

5-2008

ANAEROBIC BIODEGRADATION OF ETHYLENE DIBROMIDE AND 1,2-DICHLOROETHANE IN THE PRESENCE OF FUEL HYDROCARBONS

James Henderson

Clemson University, james.k.henderson@usa.dupont.com

Follow this and additional works at: https://tigerprints.clemson.edu/all_dissertations

 Part of the [Environmental Engineering Commons](#)

Recommended Citation

Henderson, James, "ANAEROBIC BIODEGRADATION OF ETHYLENE DIBROMIDE AND 1,2-DICHLOROETHANE IN THE PRESENCE OF FUEL HYDROCARBONS" (2008). *All Dissertations*. 213.

https://tigerprints.clemson.edu/all_dissertations/213

This Dissertation is brought to you for free and open access by the Dissertations at TigerPrints. It has been accepted for inclusion in All Dissertations by an authorized administrator of TigerPrints. For more information, please contact kokeefe@clemson.edu.

ANAEROBIC BIODEGRADATION OF ETHYLENE DIBROMIDE AND 1,2-
DICHLOROETHANE IN THE PRESENCE OF FUEL HYDROCARBONS

A Thesis
Presented to
the Graduate School of
Clemson University

In Partial Fulfillment
of the Requirements for the Degree
Doctor of Philosophy
Environmental Engineering and Science

by
James K. Henderson
May 2008

Accepted by:
Dr. Ronald W. Falta, Committee Chair
Dr. David L. Freedman
Dr. Larry W. Murdoch
Mr. Stephen H. Shoemaker
Dr. Yanru Yang

ABSTRACT

Field evidence from underground storage tank (UST) sites where leaded gasoline leaked indicates the lead scavengers 1,2-dibromoethane (ethylene dibromide, or EDB) and 1,2-dichloroethane (1,2-DCA) may be present in groundwater at levels that pose unacceptable risk. These compounds are seldom tested for at UST sites. Although dehalogenation of EDB and 1,2-DCA is known to occur, the effect of fuel hydrocarbons on their biodegradability under anaerobic conditions is poorly understood. Microcosms (2 L glass bottles) were prepared with soil and groundwater from a UST site in Clemson, South Carolina, using samples collected from the source (containing residual fuel) and less contaminated downgradient areas. Anaerobic biodegradation of EDB occurred in microcosms simulating natural attenuation, but was more extensive and predictable in treatments biostimulated with lactate. In the downgradient biostimulated microcosms, EDB decreased below its maximum contaminant level (MCL) ($0.05 \mu\text{g/L}$) at a first order rate of $9.4 \pm 0.2 \text{ yr}^{-1}$. The pathway for EDB dehalogenation proceeded mainly by dihaloelimination to ethene in the source microcosms, while sequential hydrogenolysis to bromoethane and ethane was predominant in the downgradient treatments. Biodegradation of EDB in the source microcosms was confirmed by carbon specific isotope analysis, with a $\delta^{13}\text{C}$ enrichment factor of -5.6‰. The highest levels of EDB removal occurred in microcosms that produced the highest amounts of methane. Extensive biodegradation of benzene, ethylbenzene, toluene and *ortho*-xylene was also observed in the source and downgradient area microcosms. In contrast, biodegradation of 1,2-DCA proceeded at a considerably slower rate than EDB, with no response to lactate

additions. The slower biodegradation rates for 1,2-DCA agree with field observations and indicate that even if EDB is removed to below its MCL, 1,2-DCA may persist.

Separate experiments were carried out to assess the potential inhibitory interactions between 1,2-DCA and EDB, which might explain the observed persistence of these compounds where leaded gasoline was released. Preliminary experiments were conducted to determine if an enrichment culture that chlororespires PCE and TCE developed at Clemson University was also capable of respiring EDB and 1,2-DCA. The culture was found to have the ability to rapidly dehalorespire EDB and 1,2-DCA, currently the only mixed culture known to do so. However, when the culture was fed both compounds simultaneously, it degraded EDB at the expense of 1,2-DCA in all cases. When the culture was enriched on EDB, activity on 1,2-DCA was completely inhibited, even after EDB was gone. No amount of 1,2-DCA inhibited the rate of EDB degradation down to part-per-trillion levels. Any previous exposure to EDB precluded the culture's ability to consume 1,2-DCA. Remarkably, when the culture was enriched on 1,2-DCA and subsequently exposed to both EDB and 1,2-DCA, EDB was consumed first. EDB clearly inhibited 1,2-DCA biodegradation, and the degree of 1,2-DCA inhibition was roughly proportional to the concentration of EDB. This clear pattern of 1,2-DCA inhibition by EDB may contribute to its observed persistence in laboratory and field studies and merits further evaluation.

Currently, decision makers have little information to guide remedial choices at UST sites contaminated with leaded gasoline additives. An analytical model was used to simulate the effects of partial source removal and plume remediation on EDB and 1,2-

DCA plumes at contaminated UST sites. The risk posed by EDB, 1,2-DCA, and comingled gasoline hydrocarbons varies throughout the plume over time. Dissolution from the light nonaqueous phase liquid (LNAPL) determines the concentration of each contaminant near the source, but biological decay in the plume has a greater influence as distance downgradient from the source increases. For this reason, compounds that exceed regulatory standards near the source may not in downgradient plume zones. At UST sites, partial removal of a residual LNAPL source mass may serve as a stand alone remedial technique if dissolved concentrations in the source zone are within a couple orders of magnitude of the applicable government or remedial standards. This may be the case with 1,2-DCA; however EDB is likely to be found at concentrations that are orders of magnitude higher than its low MCL of $0.05 \mu\text{g/L}$. For sites with significant EDB contamination, even when plume remediation is combined with source depletion, significant timeframes may be required to mitigate the impact of this compound. Benzene and MTBE are commonly the focus of remedial efforts at UST sites, but simulations presented here suggest that EDB, and to a lesser extent 1,2-DCA could be the critical contaminants to consider in the remediation design process at many sites.

ACKNOWLEDGMENTS

I would like to thank Dr. Ronald W. Falta and Dr. David L. Freedman for their continual guidance and support throughout this project. I would also like to thank the other members of my committee, Dr. Larry Murdoch, Dr. Yanru Yang, and Mr. Stephen H. Shoemaker. I gratefully acknowledge Bunnell-Lammons Engineering, Inc. for assistance in collecting soil and groundwater samples, Dr. John T. Coates for guidance with analytical method development, and Susan Fredendall, Audrey Bone, Ashley Eaddy, Micah Freedman, Bridget Odonague, and Ron Yu for performing headspace analyses. I am very grateful to Dr. John T. Wilson for sponsoring the ^{13}C analyses and Dr. Tomasz Kuder for performing them. I am thankful for the unwavering support of my family.

TABLE OF CONTENTS

	Page
TITLE PAGE	i
ABSTRACT	ii
ACKNOWLEDGMENTS	v
LIST OF TABLES	viii
LIST OF FIGURES	ix
 CHAPTER	
1 INTRODUCTION	1
2 MICROCOSM STUDY	3
2.1 Introduction	3
2.2 Materials & Methods	5
2.3 Results	8
2.4 Discussion	13
3 MODELING THE EFFECTS OF REMEDIATION ON EDB AND 1,2-DCA PLUMES USING REMCHLOR	26
3.1 Introduction	26
3.2 Background	27
3.3 Modeling Approach	29
3.4 Simulation Development	33
3.5 Results	42
3.6 Discussion	52
4 EVALUATION OF POTENTIAL MUTUAL INHIBITION OF EDB AND 1,2- DCA ON AN ENRICHMENT CULTURE	73
4.1 Introduction	73
4.2 Materials and Methods	76
4.3 Results	81
4.4 Discussion	87

Table of Contents (Continued)

	Page
5 SUMMARY AND IMPLICATIONS	103
APPENDICES	108
A: Appendix A	109
6.1 Microcosm Sampling and Analytical Methods.....	109
6.2 The Effect of Incubation Method on Losses of Volatile Compounds During Storage of the Microcosms.....	112
6.3 Comparison of EDB Quantification by EPA Method 8011 and Headspace Analysis.....	116
6.4 EDB and 1,2-DCA Results for Individual Microcosms.	118
6.5 Characteristics of Soil from the Source and Midgradient Zones.	121
6.6 Comparison of Gibbs Free Energies for Dehalogenation of EDB, 1,2-DCA, and Associated Daughter Products.....	122
6.6 Comparison of EDB, 1,2-DCA and BTEX First Order Biodegradation Rates.	125
B: Appendix B.....	127
7.1 Inhibition Test Results by Bottle	127
REFERENCES	137

LIST OF TABLES

Table	Page
2.1	Average initial concentrations in the microcosms18
2.2	Maximum methane produced and final EDB concentrations19
3.1	Comparison of first order biodegradation rates (yr^{-1})56
3.2	Simulation parameters, short and long plume scenarios.....57
3.3	Calculation of compound-specific simulation parameters.....58
3.4a	Maximum extent above MCL, at t = 2012, 2017, Short Plume.....59
3.4b	Maximum extent above MCL, at t = 2012, 2017, Long Plume59
4.1	Treatments used to test the effect of 1,2-DCA on EDB90
4.2	Treatments used to test the effect of EDB on 1,2-DCA90
A.1	Summary of first order loss rates from water controls with punctured and unpunctured septa.....115
A.2	Soil characteristics121
A.3	Comparison of Gibbs free energies for transformation of EDB, 1,2-DCA and associated daughter products123
A.4	Data used for Gibbs free energy calculations presented in table A.3124
A.5	Comparison of first order biodegradation rates (yr^{-1})126
A.6	Field concentration data used to calculate first order biodegradation rates for the Clemson UST site.....126

LIST OF FIGURES

Figure	Page
2.1 Average EDB and 1,2-DCA concentrations for all treatments.....	20
2.2 Pseudo first-order decay rates for the a) source zone and b) midgradient microcosms.....	21
2.3 Average BTEX concentrations for all treatments.....	22
2.4 EDB biodegradation and daughter product behavior in source zone NA replicate #3	23
2.5 Daughter products from EDB biodegradation in the source zone and midgradient microcosms	24
2.6 CSIA results for EDB for two source zone NA microcosms.....	25
3.1 Distance-time plot for advective transport with multiple sets of plume reaction rates.....	60
3.2 Site conceptual model for short and long plume cases, including biostimulation schemes	61
3.3 Short plume natural attenuation relative importance of EDB, 1,2-DCA, Benzene and MTBE in zones 1, 2 and 3	62
3.4 Long plume natural attenuation relative importance of EDB, 1,2-DCA, Benzene and MTBE in zones 1, 2 and 3	63
3.5 REMChlor simulation results of natural attenuation, short plume scenario, 2012	64
3.6 REMChlor simulation results of natural attenuation, long plume scenario, 2012	65
3.7 REMChlor simulation results of 90% source removal, short plume scenario, 2012	66
3.8 REMChlor simulation results of 90% source removal, long plume scenario, 2012	67

List of Figures (Continued)

Figure	Page
3.9 REMChlor simulation results of biostimulation, short plume scenario, 2012.....	68
3.10 REMChlor simulation results of biostimulation, long plume scenario, 2012.....	69
3.11 REMChlor simulation results of 90% source removal and biostimulation, short plume scenario, 2012.....	70
3.12 REMChlor simulation results of 90% source removal and biostimulation, long plume scenario, 2012.....	71
3.13 REMChlor simulation results of 90% source removal and biostimulation, long plume scenario, 2017.....	72
4.1 Pathways for anaerobic reduction of EDB.....	91
4.2 EDB mother bottle.....	92
4.3 1,2-DCA mother bottle.....	93
4.4 EDB inhibition test, comparison of average EDB amount per bottle by treatment.....	94
4.5 EDB inhibition test, comparison of average ethane amount per bottle by treatment.....	95
4.6 EDB inhibition test, comparison of average 1,2-DCA amount per bottle by treatment.....	96
4.7 EDB inhibition test, comparison of average methane amount per bottle by treatment.....	97
4.8 1,2-DCA inhibition test, comparison of average 1,2-DCA amount per bottle by treatment.....	98
4.9 1,2-DCA inhibition test, comparison of average EDB amount per bottle by treatment.....	99
4.10 1,2-DCA inhibition test, comparison of average ethane amount per bottle by treatment.....	100

List of Figures (Continued)

Figure	Page
4.11 1,2-DCA inhibition test, comparison of VC amount per bottle by treatment.....	101
4.12 1,2-DCA inhibition test, comparison of average methane amount per bottle by treatment.....	102
A-1 Behavior of EDB, 1,2-DCA and BTEX in triplicate water control microcosms.....	114
A-2 Source zone EDB and 1,2-DCA microcosm replicates	119
A-3 Midgradient zone EDB and 1,2-DCA microcosm replicates.....	120
B-1 EDB Inhibition test, EDB only, replicates 1 (a) and 2 (b).....	128
B-2 EDB inhibition test, EDB + Low 1,2-DCA, replicates 1 (a) and 2 (b).....	129
B-3 EDB inhibition test, EDB + Mid 1,2-DCA, replicates 1 (a) and 2 (b).....	130
B-4 EDB inhibition test, EDB + High 1,2-DCA, replicates 1 (a) and 2 (b)	131
B-5 1,2-DCA inhibition test, 1,2-DCA only, replicates 1 (a) and 2 (b).....	132
B-6 1,2-DCA inhibition test, EDB only, replicates 1 (a) and 2 (b).	133
B-7 1,2-DCA inhibition test, 1,2-DCA + Low EDB, replicates 1 (a) and 2 (b)	134
B-8 1,2-DCA inhibition test, 1,2-DCA + Mid EDB, replicates 1 (a) and 2 (b).....	135
B-9 1,2-DCA inhibition test, 1,2-DCA + High EDB, replicates 1 (a) and 2 (b).	136

CHAPTER ONE

INTRODUCTION

Society's reliance on the internal combustion engine has resulted in a legacy of environmental contamination where gasoline spilled or leaked from underground storage tank (UST) systems. Two compounds, 1,2-dibromoethane (ethylene dibromide, or EDB) and 1,2-dichloroethane (1,2-DCA) were added to leaded gasoline along with organic contaminants benzene, toluene, ethyl benzene, xylene (known collectively as BTEX), and methyl tert-butyl ether (MTBE), but have not received significant regulatory scrutiny to date (21). EDB and 1,2-DCA were present in gasoline from the 1920s through the 1980s. EDB is highly carcinogenic, with a federal Maximum Contaminant Level (MCL) of 0.05 $\mu\text{g/L}$ in groundwater, second only to that of dioxin. 1,2-DCA also has a low MCL (5.0 $\mu\text{g/L}$), comparable to that of benzene. EDB and 1,2-DCA are mobile at some sites, but the factors controlling this behavior are not well defined. Emerging evidence indicates that EDB and 1,2-DCA persist in groundwater at UST sites, but to date, no significant research identifying the extent of lead scavenger contamination in groundwater at leaded gasoline release sites has been undertaken. This research attempts to develop an understanding of the geochemical and biological components controlling the behavior of lead scavengers in the subsurface at sites where leaded gasoline was released, which in turn will permit more informed remedial decision making to achieve risk-based remedial objectives at UST sites. This dissertation documents laboratory research conducted on the biodegradation of lead additives in the presence of fuel hydrocarbons and efforts to document the potential inhibitory effects of 1,2-DCA on EDB. Using these laboratory

derived data, a new analytical model is utilized to explore potential remedial options that might be employed at UST sites. Simulations of partial source removal and plume remediation are conducted to provide UST project managers a sense of how these contaminants will respond to remediation, and how remedial actions might lessen the extent of EDB and 1,2-DCA in groundwater at UST sites.

CHAPTER TWO

MICROCOSM STUDY

2.1 Introduction

An estimated 400,000 underground storage tank (UST) releases have been documented in the US and it is possible that more undocumented releases have occurred (38). The US Environmental Protection Agency (EPA) and state regulatory programs have required that benzene, toluene, ethylbenzene, xylenes (i.e., BTEX), and, more recently methyl tert-butyl ether (MTBE) be analyzed during environmental investigations at UST sites. Two components of leaded gasoline that have received little attention are 1,2-dibromoethane (ethylene dibromide, or EDB) and 1,2-dichloroethane (DCA), which were added to leaded gasoline to prevent engine lead fouling (21). EDB is highly carcinogenic, with a drinking water maximum contaminant level (MCL) of $0.05 \mu\text{g/L}$. The MCLs for 1,2-DCA and benzene are $5.0 \mu\text{g/L}$.

Once released to groundwater, the physical properties of EDB and 1,2-DCA suggest they will be mobile. Based upon their gasoline-water partition constants, dissolved phase EDB and 1,2-DCA concentrations up to 1,900 and 3,700 $\mu\text{g/L}$, respectively, can be expected in groundwater near the source area of a leaded gasoline release (25). A review of about 1,100 UST facilities in South Carolina revealed that 537 had EDB concentrations above the MCL. Few of these sites have been tested for 1,2-DCA (25). The extent of EDB and 1,2-DCA contamination is not known for the vast majority of sites, but it is apparent that both persist at levels above the MCL at a significant percentage of sites. Despite the fact that there is an MCL for EDB, a review

of state UST regulatory program testing requirements revealed only 11 states required testing for EDB in 2003 (25).

Biodegradation of EDB and 1,2-DCA has been reported under a variety of anaerobic conditions (29, 33, 40, 45, 52, 65). However, previous research on EDB and 1,2-DCA dehalogenation focused on agricultural or industrial settings. No previous studies have investigated the effect of fuel hydrocarbons on EDB and 1,2-DCA anaerobic dehalogenation. Furthermore, little effort has been made to relate laboratory biodegradation studies to behavior observed in the field, so the geochemical and biological factors determining whether or not EDB and 1,2-DCA degrade at gasoline sites remain unclear. The purpose of this work was to evaluate biodegradation of EDB and 1,2-DCA in the presence of BTEX, MTBE and other fuel hydrocarbons.

Numerous UST sites were reviewed in a collaborative effort between Clemson University and the South Carolina Department of Health and Environmental Control (SCDHEC) in 2004 . Based on this review, a conceptual model was developed to describe the typical behavior of EDB and 1,2-DCA in gasoline-contaminated groundwater. Three distinct spatial zones can be expected. The source zone is found directly downgradient from a leaking UST or former tank excavation and is characterized by high dissolved concentrations of EDB, 1,2-DCA, BTEX, and other fuel hydrocarbons. In the midgradient zone dissolved concentrations are generally lower by orders of magnitude, which may occur at varying distances downgradient from the source. The source and midgradient zones are typically anaerobic, given the high oxygen demand of the fuel hydrocarbons. Finally, low concentrations (but above the MCL) of EDB and 1,2-

DCA may exist in the downgradient portion of the plume, where BTEX compounds may be absent and conditions are typically aerobic. The microcosms reported in this study were designed to evaluate natural attenuation (NA) or biostimulation (BST) of EDB and 1,2-DCA in the source and midgradient zones of an actual UST site.

2.2 Materials & Methods

2.2.1 Soil and Groundwater Collection

During the evaluation of SCDHEC UST sites, a facility in Clemson, SC was identified that exhibits the three spatial zones described above. High concentrations of EDB (300 $\mu\text{g/L}$) in the source zone are attenuated by orders of magnitude less than ten meters downgradient, presumptively via biodegradation. In May 2005, soil cores were collected from the source and midgradient areas. A Geoprobe® was used to advance 5.1-cm inner-diameter downhole tooling to below the water table in each zone, and two 1.5-m soil cores were collected in acetate liners. The ends of the liners were waxed to prevent volatilization and oxygen intrusion. The source and midgradient boring locations were sited adjacent to groundwater wells, and groundwater was collected using bailers (after purging the wells of three volumes).

2.2.2 Microcosms

Three treatments were prepared (June 2005) for the source area and midgradient locations (triplicate or quadruplet bottles per treatment): no amendments (to simulate NA); addition of lactate (to simulate BST); and killed controls. Microcosms were prepared in 2-liter glass Qorpak® jugs (VWR International, Inc.), which provided sufficient volume for repeated sampling without significantly disrupting the volumetric

ratio of liquid-to-headspace. Groundwater (1.5-L with 1 mg/L of resazurin added) and soil (400-g) were added to the bottles in an anaerobic chamber (approximately 99% N₂, 1% H₂), leaving 0.3-L of headspace. The bottles were capped with Teflon-backed septa (3.5-cm, Saint-Gobain Performance Plastics) and a plastic screw cap. Soil from the source zone was contaminated with light non-aqueous phase liquid; a sheen (presumably gasoline) was initially present on the water surface of these microcosms. The initial lactate addition to the BST treatments was 0.14 mM (100 times the stoichiometric amount required to reduce EDB and 1,2-DCA to ethene in the source zone microcosms). Killed controls were autoclaved for one hour on three consecutive days. Evidence of biological activity (i.e., methane and ethene formation) was noted in the controls during the first 76 days of incubation. After adding glutaraldehyde on day 76 (70 mg of 50% syrup/g soil (55)) there was no further biological activity.

EDB, 1,2-DCA, and BTEX were present in the source zone groundwater in expected amounts, so it was unnecessary to add these compounds to the source treatments. However, in two of the source zone NA microcosms (replicates #3 and #4), most of the EDB was consumed within three months of incubation. In order to confirm the occurrence of EDB biodegradation, EDB was respiked (using a water saturated solution) to the same concentration initially observed in the groundwater (Table 1). The soil sample was well-mixed prior to distribution to the microcosms and the same groundwater was used in all bottles. Nevertheless, there was considerable variability in initial concentrations. For the midgradient microcosms, the background concentrations were low relative to the source zone so EDB, 1,2-DCA and BTEX were added using

saturated water solutions. The resulting initial midgradient concentrations were approximately two orders of magnitude lower than in the source zone treatments (as in the site conceptual model), with less variability (Table 1). The microcosms were incubated at 22-24°C, in an inverted position (solids and liquid in contact with the septa), with unpunctured septa, in order to minimize loss of volatile compounds (Appendix A).

2.2.3 Chemicals

Chemicals used were EDB (99.99%, Acrōs Organics), 1,2-DCA (99.99%, Malinckrodt), benzene (99.9%, Fischer), toluene (99.0%, Fischer), ethylbenzene and *o*-xylene (99.9%, Fischer), MTBE (99.8%, Sigma-Aldrich), bromoethane (99.0%, BMD), vinyl bromide (98%, Pfaltz & Bauer), and chloroethane (99.7%, Aldrich). National Welders supplied methane (99.99%), ethane (99.99%), ethene (99.99%) and hydrogen (99.999%).

2.2.4 Analytical Methods

EDB, bromoethane, vinyl bromide, 1,2-DCA, BTEX and MTBE were monitored by headspace analysis using a 5890 Series II Plus Hewlett-Packard gas chromatograph (GC), equipped with both a ⁶³Ni electron capture detector (ECD) and a flame ionization detector (FID). Headspace analysis was used because it allows for detection of all compounds to below their MCL and does not require an extraction step, as with EPA Method 8011. Two headspace samples were taken simultaneously with separate syringes, and samples were manually injected, one immediately after the other, onto separate columns on the same GC (Appendix A). Compound-specific isotope analysis

(CSIA) was performed for EDB and 1,2-DCA using procedures described in Appendix A.

Chloroethane and vinyl chloride were quantified by headspace analysis with an FID-equipped GC (5890 Series II Plus Hewlett-Packard) and a packed Carbopack™ B column (28). Methane, ethane, and ethene were quantified on the same GC using a Carbosieve™ S-II molecular sieve column (3.2-mm x 3.2-m; 200°C isothermal, 28.5 mL/min N₂ carrier gas; injector and detector at 250°C) and FID at 200°C. Bromide, chloride, nitrate, sulfate, iron and organic acids were analyzed using standard procedures (Appendix A).

2.3 Results

2.3.1 Biodegradation Trends

In the source zone microcosms, average results indicated significantly better removal of EDB in the BST treatment than in the NA treatment (Fig. 2.1a). Less than 1% of initial EDB remained at 380 days of incubation, versus 22% in NA treatment and 50% in killed controls. Although the average dehalogenation rate for NA was less than BST, EDB was initially consumed in two NA replicates (#3 and #4) at a faster rate than the BST microcosms (results for individual microcosms are presented in Appendix A). This activity was confirmed by respiking EDB to the same initial concentration (Table 2.1) in both microcosms. Rapid EDB consumption continued in one NA replicate (#3) to below the MCL while the rate of dehalogenation in the other (NA #4) slowed. The other source zone NA replicates (#1 and #2) and all three of the BST replicates were at µg/L levels at day 380 (and consequently were not respiked with EDB). Average losses of 41% in the

killed controls occurred mainly during the first 76 days due to biological activity, since autoclaving was insufficient. After addition of glutaraldehyde (day 76), EDB decreased by only 9% through day 380. EDB losses from water controls averaged 11% over this same period (data not shown).

In the midgradient microcosms, the BST treatment also outperformed NA in terms of EDB removal (Fig. 2.1b). Less abiotic losses occurred from midgradient killed controls ($11.1\% \pm 10.5\%$). The midgradient BST treatment is notable since EDB was degraded below the MCL in all replicates. Lactate was monitored approximately twice per month; whenever it was consumed, more was added. Approximately 12 times more lactate was consumed in the midgradient bottles and both NA and BST replicates behaved more uniformly compared to the source zone.

Pseudo-first order degradation rates for EDB degradation are shown in Figure 2.2. The source zone BST rate is approximately four times higher than for NA and the controls. Although the average rate for NA was higher than for the controls, they were not statistically different (Student's *t*-test, $\alpha = 0.05$). In midgradient microcosms, the BST rate was significantly greater than for NA, and both were significantly greater than the killed controls.

Much less 1,2-DCA was degraded in source (Fig. 2.1c) and midgradient microcosms (Fig. 2.1d) compared to EDB. 1,2-DCA did not decrease below its MCL in any of the microcosms. The first order rates for 1,2-DCA in NA and BST treatments were statistically higher than for the controls in the source, but not in the midgradient microcosms (Fig. 2.2), and lower abiotic losses of 1,2-DCA occurred in the controls

relative to EDB. Consumption of lactate did not have as significant a stimulatory effect on 1,2-DCA; the degradation rates for NA and BST treatments were not statistically different in the source or midgradient treatments. A notable departure from these trends occurred in the source zone NA microcosm (replicate #3) that exhibited extensive and rapid EDB biodegradation. In this bottle, 1,2-DCA declined from 565 to 13 $\mu\text{g/L}$, with approximately an equimolar amount of chloroethane produced (Appendix A).

The pattern of BTEX degradation varied between source and midgradient microcosms (Fig. 2.3). A considerable amount of benzene was biodegraded in source and midgradient NA and BST treatments. The first order rate for benzene was higher in the source BST versus NA microcosms (Fig. 2.2a). There was no significant difference in the midgradient BST and NA rates (Fig. 2.3b), although the average amount of benzene consumed was greater in the NA treatment (Fig. 2.3b). Toluene loss from the source zone killed controls was considerable (Fig. 2.3c). Consequently, the first order rate for the BST treatment was not statistically higher than the killed controls (Fig. 2.2a). Abiotic losses were negligible in midgradient microcosms (Fig. 3d), in which toluene degradation was extensive and comparatively fast in live treatments (Fig. 2.2b). Extensive biodegradation of ethylbenzene and *o*-xylene occurred in the source and midgradient microcosms (Fig. 2.3e-h), at rates similar to toluene and well above killed controls (Fig. 2.2). Statistically higher rates of removal were observed in the source zone NA treatment for ethylbenzene and *o*-xylene, whereas there was no significant difference in rates for these compounds in the midgradient microcosms. In both source and

midgradient microcosms, there was no significant loss of MTBE from the live treatments or the killed controls (data not shown).

2.3.2 EDB Daughter Products

Biodegradation of EDB was accompanied by stoichiometric increases in ethene and bromoethane (Fig. 2.4). Vinyl bromide was not detected in any microcosms. After EDB decreased below detection, the amount of bromoethane and ethene also declined. In water controls containing methane, ethene, ethane, and chloroethane, losses ranged from 11.2% for ethane to 25.9% for methane over 280 days of incubation. This indicates the extensive and rapid decreases in EDB daughter products from live bottles (e.g., Fig. 2.4) cannot be attributed solely to diffusive losses.

Figure 2.5 shows the amount of daughter products for each treatment at the midpoint of the incubation period (when 40-70% of the EDB had been consumed) and the end of the incubation period. At the midpoint, daughter products accounted for 66-88% (molar basis) of the EDB consumed, with ethene predominant in the source and bromoethane in the midgradient treatments. Ethane was insignificant in the source zone but was similar in magnitude to ethene in the midgradient treatments. It is not known if ethane was formed via reduction of bromoethane, ethene, or both. At the end of the incubation, significant decreases in daughter products occurred (also shown in Fig. 2.4); less than 18% remained in the source microcosms and none were detectable in the midgradient microcosms.

2.3.3 Electron Acceptors and Methane Production

Nitrate was not detected at any time. Sulfate was not detected in the midgradient microcosms. In most of the source zone bottles, sulfate ranged from 13 to 43 mg/L, with no apparent fluctuations in concentration between days 130-251, when most of the samples were taken. However, in the two source zone NA replicates with the lowest EDB concentrations (#3 and #4, Table 2), sulfate was less than 2.0 mg/L over the same interval. Soluble iron at the end of the experiment averaged 4.1 (± 4.3) mg/L in the source zone and 17.5 (± 4.6) mg/L in the midgradient microcosms. Soil from the source and midgradient zones contained low levels of total iron (Appendix A).

Methane production was highest in microcosms that exhibited decreases in EDB to below the MCL (Table 2.2). For example, methane output was highest in source zone NA replicate #3; EDB in this bottle decreased to non-detect. Methane output was considerably higher and EDB degradation more extensive in the midgradient BST treatment compared to NA. The highest amount of methane that accumulated in the midgradient bottles (0.24 mmol) accounted for 9.4% of the electron equivalents of the lactate consumed (1.7 mmol), while acetate and propionate accounted for approximately 23%.

2.2.4 Compound-specific isotope analysis

Samples for CSIA were taken from two source zone NA microcosms (days 189 and 259). On day 259 extensive dehalogenation was noted for EDB (Fig. 2.1a), but less for 1,2-DCA (Fig. 2.1c). The values of $\delta^{13}\text{C}$ in the four samples increased as the EDB concentrations decreased relative to the initial concentrations (Fig. 2.6). The observed

increase of $\delta^{13}\text{C}$ associated with a reduction in EDB concentration is consistent with EDB dehalogenation (47). The same trend in isotope fractionation was observed in both NA microcosms. In NA samples, the enrichment factor is -5.6‰ ($\pm 1\text{‰}$ at 95 % confidence level). Significant attenuation of 1,2-DCA occurred only in NA replicate #3, in which the $\delta^{13}\text{C}$ of 1,2-DCA was $+15\text{‰}$. This was also the only source zone microcosm in which EDB decreased below the MCL and a significant amount of methane was produced (Table 2.2). In replicate #2, with no apparent 1,2-DCA attenuation, the $\delta^{13}\text{C}$ of 1,2-DCA was -26‰ .

2.4 Discussion

This results of this study are the first to conclusively demonstrate anaerobic biodegradation of EDB in the presence of fuel hydrocarbons from release of leaded gasoline to groundwater. However, considerably less dechlorination of 1,2-DCA occurred in the presence of fuel hydrocarbons, in spite of previous studies that have demonstrated anaerobic degradation of 1,2-DCA when it is the sole contaminant.

Rapid EDB dehalogenation in the source zone (in the presence of high concentrations of BTEX and other fuel hydrocarbons) to below the MCL is possible with NA. However, the average rate of EDB removal was faster and less variable with BST. The reasons for variability in source zone EDB NA rates are not yet known but are likely related to high levels of other hydrocarbons also undergoing biodegradation. The source zone microcosms contain high levels of organic acids (data not shown) that may be enhancing (by providing electron donor) or inhibiting (due to the potential toxicity of longer chain fatty acids) EDB and 1,2-DCA dehalogenation. Faster anaerobic decay of

EDB may occur downgradient of gasoline source zones due to lower hydrocarbon concentrations.

The pattern of isotope fractionation observed in this study is consistent with a degradative process, such as bio-dehalogenation. No previous studies were found with stable isotope data for reductive debromination of EDB. The value for the enrichment factor in this study ($-5.6 \pm 1\text{‰}$) is within the range of those reported for reductive dechlorination of tri- and tetrachloroethene (-2.5 to -13.8‰ and -2 to -5.5‰ , respectively (19)), but is lower than the values reported for dechlorination of 1,2-DCA (-27 to -33‰ (19)). The magnitude of $\delta^{13}\text{C}$ enrichment for 1,2-DCA, from -26‰ in a specimen with no apparent attenuation of the compound to $+15\text{‰}$ in the NA microcosm showing advanced attenuation of 1,2-DCA, agrees well with previous reports on dechlorination of 1,2-DCA (19). The relatively large isotope effects observed in this study suggest that CSIA may be used to document dehalogenation of EDB and 1,2-DCA in the field.

The slower rate of 1,2-DCA dehalogenation compared to EDB is consistent with field observations (21). Given 1,2-DCA's low MCL ($5.0 \mu\text{g/L}$) and the fact that few states currently sample for this compound, it may present a significant risk at leaded gasoline UST sites. 1,2-DCA removal to near its MCL in one of the source zone microcosms (confirmed by CSIA) suggests this compound can be biodegraded at UST sites, but as with EDB, source zone NA results were variable. Biodegradation of brominated organics is generally faster than chlorinated compounds (61) and thermodynamics slightly favor dehalogenation of EDB over 1,2-DCA (Appendix A).

Given that the same type of microbes (i.e., *Dehalococcoides*) dehalorespire both compounds (33), EDB biodegradation may have to occur before activity commences on 1,2-DCA. pH may also influence the rate of dehalogenation, since the activity of *Dehalococcoides* declines below a pH of approximately 6.5. Groundwater at the Clemson UST site and in the microcosms is approximately 6.4. In addition to *Dehalococcoides*, rapid chlororespiration of 1,2-DCA has been reported with *Desulfotobacterium dichloroeliminans* strain DCA1 (45); it is not known if these microbes are present at the Clemson UST site.

First order biodegradation rates observed for EDB, 1,2-DCA and BTEX were similar to in situ rates at the Clemson UST site and published rates (57) (Appendix A). Such comparisons must be viewed with caution due to variability in field and laboratory conditions, including factors such as biomass and contaminant concentrations. The biodegradation rate for benzene in the source zone microcosms was comparable to the other BTEX compounds, although it was comparatively slower in the downgradient bottles. The fact that biodegradation of benzene occurred is noteworthy because this compound is often regarded as refractory under anaerobic conditions (57).

The effect of lactate addition on BTEX biodegradation varied. It appeared to be beneficial in the case of benzene, negligible in the case of toluene, and inhibitory for ethylbenzene and *o*-xylene in the source zone. Nevertheless, the benefits of biostimulation with respect to EDB are clear, and any potential inhibitory effects of lactate on hydrocarbons is less of a concern in the source zone since these compounds

biodegraded at a faster rate in the midgradient zone (Fig. 2), do not persist in downgradient aerobic zones, and are less toxic (21).

Most previous studies report anaerobic dehalogenation of EDB occurring primarily via dihaloelimination to ethene, with hydrogenolysis to bromoethane and dehydrohalogenation to vinyl bromide being minor (52). However, hydrogenolysis to bromoethane was prominent in this study, particularly in the midgradient treatments. Bromoethane is present in groundwater at the Clemson UST site (unpublished data), confirming the occurrence of EDB hydrogenolysis in situ. While ethene and ethane are harmless, several toxicological effects are associated with bromoethane, including neurotoxicity, hematological and hepatic toxicity, irritation of the respiratory tract, damage to genetic material, and carcinogenicity (<http://www.inchem.org/documents/cicads/cicads/cicad42htm>). The possibility of groundwater contamination by bromoethane, which is not tested for at UST sites, is a concern, although an MCL has not been established. It is unclear what factors determine the predominant pathway for anaerobic dehalogenation of EDB.

The significant decrease in ethene and bromoethane from source and midgradient microcosms in comparison to water controls indicates that a degradation mechanism other than reduction is responsible. Anaerobic oxidation of ethene has been reported under sulfate reducing conditions (9). Sulfate reduction was observed in several source zone NA microcosms and the amount of sulfate required for ethene oxidation was less than 1 mg/L. A modest level of iron reduction occurred in the midgradient treatments and bio-oxidation of vinyl chloride has been demonstrated with iron as the terminal electron

acceptor (10, 11). It is not known if anaerobic bio-oxidation is also possible for ethane and bromoethane. The product(s) from oxidation (CO_2 and Br^-) are not readily detectable in situ, so that disappearance of EDB daughter products complicates documenting natural attenuation of EDB at UST sites. Methanogenesis may serve as an indirect predictor of EDB and daughter product biodegradation. We found a consistent correlation between EDB decay below its MCL and the presence of high levels of methane in microcosms.

The microcosm results from the Clemson UST site indicate that natural attenuation of EDB from leaded gasoline spills is possible, but may be difficult to predict and document. Biostimulation increased the rate of EDB biodegradation and permitted consistent removal to below the MCL. Based on growing experience with electron donor addition to enhance removal of chlorinated ethenes, the same in situ approach should be transferable to UST sites. If the necessary microbes are not present, bioaugmentation may be necessary using cultures that dehalorespire EDB and 1,2-DCA.

Table 2.1. Average Initial Concentrations in the Microcosms

Compound	Source Zone ($\mu\text{g/L}$)	Midgradient Zone ($\mu\text{g/L}$)
EDB	343 ± 186^a	10.5 ± 1.9
1,2-DCA	575 ± 156	19.1 ± 5.2
Benzene	$25,000 \pm 11,800$	116 ± 25
Toluene	$7,950 \pm 4,560$	28.3 ± 1.6
Ethylbenzene	$2,350 \pm 1,090$	16.2 ± 2.4
<i>o</i> -Xylene	$3,670 \pm 1,550$	17.3 ± 2.6

^a \pm standard deviation for three or four microcosms.

Table 2.2 Maximum Methane Produced and Final EDB Concentrations

Rep.	Source Zone				Midgradient Zone			
	NA		BST		NA		BST	
	CH ₄ (μ mol/ bottle)	EDB _f ^a (μ g/L)	CH ₄ (μ mol/ bottle)	EDB _f (μ g/L)	CH ₄ (μ mol/ bottle)	EDB _f (μ g/L)	CH ₄ (μ mol/ bottle)	EDB _f (μ g/L)
1	1.2	120	1.5	0.4	1.5	0.33	244	ND ^b
2	3.0	67	1.8	1.4	2.4	0.24	94	ND
3	1,550	ND ^b	2.3	3.4	1.1	0.20	224	ND
4	219	7.3	-	-	-	-	-	-

^a EDB_f = final EDB concentration. ^b ND = non-detect (<0.03 μ g/L).

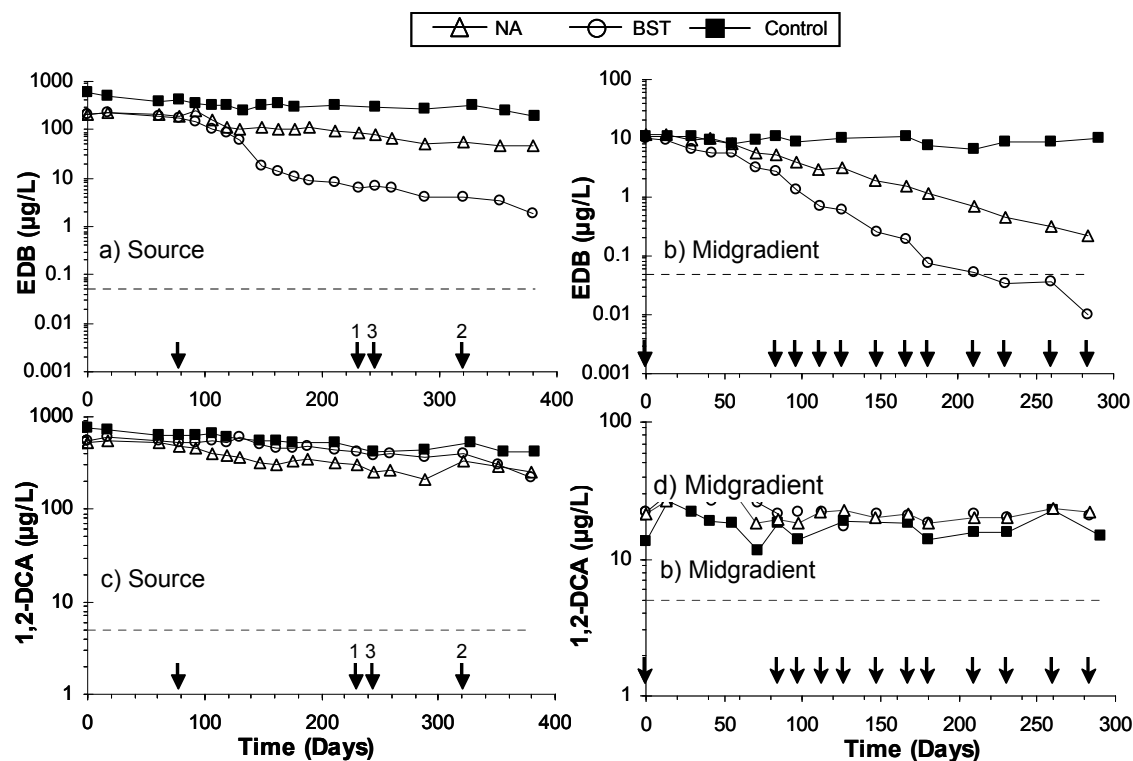


FIGURE 2.1 Average EDB and 1,2-DCA concentrations for the NA treatment (Δ), BST treatment (\circ), and killed controls (\blacksquare) in the source zone (a and c) and midgradient (b and d) microcosms. Arrows (\downarrow) indicate when lactate was added to all replicates within a BST treatment. An arrow with a number above it indicates that lactate was added only to that replicate. New lactate additions were made only when the previous addition was completely consumed. Dashed horizontal lines indicate the MCL for EDB and 1,2-DCA.

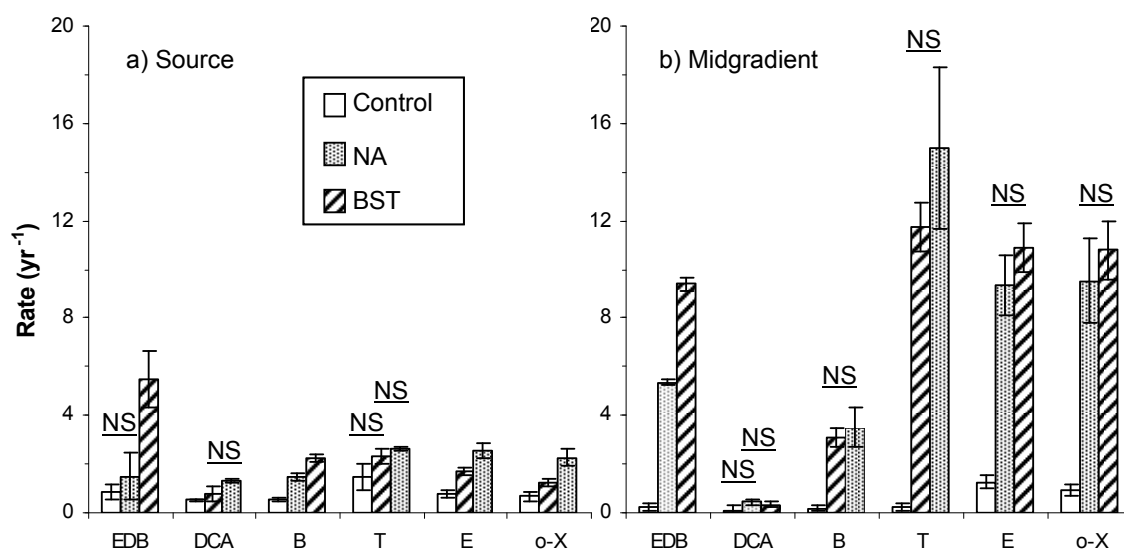


FIGURE 2.2 Pseudo first-order decay rates for the source zone (a) and midgradient (b) microcosms. Rates were determined from the pooled data for triplicate or quadruplicate bottles. Error bars represent the standard error of the slope of the regression line used to determine the rates. Horizontal lines above adjacent treatments indicate there is not a statistically significant difference between the two rates (NS = not significant); the absence of a horizontal line over adjacent treatments indicates they are statistically different (Student's *t*-test on the slopes of the regression lines, $\alpha = 0.05$).

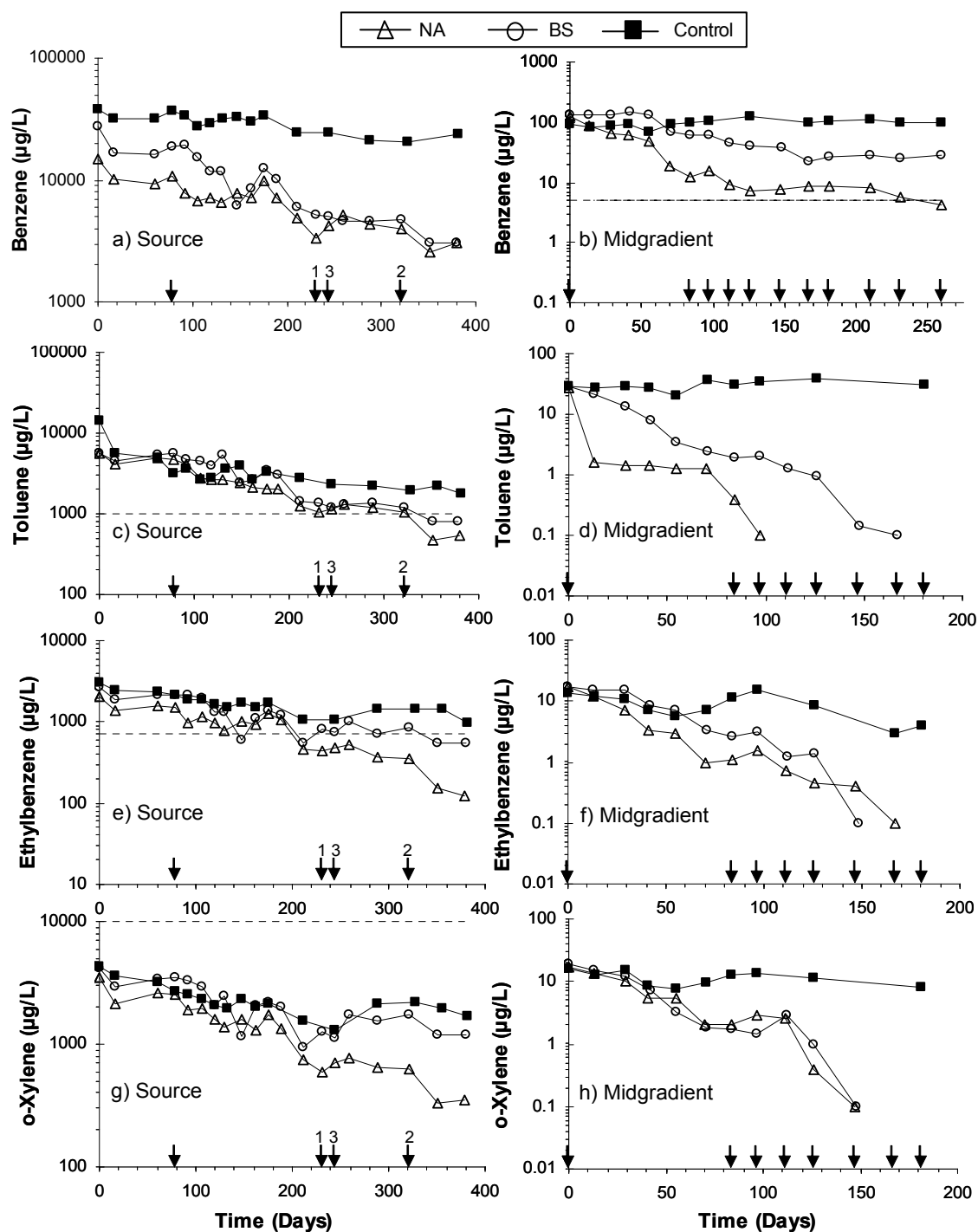


FIGURE 2.3 Average BTEX concentrations for the NA treatment (Δ), BST treatment (o), and killed controls (\blacksquare) in the source zone (a, c, e, and g) and midgradient (b, d, f, and h) microcosms. Arrows (\downarrow) indicate when lactate was added to all replicates within a BST treatment. An arrow with a number above it indicates that lactate was added only to that replicate. MCL values are shown as dashed horizontal lines when they are within the y-axis.

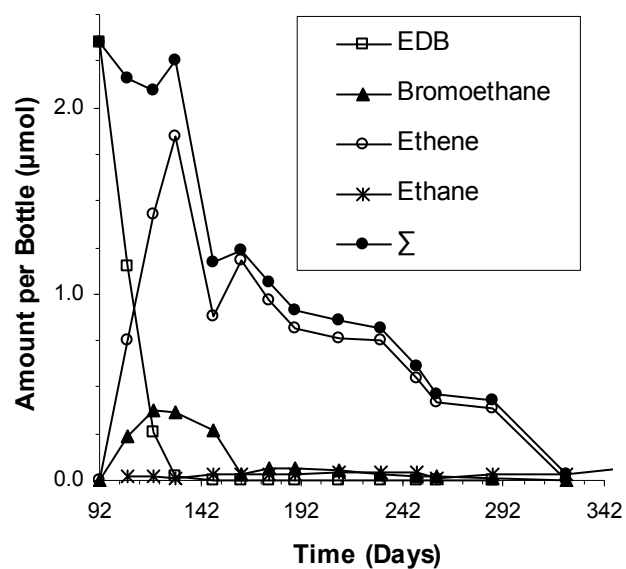


FIGURE 2.4 EDB biodegradation and daughter product behavior in source zone NA replicate #3. Σ = sum of (EDB + bromoethane + ethene + ethane).

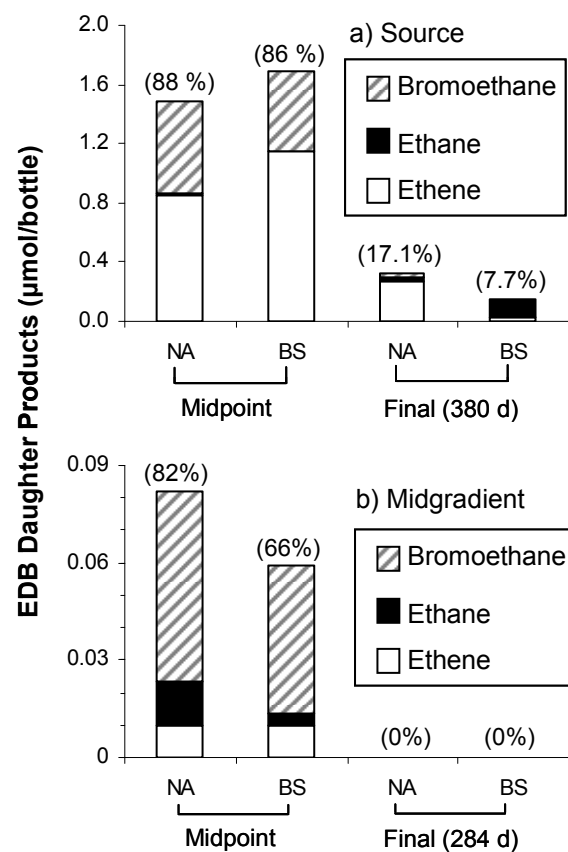


FIGURE 2.5 Daughter products from EDB biodegradation in the source zone (a) and midgradient (b) microcosms. Midpoint refers to the approximate half way period of incubation, when EDB biodegradation was 40-70% complete and daughter product accumulation was close to the maximum. Numbers above the bars indicate the molar percentage of EDB daughter products relative to the total amount of EDB consumed.

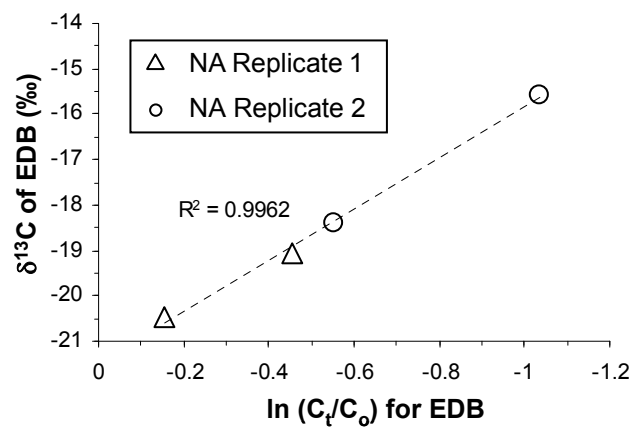


FIGURE 2.6 CSIA results for EDB for two source zone NA microcosms. C_t is the concentration of EDB at the time of sampling; C_o is the initial concentration of EDB. The enrichment factor (slope of the regression line) is -5.6‰ .

CHAPTER THREE

MODELING THE EFFECTS OF REMEDIATION ON EDB AND 1,2-DCA

PLUMES USING REMCHLOR

3.1 Introduction

Organic contaminants benzene, toluene, ethylbenzene, xylene (known collectively as BTEX), and methyl tert-butyl ether (MTBE), are commonly encountered in soil and groundwater at sites where gasoline spilled or leaked from underground storage tank (UST) systems. In the United States alone, an estimated 400,000 UST releases have been documented (38). Though gasoline is a complex mixture of hundreds of hydrocarbons, historically the United States Environmental Protection Agency (USEPA) and state regulatory programs have required that only BTEX and a small number of other organic contaminants be analyzed during environmental investigations. Two components of leaded gasoline that have not received significant regulatory scrutiny to date are 1,2-dibromoethane (ethylene dibromide, or EDB), and 1,2-dichloroethane (1,2-DCA), which were added to leaded gasoline to prevent engine lead fouling (21). EDB is highly toxic, with the lowest federal Maximum Contaminant Level (MCL) ($0.05 \mu\text{g/L}$) for any compound except dioxin (21). 1,2-DCA is also toxic and a suspected carcinogen, and has the same MCL as benzene (5.0 g/L). Emerging evidence indicates that EDB and 1,2-DCA persist in groundwater, but to date, no significant research identifying the extent of EDB and 1,2-DCA contamination in groundwater at leaded gasoline release sites has been undertaken, nor is their behavior in the subsurface well understood (21).

The objective of this study is to evaluate the effects of partial LNAPL source removal and plume remediation on EDB, 1,2-DCA, and hydrocarbon plumes at leaded gasoline UST sites. Experience with natural attenuation as a remedy for plume management has shown that mathematical models can play an important role in selection of a remedy (2, 50, 64). In many cases, screening level simulations performed with analytical models such as BIOCHLOR (3) or BIOSCREEN (49) are effective for demonstrating the applicability of natural attenuation as a remedy. This study uses an analytical model called REMChlor (Remediation Evaluation Model for Chlorinated Solvents) (22, 23), which accounts for variable source and plume remediation. REMChlor simulations will be used to evaluate the effects of partial source removal and plume bioremediation on EDB, 1,2-DCA and hydrocarbon plumes at UST sites. It is anticipated that the results of these simulations will be useful to remedial decision makers, who currently have little or no information about how these leaded gasoline additives might respond to remediation.

3.2 Background

Premature ignition, otherwise known as “knocking,” was a significant obstacle to the development of the internal combustion engine in the early part of the 20th century (8). In 1921, researchers discovered that the addition of tetraethyl lead prevented knocking, but found that it also formed solid lead deposits on valves and spark plugs, a condition known as engine fouling (37). EDB and 1,2-DCA were added to gasoline because they form volatile lead halides which can easily be removed in exhaust. These compounds were present in virtually all leaded gasoline sold, and are commonly referred

to as “lead scavengers” (37). In countries where leaded gasoline is still marketed, lead scavengers remain part of the fuel mix formulation (25). Once released to groundwater, the physical properties of EDB and 1,2-DCA suggest they will be mobile. EDB is a moderately soluble compound, with an aqueous solubility of 4,300 milligrams per liter (mg/L) (48); the solubility of 1,2-DCA is 8,500 mg/L (5). Based upon these solubilities and their gasoline-water partition constants, dissolved phase EDB and 1,2-DCA concentrations up to 1,900 and 3,700 $\mu\text{g/L}$ can be expected in groundwater near the source area of a leaded gasoline release (21). Both EDB and 1,2-DCA have low air-water, soil-water and octanol-water partition constants, so they will not partition out of groundwater into air and soil to any great degree. These factors indicate lead scavengers could form dissolved phase plumes downgradient of the release source zone.

Sites where leaded gasoline LNAPL contamination exists pose significant technical challenges and potential long-term risk to human health and the environment. Though little information exists on the prevalence of LNAPL source zones at sites where USTs leaked, it is commonly assumed that residual LNAPL source zones can be expected at sites where persistent and high-concentration plumes are present (67). Such sites would be characterized by two primary zones, 1) the source, defined as the area of aquifer or vadose zone where LNAPL is in contact with aquifer materials, and 2) the plume, where contamination is present in adsorbed and dissolved form. Recent attention has focused on the suitability of remediation of NAPL source zones at these sites, where short and long term remedial goals may necessitate source removal as well as plume remediation (23). As a consequence, the debate regarding source remediation versus

plume remediation has particular relevance to UST sites in general and lead scavengers in particular. Source removal is usually accomplished in order to minimize downgradient impacts of the contaminant plume (23), but currently metrics for establishing the efficacy of such actions are poorly defined, and no tools are in use to promote such an assessment.

3.3 Modeling Approach

Following Parker and Park (2004), Zhu and Sykes (2004), and Falta et al., (2005a), a mass balance on a contaminant species of interest in LNAPL source zone can be written as

$$\frac{dM}{dt} = -QC_s(t) \quad (3.1)$$

where Q is the water flow rate through the source zone due to infiltration or groundwater flow, $C_s(t)$ is the average dissolved concentration of contaminant species leaving the source zone, and M is the mass of the contaminant species in the source zone. The source mass is linked to the source discharge through a power function (43, 57, 60, 61, 80):

$$\frac{C_s(t)}{C_0} = \left(\frac{M(t)}{M_0} \right)^\Gamma \quad (3.2)$$

where C_0 and M_0 are the initial source dissolved concentration and mass of the contaminant species, respectively. The solution of (3.1) with the power function (3.2) can be used to estimate the time-dependent depletion of the source zone mass by dissolution. The time-dependent mass is then used in (3.2) to calculate the time-dependent source discharge. This model can simulate a wide range of source responses to mass loss, depending on the value of Γ . The effect of this parameter is discussed in Parker and Park (2004), Zhu and Sykes (2004) and Falta et al. (2005a), but an important special case

occurs when $\Gamma=1$, and the source contaminant mass and discharge are linearly related. As will be shown, $\Gamma=1$ may be a good approximation for modeling source behavior at sites contaminated with gasoline. If (1) and (2) are solved with $\Gamma=1$, the source discharge and mass decline exponentially with time (49, 51, 69).

Gasoline is a multicomponent LNAPL. It can be shown that to a reasonable approximation, components of a multicomponent NAPL will weather out of the NAPL according to a first order process. Assuming linear equilibrium phase partitioning, the following partition coefficients are defined:

$$K_{pnw} = \frac{C_n}{C_w}; \quad (3.3)$$

$$H = \frac{C_g}{C_w}; \quad (3.4)$$

$$K_D = \frac{X_s}{C_w} \quad (3.5)$$

where K_{pnw} is the NAPL-water partition constant, C_n is the mass concentration of the component in the NAPL, C_w is the aqueous mass concentration of the component, H is the dimensionless Henry's constant, C_g is the mass concentration in the gas phase, K_D is the soil water distribution coefficient, and X_s is the mass fraction adsorbed to soil. The NAPL-water partition coefficient, K_{pnw} can be calculated assuming Raoult's law, using the component and mixture molecular weights, the NAPL density, and the component pure solubility (14):

$$K_{pnw} = \frac{M_{wt} \rho_n}{M_{wt}^{ave} C_w} \quad (3.6)$$

where M_{wt} is the compound's molecular weight, ρ_n is NAPL density, M_{wt}^{ave} is the average molecular weight of the NAPL, and \bar{C}_w is the component's pure solubility in water. The total concentration (C_T) of the gasoline component is defined as follows:

$$C_T = \phi S_w C_w + \phi S_g C_g + \phi S_n C_n + \rho_b K_D C_w \quad (3.7)$$

where ϕ is porosity, S_w is water phase saturation, S_g is gas phase saturation, S_n is NAPL phase saturation, and ρ_b is bulk soil density. For a multicomponent NAPL with linear phase partitioning, C_T is a linear function of any phase concentration. The mass balance on a control volume containing soil, gas, water, and NAPL, with gas and water flushing, and first order aqueous phase decay of the species leads to a differential equation:

$$V \frac{dC_T}{dt} = -Q_w C_w - Q_g C_g - \nabla \phi S_w C_w \lambda \quad (3.8)$$

Where V is the volume of the system, Q_w and Q_g are the water and gas flushing rates (volume per time), and λ is the pseudo first order decay rate. C_T can be defined in terms of the aqueous concentration using the phase partitioning relationships in equations (3.3), (3.4), and (3.5):

$$C_T = (\phi S_w + \phi S_g H + \phi S_n K_{pmw} + \rho_b K_D) C_w = K_w^* C_w \quad (3.9)$$

If the phase saturations and partition coefficients are constant, then K_w^* is constant.

Substituting, we get:

$$\frac{dC_w}{dt} = - \left(\frac{Q_w + HQ_g}{K_w^* V} + \frac{\phi S_w \lambda}{K_w^*} \right) C_w = -k_s C_w \quad (3.10)$$

So, for constant phase saturations and partition coefficients, NAPL weathering is a first order decay process with an exponential decay solution:

(3.11)

with a source decay rate of k_s . The source decay rate is a measure of processes such as dissolution, volatilization, and aqueous phase biodegradation that over time remove the LNAPL component from the source zone. Since all of the concentrations are linearly related, they will all decline exponentially, with the same source decay rate coefficient:

$$\frac{C_w}{C_{w,0}} = e^{-k_s t} \quad (3.12)$$

Therefore, this equation can be used to model NAPL composition, soil mass fractions, and dissolved concentrations in the source zone. Because the decay of the source zone is exponential, it can thus be assumed that Γ is equal to 1 in Equation (3.2). If the only depletion process taking place in the source zone is aqueous dissolution of the LNAPL component, then using Equations (3.1) and (3.2) (or Equation 3.10 with no gas flushing or biodegradation) leads to an exponential decay solution:

$$C_s(t) = C_o e^{-\frac{QC_o}{M_o} t} \quad (3.13)$$

and

$$M(t) = M_o e^{-\frac{QC_o}{M_o} t} \quad (3.12)$$

The REMChlor code simulates source depletion by dissolution, first order decay (by biological or chemical processes), and aggressive source remediation. Aggressive source remediation involves removing a large fraction of the source mass in a short period of time. REMChlor simulates this by simply rescaling the source zone mass, M , to reflect the fraction of the source that was removed. Then the source concentration, C_s , is recalculated using the power function defined by equation (3.2), and the mass balance

equation (3.1) is solved using these new values as the initial condition. Full details of this source model are given in (23) and (20).

The REMChlor model also includes an analytical model capable of simulating plume remediation of compounds that is variable in space and time (22). This plume model can consider independent variations in parent and daughter compound decay rates and yield coefficients in the plume. The plume model is based on a distance-time plot for the plume behavior (Figure 3.1). Here, distance is the distance downgradient of the LNAPL source, and time is the time since the LNAPL release. The distance-time domain is divided into 9 “reaction zones”, where the contaminant first order decay rates are independently specified. Thus the code can simulate temporal and spatial changes in the contaminant decay rate that arise from natural and enhanced plume biodegradation. These space-time reaction zones are described in more detail below.

3.4 Simulation Development

The conceptual plume model employed here incorporates three spatial zones. The first, termed zone 1, is found directly downgradient from the contamination source (a leaking UST or former tank excavation), and is characterized by high dissolved phase concentrations of EDB, 1,2-DCA, and BTEX (Figure 3.2). At sites where historic releases of leaded gasoline are commingled with later releases of unleaded fuel, oxygenates such as MTBE may also be present. In zone 2, dissolved phase concentrations decline by orders of magnitude at varying distances downgradient from the source depending on site conditions. Both zones 1 and 2 are assumed to be anaerobic, given that available oxygen is depleted quickly by an abundance of fuel hydrocarbons, some of

which can serve as electron donors in anaerobic dehalogenation processes (57). Finally, low concentrations (but above the MCL) of EDB and 1,2-DCA may exist in the downgradient portion of the plume, though BTEX compounds may not be present, given that these compounds tend to be more biodegradable in the aerobic setting (57) (Figure 3.2). The downgradient zone is usually aerobic, and is termed here zone 3.

We consider two extremes in UST plume behavior. At sites where natural attenuation processes are robust, EDB and 1,2-DCA plumes are likely to be short, but at other sites, long plumes of either or both contaminants may exist (Figure 3.2). The short plume simulations are based on a site in Clemson, SC where EDB and 1,2-DCA plume extent is limited. In June 2005, three soil borings were advanced at the Former Clemson Tiger Mart in zones 1, 2 and 3, and soil and groundwater collected for the purpose of establishing laboratory microcosms (34). This site sold leaded gasoline and various formulations of unleaded gasoline until the tanks were removed in 2000 (7). Subsequent groundwater investigations revealed high levels of EDB, 1,2-DCA, BTEX, and MTBE downgradient of the source zone. Concentrations of EDB and 1,2-DCA are approximately 300 µg/L and 800 µg/L respectively in this area. High part-per-million concentrations of BTEX and MTBE are present in ground water in zone 1. The presence of MTBE is attributable to a later release of unleaded fuel, since this compound would not have been present in the original release of leaded fuel. Over the next 10 meters downgradient, concentrations are attenuated by one to two orders of magnitude (zone 2). Site lithology at the Former Clemson Tiger Mart consists of poorly sorted sand, clay and silt (7) with a groundwater Darcy velocity is approximately 10 meters per year.

In anaerobic laboratory microcosms, EDB was observed to degrade to its low MCL of 0.05 µg/L in the presence of 1,2-DCA and fuel hydrocarbons (34). However, 1,2-DCA was not significantly biodegraded. Biodegradation of BTEX was also observed in the anaerobic microcosms. The addition of lactate greatly stimulated biodegradation of EDB, but had no apparent effect on 1,2-DCA in the microcosm experiments. The addition of lactate yielded mixed effects in the case of the BTEX compounds. Table 3.1 summarizes pseudo first order decay rates derived from incubating the microcosms from 284 to 380 days for EDB, 1,2-DCA, and benzene. These laboratory-derived biodegradation rates are used in the present study and are assumed to be representative of in-situ rates at similar UST sites. Aerobic degradation rates for benzene, and aerobic and anaerobic degradation rates for MTBE were taken from Schmidt et al. (2003) (Table 3.1).

The second set of simulations is based on a site where long EDB plumes have been extensively delineated. The Massachusetts Military Reservation (MMR) is situated on Cape Cod, and has been in operation since 1911, providing mechanized and aircraft training for the Army and Air Force. A total of four EDB plumes exist at MMR, ranging in length from 1,400 to 2,400 meters (21). Concentrations of EDB detected in the subsurface at MMR range from 0.071 to over 600 µg/L (21). Geology at MMR is comprised of glacial deposits characterized by fine to coarse sands and groundwater seepage velocity ranges from 100 to 200 meters per year (21). Concentrations of EDB in several of these plumes have declined little, which would indicate that natural attenuation processes are not effective at limiting the transport of EDB (12). Based upon available groundwater concentrations of EDB in one of the plumes at MMR, the computed EDB

in-situ degradation rate at MMR was estimated at 0.04 yr^{-1} , or a half-life of approximately 18 years (24).

Table 3.2 compares parameters used to model the short plume and long plume scenarios. A catastrophic release of 18,927 liters (5,000 gallons) of leaded gasoline is assumed to have occurred in 1987, which is roughly when leaded gasoline was phased out of existence in the US. This release would have contained EDB, 1,2-DCA and BTEX, but not MTBE. A second, smaller release of 3,785 liters (1000 gallons) will be modeled ten years afterwards (in 1997). Such a release could have resulted from an overfill or localized piping leak, and it would have contained MTBE and BTEX, but not EDB and 1,2-DCA, since only unleaded gasoline was marketed at this point. Benzene is thus the only contaminant of concern that is common to both releases. Both releases would have contained other hydrocarbons that will not be simulated here (although they could contribute to the formation of the anaerobic zone geometry).

Basic simulation parameters for the short and long plume cases are similar for most parameters, save for groundwater Darcy velocity, which is assumed in the long plume case to be double (20 m/yr) the value of the short plume case (10 m/yr), and for the source zone dimensions (Table 3.2). It is to be expected that faster groundwater velocity will form longer plumes. Small transverse and vertical dispersivities of 0.05 and 0.005 meters, respectively, are selected to emphasize contaminant destruction and removal effects on the plumes, rather than dilution effects. In REMChlor, longitudinal dispersivity is scale dependent, and is calculated as

$$\alpha_x = \frac{1}{2} \left(\frac{\sigma_v^2}{\bar{v}^2} \right) \bar{x} \quad (3.13)$$

where α_x is longitudinal dispersivity, σ_v/\bar{v} is the ratio of pore velocity standard deviation to the mean pore velocity, and \bar{x} is the average of the front location at a given time (22). A σ_v of 0.1 produces a longitudinal dispersivity of 1/200 the travel distance, and this value is used here.

EDB and 1,2-DCA concentrations in gasoline ranged from about 0.3 g/L before the 1970s to around 0.07 g/L at the time leaded gasoline was banned (24). The lower value is selected here because it was assumed that the first release occurred in 1987, when leaded gasoline was phased out of existence and concentrations of the lead additives were at their lowest. This would produce a total mass of 1.3 kg of EDB and 1,2-DCA in the subsurface if 18,927 liters (or the entire contents of a 5,000-gallon UST) were released. Historical releases of leaded gasoline that occurred prior to the late 1980s would have contained higher concentrations of EDB and 1,2-DCA, which would result in proportionately greater EDB and 1,2-DCA mass in the subsurface, so in this respect the selection of lower concentrations used in these simulations is conservative. Benzene concentrations in leaded and unleaded gasoline have also varied over time (63). In release 1, a two percent benzene content by mass in leaded gasoline was assumed, producing a benzene concentration of 13 g/L (21), or a total mass of benzene of 246 kg released into the subsurface. For the second, smaller release in 1997, benzene concentrations would have been different, and probably lower. Based on data from (63), a benzene concentration of 3.8 g/L was used for the smaller 1997 release, producing 14 kg of benzene mass added to the source. The addition of benzene from the second release was

modeled additively; the source mass of benzene at the point of the second release equals residual mass from the first release at that time plus the mass attributable to the second release. This resulted in an increase in benzene concentration discharging from the source zone at the time of the second release. Modeling the benzene release in this fashion will mimicked the effects of multiple releases at UST sites. MTBE concentration in the gasoline at the time of the second release was taken from data characterizing conventional fuel marketed in 1997 in Charleston, SC (63). Using a concentration of 13.8 g/L (1.8% by mass), a 1,000 gallon release would result in 52 kg of MTBE in the source zone. We note that reformulated gasolines that were used in many parts of the country could contain as much as eight times this amount of MTBE.

For release 1, cross-sectional (perpendicular to flow) source zone dimensions of 10 meters wide by 3 meters deep were specified in REMChlor. Dissolution of source mass occurs when groundwater flux discharges from this 30 square meter area, but the total volume of gasoline resulting from the releases would be dispersed throughout the subsurface, as calculated by the equation

$$V_{tot} = \frac{V_n}{\phi S_n} \quad (3.14)$$

where V_{tot} is the contaminated volume of soil in the subsurface, V_n is the volume of NAPL (18,927 liters, or 18.9 m³), ϕ is porosity (assumed to be 0.35), and S_n is NAPL saturation (assumed to be 0.3). This calculation yields a total contaminated volume of 180 m³. The 1997 release was assumed to be one-fifth the volume of the first release, so benzene and MTBE mass from this release would likely spread over a smaller volume. If the flux plane is 30 meters squared for the first release, then the second release might

discharge through a flux plane of 6 meters squared. Aqueous concentrations are highest immediately downgradient of the source, and can be estimated using gasoline-water partition constants (Table 3.3). It is unlikely that field scale groundwater concentrations downgradient of the NAPL source would be this high due to mixing and dilution with clean groundwater (24), and therefore, initial groundwater concentrations in the NAPL source zone are assumed to be half of the highest concentrations that might be expected due to equilibrium with the NAPL source. On this basis, calculated initial source concentration of EDB and 1,2-DCA would be 230 µg/L and 417 µg/L, respectively. Similarly, modeled initial source benzene concentrations of 18,571 µg/L and 5,441 µg/L were calculated for releases 1 and 2 respectively. The initial MTBE source concentration was 446,528 µg/L. As noted earlier, these source concentrations (C_s) will tend to decline exponentially as groundwater flows through the source zone. Retardation coefficients for the 4 contaminants were calculated assuming an organic carbon fraction of 0.001 (62). Of the four compounds modeled here, benzene is the most retarded in groundwater (1.24), while MTBE is the least (1.02) (Table 3.3), and, as a whole, retardation plays a relatively small role in the transport of these compounds.

Following the conceptual model, natural attenuation biodegradation rates from the laboratory microcosms were applied to zones 1, 2 and 3 for the short plume scenario (Table 3.1). Rates utilized in the short and long plume case were identical through zones 1 and 2, but an arbitrarily selected low rate of 0.5 yr⁻¹ was assigned to both EDB and 1,2-DCA in the aerobic zone (zone 3) for the long plume case.

It should be noted that for EDB, the assumed aerobic decay rate for the long plume scenario is much higher than the rate of 0.038 yr^{-1} estimated at the MMR site (24). Similarly low aerobic rates have been inferred for 1,2-DCA based on UST field data (25). In this respect, use of these rates are conservative, since they will result in faster simulated aerobic decay than that evident at some sites. Aerobic rates for benzene and MTBE, and anaerobic rates for MTBE, are taken from Schmidt et al. (2003), as summarized in Table 3.1. The MTBE aerobic rate (8.0 yr^{-1}) selected for the short plume case is a rough median of values reported in Schmidt et al. (2003). The long plume aerobic rate (0.365 yr^{-1}) is the lowest aerobic rate cited in Schmidt et al (2003). Anaerobic rates for natural attenuation and biostimulation are the low and high ends of the range observed by Wilson et al (2000) in a field study, as reported in the Schmidt et al. (2003) survey.

A total of four remediation scenarios are presented for both the short and long plume case:

- (1) *Natural attenuation of both the LNAPL source and the plume.* Natural attenuation was modeled by incorporating biodegradation rates from Clemson University microcosms over nine spatial-temporal plume zones (Figure 3.1, Table 3.1). The purpose of these simulations is to illustrate the behavior of each of the modeled compounds at UST sites in the absence of remediation, thereby permitting a point of comparison for remedial simulations.
- (2) *Aggressive LNAPL source remediation with natural attenuation of the plume.* The effects of LNAPL source remediation were modeled to determine how such a

remedial action might decrease the extent of the EDB, 1,2-DCA, benzene and MTBE plumes. An assumed 90% removal of residual LNAPL source mass was modeled 20 years after the first release (i.e. in 2007) as a one-time event. It should be noted that REMChlor can simulate removal of any fraction of the source over any time frame (20). Prior to the source remediation effort, the system underwent only natural attenuation, as in scenario (1), above

- (3) *Natural attenuation of the LNAPL source with enhanced biodegradation in the plume.* Given EDB's positive response to lactate addition in laboratory microcosms (Henderson et al., 2008), the second set of remedial simulations explore plume remediation through biostimulation. This would involve providing electron donor to microorganisms through direct injection or some other in-situ delivery method. Degradation rates achieved in microcosms through addition of lactate were used (Table 3.1) and are thus assumed to be uniformly achievable at the field scale. Lactate would be applied in 2007 for five years (i.e., from 20 to 25 years after the initial release) in the anaerobic areas of the plume (zones 1 and 2), where abundant fuel hydrocarbons rapidly deplete available oxygen (57). Accelerated biostimulation would occur in near downgradient areas of the source but not in downgradient aerobic portions of the plume. Figure 3.2 provides a graphical comparison of the location of biostimulated zones within short and long plumes, showing clearly that as a percentage of total plume area, biostimulation occurs over a very small portion of the long plume case, relative to the short plume case.

(4) *Aggressive LNAPL source remediation combined with enhanced plume biodegradation.* The combined effects of source removal and biostimulation were simulated, following the methods described above. The purpose of these simulations is to determine the benefit of applying both partial source removal and plume remediation at UST sites, relative to relying on one or the other technique. It is anticipated that this will permit a determination of the maximum benefits that might be expected through the best possible use of remedial technology at UST sites.

3.5 Results

The simulations demonstrate how the impact of source and/or plume remediation of each contaminant varies over time throughout the plume. To facilitate comparison of the modeled compounds, concentrations are normalized by dividing by the applicable standard (i.e., the MCL) and evaluating how this ratio (termed here “relative importance”) changes over time along the plume center line. Relative importance can be considered a surrogate indicator of the risk posed by each compound. Federal MCLs exist for EDB ($0.05 \mu\text{g/L}$), 1,2-DCA and benzene ($5.0 \mu\text{g/L}$), but not for MTBE, for which the US EPA Region 9 drinking water Preliminary Remediation Goal (PRG) ($11.0 \mu\text{g/L}$) is used as an applicable regulatory standard (59).

Figure 3.3 presents the relative importance of EDB, 1,2-DCA, benzene, and MTBE over 100 years in the short plume natural attenuation case at three points within the plume: a) 0 meters (discharging source concentrations), b) 15 meters downgradient of the source zone, and c) 25 meters downgradient of the source zone. Over time, concentrations discharging from the source zone (Figure 3.3a) change according to

equation (3.11), and since Γ is assumed to be 1, the relationship between source discharge and source mass is linear.

At the time of release 1 (1987), the ratio of source discharge concentrations of EDB and benzene to their MCLs is similar (4,600 and 3,714 times, respectively). Though discharging concentrations of EDB are lower, so too is its MCL when compared to benzene's. By contrast, 1,2-DCA discharges from the source at an initial concentration that is 83 times its MCL ($5.0 \mu\text{g/L}$). The second release (in 1997) adds benzene mass to the source, increasing its concentration and relative importance (Figure 3.3a). MTBE is a constituent of the second release but not the first. Given its higher solubility, it exceeds the applicable standard ($11.0 \mu\text{g/L}$) 40,581 times, more than both EDB and benzene at the time of its release. Figure 3.3a demonstrates how the source strength varies as a function of time under natural dissolution conditions; this process depends on the dissolution characteristics of each contaminant. Compounds that have high aqueous solubility can be expected to wash out of the source zone quickly. This characteristic of source strength (23) has its mathematical expression in the exponent of equation (3.11). If the initial concentration (C_o) is large relative to the initial mass, the magnitude of the negative exponent is larger, producing accelerated source dissolution. Near UST source zones where more recent releases of conventional unleaded fuel occurred, MTBE may be a regulatory driver, but this condition will tend to be short-lived based upon its dissolution characteristics. EDB and benzene attenuate from the source more slowly, exceeding applicable standards in 2087 by 27 and 540 times respectively, 100 years after the initial

release of leaded gasoline. In contrast, 1,2-DCA and MTBE do not exceed their respective screening values after 2034 and 2019, respectively.

Figure 3.3b portrays relative importance 15 meters from the source, at the end of the anaerobic portion of the plume. Because EDB was assigned a higher decay rate in the anaerobic zone, its relative importance decreases somewhat compared to benzene at this location. The MTBE concentration drops quickly because of its short residence time in the source zone. EDB and 1,2-DCA are much less biodegradable in the aerobic zone than benzene and they appear to have first order decay rates roughly similar to MTBE. Figure 3.3c shows relative importance 25 meters downgradient of the source, or ten meters into the aerobic zone. At this location, the benzene plume has completely attenuated below its MCL concentration, and the plume risk is dominated by EDB concentrations except for a brief period where MTBE concentrations are high. EDB requires 96 years to decline below its MCL 25 meters downgradient of the source zone; 39 years would be required for 1,2-DCA to degrade to its MCL at the same location. This suggests that EDB (and to a lesser degree, 1,2-DCA) are likely to be regulatory drivers where aerobic conditions predominate. While EDB requires nearly 100 years to decline below its MCL 25 meters downgradient of the source, MTBE drops below its regulatory standard in 13 years at this location. Longer-lasting MTBE plumes result if lower aerobic rates are used. For example, if a rate of 4.0 yr^{-1} is used instead of 8.0 yr^{-1} , 16 years are required to attenuated MTBE at 25 meters downgradient to below its PRG.

Relative importance is presented for the long plume case at 0, 200 and 500 meters (Figures 3.4a, 3.4b, and 3.4c, respectively). At the time of release (1987) the ratio of

source discharge concentrations of EDB (4,600) and benzene (3,714) is identical to the short plume case. Darcy velocity used in long plume simulations is twice that of the short plume case, and since higher groundwater flow through the source area accelerates dissolution of the source, source discharging concentrations are sustained for a shorter period of time. However, at the time of release, this difference has not yet impacted the dissolution profile, and so the relative importance of the modeled compounds is the same for both the short and long plumes. Over time, the relative importance of the compounds declines more quickly than in the short plume case. EDB concentrations in groundwater discharging from the source drop below the MCL in 2067 (80 years after release 1). By comparison, the short plume requires 161 years to do so at the same point in space. Likewise, benzene, MTBE, and 1,2-DCA require shorter timeframes to discharge at concentrations below their respective screening levels in the long plume. Benzene is attenuated in 2177 (190 years after release 1) to below its MCL, but in the short plume case, 340 years are required. 1,2-DCA and MTBE decline below their respective screening values in 25 and 12 years, respectively, compared to 48 and 22 years in the short plume case (Figure 3.3a and 3.4a).

Higher groundwater flow and low aerobic plume degradation rates increase relative importance farther away from the source in the long plume, and this relationship is portrayed at 200 and 500 meters in Figure 3.4b and 3.4c, respectively. Benzene does not appear because it is degraded below its MCL by plume aerobic biodegradation prior to 200 meters. EDB presents the most sustained risk at 200 meters, persisting above its MCL for 62 years (2049). 1,2-DCA and MTBE exceed their applicable standards until

2010 and 2012, respectively. Only EDB and MTBE are detected 500 meters downgradient of the source (Figure 3.4c). Though 1,2-DCA is present 200 meters downgradient, the plume degradation rate of 1.46 yr^{-1} is sufficient to attenuate its concentration to below the MCL before 500 meters. At 500 meters, EDB persists until 2024, MTBE until 2012.

Given the range of behaviors detailed above, contaminant response to remediation varies significantly. Table 3.4 summarizes the maximum plume center line extent above applicable regulatory standards in 2012 (25 years after release 1) and 2017 (30 years after release 1). These times do not necessarily correspond to maximum plume lengths for the various compounds, but were selected in order to be able to compare the future effect of actions taken in 2007. The maximum plume lengths for EDB and 1,2-DCA occurred well before this date.

The effect of natural attenuation processes on plume length is portrayed in plume centerline plots for EDB, 1,2-DCA, benzene and MTBE in the short and long plume cases in 2012, 25 years after release 1 (Figures 3.5 and 3.6, respectively). The MCLs of the compounds are shown as horizontal dashed lines, and markers suspended above the plots represent the start of zones 1, 2, and 3. Under natural attenuation short plume conditions, EDB and 1,2-DCA have roughly the same extent in 2012 (54 and 52 meters, respectively), while benzene and MTBE have shorter plume lengths due to their higher aerobic decay rate in this case (Figure 3.5). As discussed above, benzene is completely biodegraded at the start of the aerobic zone, extending no further than 17 meters, indicating that even where multiple historic releases have occurred, benzene plumes are

likely to be short at sites where aerobic conditions predominate in downgradient areas of the plume. MTBE is less biodegradable aerobically than benzene, but the rate (8.0 yr^{-1}) is still high in this case so it extends a short distance into the aerobic zone. If a rate of 4.0 yr^{-1} is used instead, MTBE plume length in 2012 is 27 meters; under this scenario, it attains a maximum plume length of 76 meters within four years of its release. Comparing the plume lengths in 2012 to the plume lengths in 2017 (Table 3.4), one could conclude that the EDB and benzene plumes are stable, while the 1,2-DCA and MTBE plumes are shrinking.

As discussed above, short and long plume simulations are differentiated by aerobic rate (lower rates are used for the long plume case, Table 3.1) and groundwater flow (lower Darcy velocity is used for the short plume case, Table 3.2), with the expectation that these differences will produce markedly different plumes lengths. This effect is most striking in the case of EDB, which in the long plume simulations extends downgradient 605 and 535 meters in 2012 and 2017, respectively (Figure 3.6) (Table 3.4). In contrast to EDB, 1,2-DCA centerline extent above its MCL in 2012 is zero. Higher groundwater velocity produces more flushing of the source zone, and since both 1,2-DCA's solubility and MCL are higher than EDB's, this compound dissolves away more quickly. However, this also means that longer plume lengths of these compounds result at earlier timeframes, which is not reflected in Table 3.4. For example, 1,2-DCA achieves a maximum plume length of approximately 400 meters in 1995, 8 years after the release. The lower aerobic rate also produces a longer benzene plume (Figure 3.6) (57 and 56 meters in 2012 and 2017, respectively), but like 1,2-DCA, MTBE washes out of

the source zone before 2012. When combined with its low aerobic rate (0.365 yr^{-1}) (Table 3.1), MTBE's source dissolution profile produces complete separation of the MTBE plume. In 2012, MTBE concentrations above $11 \mu\text{g/L}$ occur between 620 and 915 meters downgradient of the source, peaking at a concentration of $29 \mu\text{g/L}$ (Figure 3.6). A maximum MTBE extent of approximately 935 meters occurs 16 years after release 2.

3.5.1 Source Remediation Case

The effect of removing 90% of the LNAPL source is portrayed in plume centerline plots for EDB, 1,2-DCA, benzene and MTBE in the short and long plumes (Figures 3.7 and 3.8, respectively), and both natural attenuation and source removal results are shown for the sake of comparison. Results are portrayed in 2012 because this provides time (five years) for the effects of source remediation to propagate downgradient of the source. Given that Γ in equation (3.2) equals 1.0, 90% source removal produces a like decrease in concentrations discharging from the source zone. Five years after the removal, the extent of EDB has dropped from 54 to 37 meters, though EDB concentrations continue to discharge from the source zone several orders of magnitude above the MCL. By contrast, source removal lowers concentrations of 1,2-DCA to below its MCL throughout the plume in the short plume case. Partial source depletion has negligible impact on benzene extent, which is more effectively limited by its high aerobic biodegradation rate, but does shorten MTBE maximum extent from 21 to 15 meters in 2012. In 2017, MTBE does not occur above the regulatory standard with source removal (Table 3.4).

The effects of 90% source removal in the long plume case are portrayed in 2012 (Figure 3.8). The maximum extent of EDB is the same in 2012 as in the natural attenuation case (605 meters), given that insufficient time has elapsed for reduced concentrations to propagate downgradient. Over longer timeframes the reduced concentrations caused by source removal continue to propagate downgradient, shortening the length of the plume from 535 to 265 meters ten years after the removal (Table 3.4). Though this represents roughly a 50% reduction in plume extent, longer plumes will require significant timeframes to realize the benefits of source depletion in downgradient plume zones. No removal would be necessary for 1,2-DCA and MTBE because both are attenuated by dissolution of the source in the long plume case. In other words, source removal that occurs 20 years after a release will not lessen the impact of compounds like 1,2-DCA, whose maximum extent occurs earlier, or MTBE, which forms a detached plume that is logically not affected by a source removal action. Benzene extent is shortened from 57 to 42 meters in 2012 and 56 to 41 meters in 2017 (Figure 3.8, Table 3.4).

3.5.2 Biostimulation Case

In the short plume case, biostimulation yields similar results to partial source removal for EDB (Figure 3.9). Biostimulation produces accelerated decline in plume concentration relative to the natural attenuation case, as evidenced by the steeper slope of the biostimulated trend line. This contrasts with the partial source removal case, in which EDB concentrations discharging from the source zone are 90% lower initially, while plume concentrations decline at the same rate (i.e., the slopes of the natural attenuation

and source removal trend lines are parallel). The maximum extent of EDB above its MCL in 2012 in the biostimulated short plume is 41 meters, compared to 37 meters in the 90% source removal case (Table 3.4). Unlike partial source removal, lasting change in plume concentrations is not achieved through biostimulation because source mass is unaffected. Upon cessation of biostimulation in 2012, plume concentrations begin to return to natural attenuation conditions, and by 2017, the EDB extent matches the natural attenuation case (52 meters) (Table 3.4). Therefore, in this case, biostimulation is capable of shortening plume length, but only so long as it is actively applied. In laboratory microcosms, addition of lactate had little effect on 1,2-DCA, and as a consequence, little change in maximum 1,2-DCA extent is evident in biostimulation simulations (Figure 3.9). Likewise, biostimulation does not alter the maximum extent of the benzene plume, though MTBE plume extent is shortened from 21 to 15 meters in 2012. Like EDB, MTBE plume extent returns to natural attenuation conditions in 2017, upon cessation of biostimulation (Figure 3.9, Table 3.4).

Figure 3.10 shows the effects of biostimulation on EDB in the long plume case. Temporary reductions in EDB concentrations are achieved by 2012, but they are limited in extent (by the advective velocity of the plume), and concentrations remain an order of magnitude above the MCL. In 2017 (not shown) concentrations of EDB return to pre-biostimulation concentrations in the near-downgradient portions of the plume, but by this time reduced concentrations brought on by biostimulation have moved into the far downgradient portions of the plume, decreasing maximum plume extent from 535 to 408 meters (Table 3.4). This represents a 24% reduction in plume extent, compared to the

roughly 50% reduction that was achieved in the source removal case. However, for reasons stated above, the EDB plume would begin to lengthen and eventually stabilize at natural attenuation length once biostimulation ceases. Given the similarity of benzene natural attenuation and biostimulation rates, there is negligible difference in their plume extent (Table 3.4). No remediation would be necessary for 1,2-DCA since it attenuates below the MCL by 2012. As discussed above, MTBE forms a detached plume between 600 and 900 meters downgradient in the long plume case, but this would logically not be affected by plume biostimulation that only extends 15 meters from the source.

3.5.3 90% Source Removal + Biostimulation

Figures 3.11, 3.12 and 3.13 present results of applying 90% source removal in 2007 and simultaneously biostimulating with lactate from 2007 to 2012. Figure 3.10 shows plume extent in the short plume case in 2012. The combined action of partial source removal and biostimulation effectively halves the maximum extent of EDB to 21 meters in the short plume case (Figure 3.11). An immediate 90% reduction in concentrations discharging from the source zone is achieved through source depletion, but additional plume destruction occurs for 15 meters downgradient of the source. Biostimulation ceases in 2012, and as a result EDB extent in 2017 (not shown) matches that of source removal alone (35 meters) (Table 3.4). Because 1,2-DCA and benzene did not respond to lactate addition in the laboratory, the results of these simulations were not substantially different from those in which source removal alone was evaluated (Table 3.4). Source depletion and biostimulation together reduce MTBE extent to six meters in 2012 (Figure 10) and 0 meters in 2017 (Table 3.4).

More extensive timeframes are necessary for the benefits of remediation to propagate downgradient in long plumes, so maximum plume extent is presented within five (i.e., in 2012) and ten (i.e., in 2017) years of the onset of remediation (Figures 3.11 and 3.12, respectively). Partial source depletion and plume remediation together are not sufficient to reduce concentrations of EDB to its MCL at any point in the plume within five years of the start of remediation. However, ten years after the onset of remediation, reduced concentrations brought on by remediation have had sufficient time to propagate farther downgradient, shortening the plume to 239 meters, or a 55% reduction. This represents only a 10% percent improvement relative to applying source removal alone, indicating that biostimulation over relatively short distances and timeframes will yield little additional benefits at sites where long plumes of EDB exist. Little additional benefits results for 1,2-DCA and benzene (Figures 3.12 and 3.13) for reasons stated above. Combined source and plume remediation do not attenuate the detached MTBE plume in 2012 (Figure 3.12); in 2017, natural attenuation processes alone are sufficient to decrease MTBE plume concentrations to below 11 $\mu\text{g/L}$ (Figure 3.13).

3.6 Discussion

It is difficult to compare this evaluation to other studies, given that such an analysis has not been conducted for EDB and 1,2-DCA, and the fact that other screening level analytical models do not simulate the effects of variable source depletion and plume remediation. Relative importance, an indirect measure of the risk posed by each compound (the ratio of aqueous concentration to applicable regulatory screening value), varies by contaminant across space and time. Near UST source zones, EDB and benzene

can have similar relative importance. If later releases of unleaded gasoline occur, the relative importance of benzene (and other hydrocarbons) will increase. The relative importance of MTBE is greatest among the four compounds modeled here, but it sustains brief (but mobile) plumes, given rapid source dissolution. Plume biodegradation is not likely to significantly attenuate high MTBE concentrations, and significant detached MTBE plumes may result. To our knowledge, no studies have evaluated the co-occurrence of the lead additives and MTBE at UST sites. The relative importance of 1,2-DCA near the source zone is lowest of the four compounds due to its lower ratio of source concentration to MCL. Plume degradation rates become more important as distance downgradient of the source zone increases, and the order of relative importance may change as a result. One case in point is benzene, which has high relative importance in anaerobic near-source zones, but due to its aerobic biodegradability may not occur at all in downgradient areas. Although EDB and 1,2-DCA are aerobically biodegradable, field evidence suggests they degrade in the aerobic setting at much slower rates compared to other components of gasoline and they may persist downgradient of the source even when they are released prior to other hydrocarbons (25).

A single remedial technique may not adequately address commingled plumes of lead scavengers, hydrocarbons, and oxygenates. If equilibrium aqueous concentrations exceed regulatory standards by more than a couple of orders of magnitude, and plumes are already established, source depletion alone is unlikely to be protective. Source depletion and plume remediation together achieve roughly two orders of magnitude

reduction in EDB concentration (a 99% decrease in mass) in these simulations, although this may still not be enough to achieve its low MCL of $0.05 \mu\text{g/L}$.

Remediation will occur decades after EDB and 1,2-DCA were released to the environment, so extensive timeframes may be required for the positive effects of treatment to be realized where long plumes exist. If robust aerobic degradation occurs, benzene may degrade very quickly, but this same condition favors the persistence of EDB and 1,2-DCA. In the event plume remediation of both EDB and benzene are required, sequenced treatment may be necessary, one near the source zone that focuses on anaerobic degradation of EDB, and another downgradient where aerobic degradation of benzene can be effected without the risk of encouraging the persistence of EDB (and 1,2-DCA). Given the toxicity of EDB, it may be preferable that this compound be treated at the expense of increasing benzene transport so long as the benzene can be expected to degrade readily in downgradient aerobic zones. Such spatial considerations and sequenced plume remediation has not typically been required at UST sites. Given rapid source dissolution of MTBE, this compound may no longer be present at all at UST sites where remediation of EDB and 1,2-DCA is undertaken, despite the fact that more recent releases may have occurred.

As experience with commingled plumes of EDB, 1,2-DCA, fuel hydrocarbons, and oxygenates grows, the efficacy of source and plume remediation will improve. Plume bioremediation might be optimized by increasing the area over which it is applied, and bioaugmentation might also be implemented for 1,2-DCA, which did not respond to biostimulation with lactate in laboratory microcosms (34). Bioaugmentation may also be

used to increase anaerobic biodegradation rates for EDB, although commercial cultures for this purpose are not yet available. Where both source and plume remediation are necessary, it is unclear if source removal would perturb subsurface conditions and have negative impacts on downgradient plume bioremediation. It is important that aerobic remedial techniques for EDB and 1,2-DCA be explored at UST sites. Aerobic bioremediation may hold promise given that both EDB and 1,2-DCA serve as growth substrate under these conditions. Currently there is no S_{min} value (the minimum substrate concentration that supports growth) (54) for EDB, so it is impossible to say if aerobic biodegradation can be sustained at the very low levels necessary to attain its MCL.

Table 3.1. Comparison of First Order Biodegradation Rates (yr⁻¹)^a

Short Plume					
	Zone 1		Zone 2		Zone 3
	Natural Attenuation	Biostimulation	Natural Attenuation	Biostimulation	Natural Attenuation
EDB	1.49	5.47	5.37	9.4	3.93
1,2-DCA	1.34	0.77	0.34	0.43	1.46
Benzene	1.47	2.26	3.5	3.09	122 ^b
MTBE	2.2 ^c	5.0 ^d	2.2 ^c	5.0 ^d	8.0 ^g
Long Plume					
EDB	1.49	5.47	5.37	9.4	0.5 ^f
1,2-DCA	1.34	0.77	0.34	0.43	0.5 ^f
Benzene	1.47	2.26	3.5	3.09	9.13 ^e
MTBE	2.2 ^c	5.0 ^d	2.2 ^c	5.0 ^d	0.365 ^g

56 ^aUnless otherwise noted, rates are calculated as triplicate mean ± one standard deviation from Clemson University microcosm study.

^bBenzene aerobic biodegradation was not evaluated in the Clemson University microcosms study. This value represents the mean of surveyed field and laboratory rates in (57)

^cRate represents low value in range of anaerobic rates under methanogenic conditions reported by Wilson et al. (2000), as cited in (56)

^dRate represents high in range of anaerobic rates under methanogenic conditions reported by Wilson et al. 2000, as cited in (56)

^eValue represents the geometric mean of surveyed field and laboratory benzene first-order aerobic rates in (57)

^fArbitrarily selected low rate, based in part on Massachusetts Military Reservation EDB case described in (21)

^gRate represents low aerobic rate reported by Borden et al. 1997, as cited in (56)

^eRate represents approximate median aerobic rate from Landmeyer et al. 2001, Kane et al. 2001, Hunkeler et al. 2001, Schirmer et al. 2003, Zoekler et al. 2003, as summarized in (56)

Table 3.2. Simulation Parameters, Short and Long Plume Scenarios

Simulation Parameters	Value
Volume of release 1 (1987) ^a	18,927 L (5,000 gallons)
Volume of release 2 (1997) ^b	3,785 L (1,000 gallons)
Release 1 source depth	3 m
Release 1 source width	10 m
Release 2 source depth	2
Release 2 source width	3
Gamma (Γ)	1
Short plume Darcy velocity	10 m/yr
Long plume Darcy velocity	20 m/yr.
Porosity ^c	0.35
Coefficient of variation, velocity field	0.1
Transverse dispersivity	0.05
Vertical dispersivity	0.005
Soil bulk density ^c	1.4 g/mL
Fraction of organic carbon ^c	0.001
Spatial zone 1 (near source, anaerobic)	0 - 5 m
Spatial zone 2 (midgradient, anaerobic)	5 - 15 m
Spatial zone 3 (downgradient, aerobic)	>15 m
Time period 1 (pre-remediation)	1987 - 2007
Time period 2 (active remediation)	2007 - 2012
Time period 3 (post-remediation)	> 2012

^aRelease of leaded gasoline containing EDB, 1,2-DCA, and BTEX

^bRelease of conventional unleaded gasoline containing MTBE and BTEX

^cTaken as reasonable median value from (62)

Table 3.3. Calculation of Compound-specific Simulation Parameters

Compound	Concentration in Gasoline (g/L)	Gasoline Water Partition Coefficient	Modeled Aqueous Concentration ($\mu\text{g/L}$) ^e	Initial Source Mass (Kg)	Organic Carbon Partition Constant (mL/g)	Retardation Coefficient ⁱ
EDB	0.07 ^a	152 ^b	230	1.3 ^f	44.0 ^h	1.18
1,2-DCA	0.07 ^a	84 ^b	417	1.3 ^f	17.4 ^h	1.07
Benzene	13 ^b / 3.8 ^c	350 ^b	18,571 ^f / 5,441 ^g	246 ^f – 14 ^g	58.9 ^h	1.24
MTBE	13.8	15.5 ^d	446,528	52 ^g	6.0 ^h	1.02

^a Approximate concentration in 1984, leaded gasoline (25)

^b As reported by Falta (21)

^c Conventional unleaded gasoline, calculated from the average of available data on fuel marketed in Charleston, SC in 1997 (63)

^d Schmidt et al. (56)

^e Equal to one-half the equilibrium aqueous concentration

^f From release of 5,000 gallons of leaded fuel, 1987

^g From release of 1,000 gallons of conventional unleaded gasoline, 1997

^h USEPA(59)

ⁱ Calculated using values for porosity, fraction organic carbon content, and soil bulk density listed in Table 3.2

Table 3.4a. Maximum Extent Above MCL^a in the years 2012 and 2017, Short Plume

Simulated Scenario			Plume Length (m) ^a			
	Yr. ^b	Plume Length	EDB	1,2-DCA	Benzene	MTBE
Natural Attenuation	2012	Short	54	52	17	21
	2017	Short	52	41	15	6
90% Source Removal	2012	Short	37	0	15	15
	2017	Short	35	0	15	0
Biostimulation	2012	Short	41	53	17	15
	2017	Short	52	45	15	6
90% Source Removal + BST ^c	2012	Short	21	0	15	8
	2017	Short	35	0	15	0

Table 3.4b. Maximum Extent Above MCL^a in the years 2012 and 2017, Long Plume

Simulated Scenario			Plume Length (m) ^a			
	Yr. ^b	Plume Length	EDB	1,2-DCA	Benzene	MTBE
Natural Attenuation	2012	Long	605	0	57	911 ^d
	2017	Long	535	0	56	0 ^e
90% Source Removal	2012	Long	605	0	42	911 ^d
	2017	Long	265	0	41	0 ^e
Biostimulation	2012	Long	605	0	57	911 ^d
	2017	Long	408	0	57	0 ^e
90% Source Removal + BST ^c	2012	Long	605	0	43	911 ^d
	2017	Long	239	0	41	0 ^e

^aYr. = Plume length is defined as maximum extent above the MCL (EDB MCL = 0.05 µg/L; 1,2-DCA = 5.0 µg/L; benzene MCL = 5.0 µg/L; no MCL available for MTBE, USEPA Region 9 Tap Water Preliminary Remediation Goal = 11.0 µg/L (59))

^bYr. = Years following release

^cBST = Biostimulation

^dRapid source dissolution and low aerobic decay of MTBE in the long plume case produces detached plumes downgradient of the source.

^eDetached plume still exists, but at concentrations just below 11 µg/L.

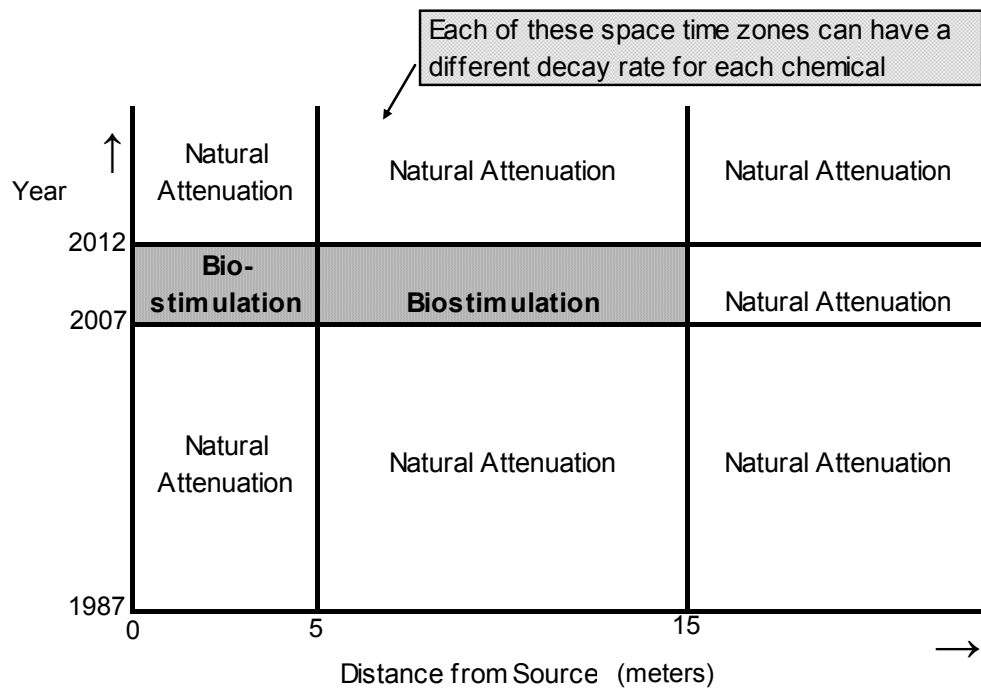


FIGURE 3.1 Distance-time plot for advective transport with multiple sets of plume reaction rates.

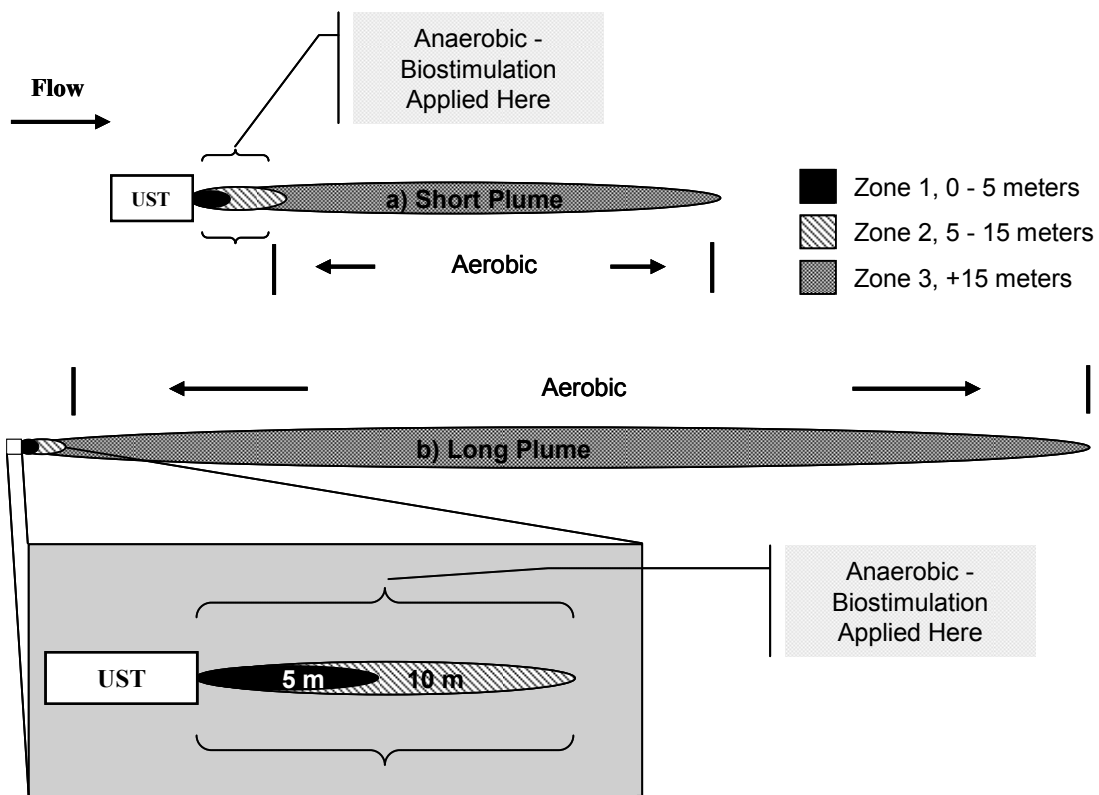


FIGURE 3.2 Site conceptual model for short and long plume cases (not drawn to scale), including biostimulation schemes

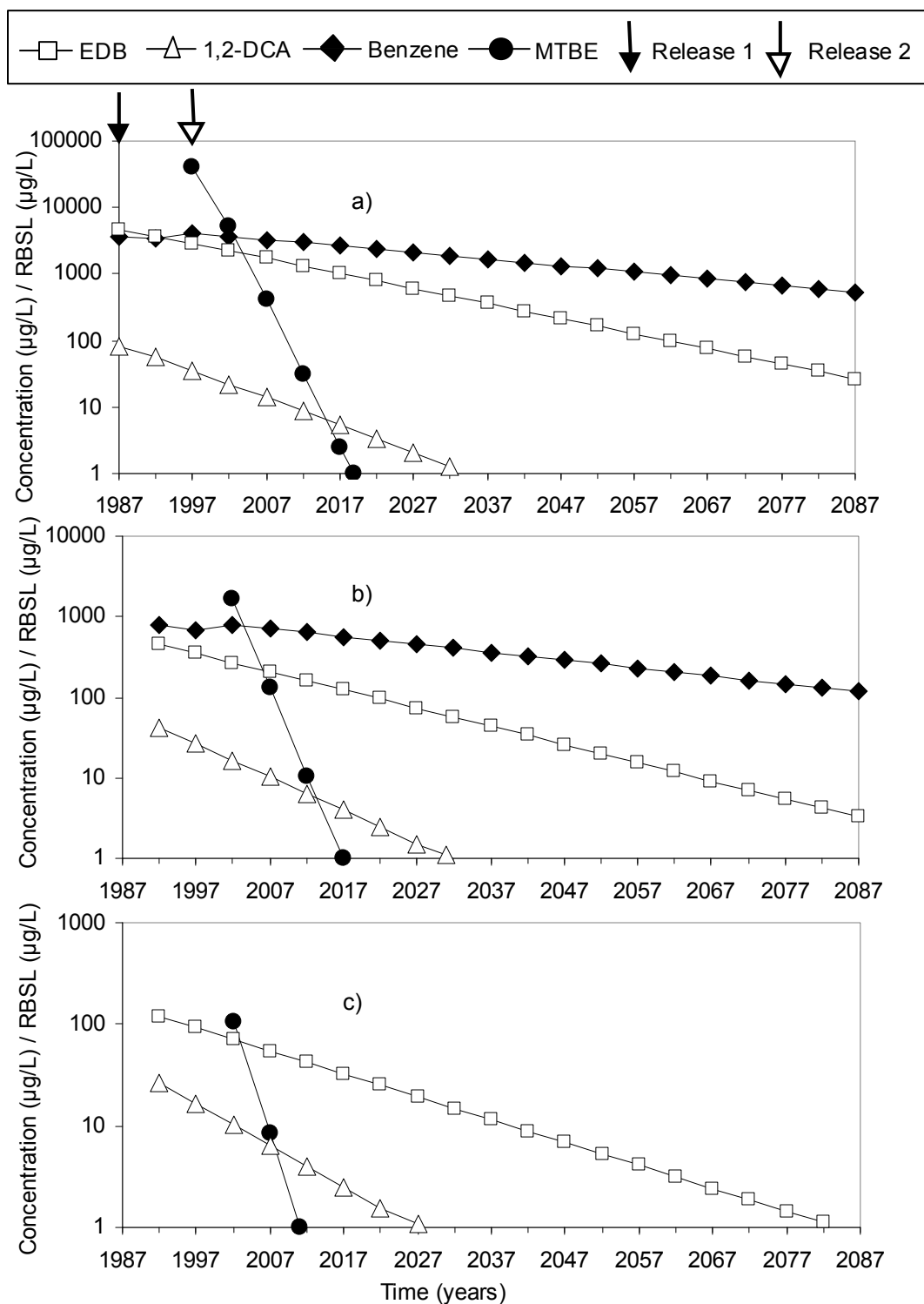


FIGURE 3.3 Short plume natural attenuation relative importance (concentration divided by risk-based screening level (RBSL)) of EDB, 1,2-DCA, benzene and MTBE at a) 0 meters, b) 15 meters, and c) 25 meters. Compounds not graphed are degraded below the RBSL.

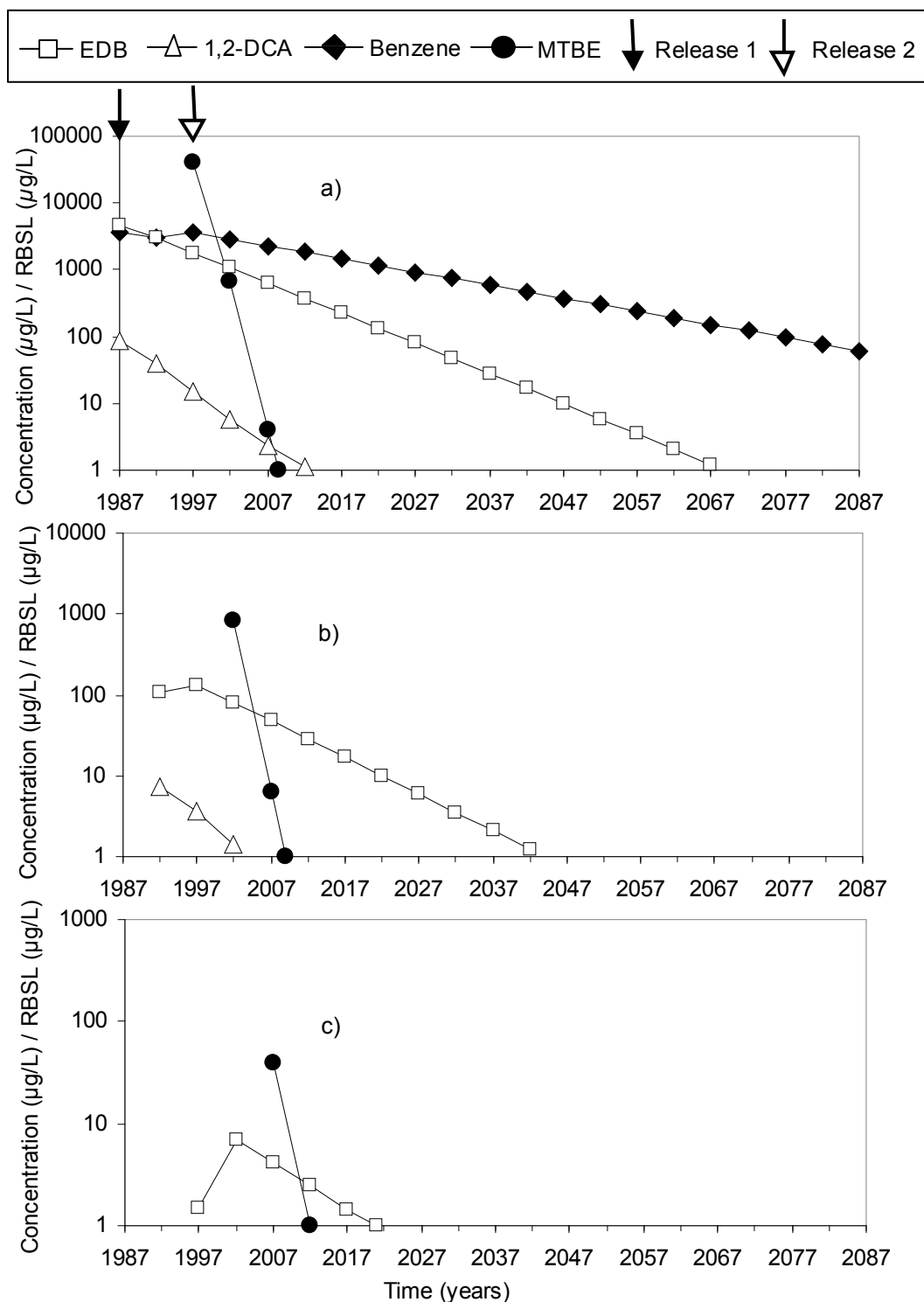


FIGURE 3.4 Long plume natural attenuation relative importance (concentration divided by risk-based screening level (RBSL)) of EDB, 1,2-DCA, benzene and MTBE at a) 0 meters, b) 200 meters and c) 500 meters. Compounds not graphed are degraded below the RBSL.

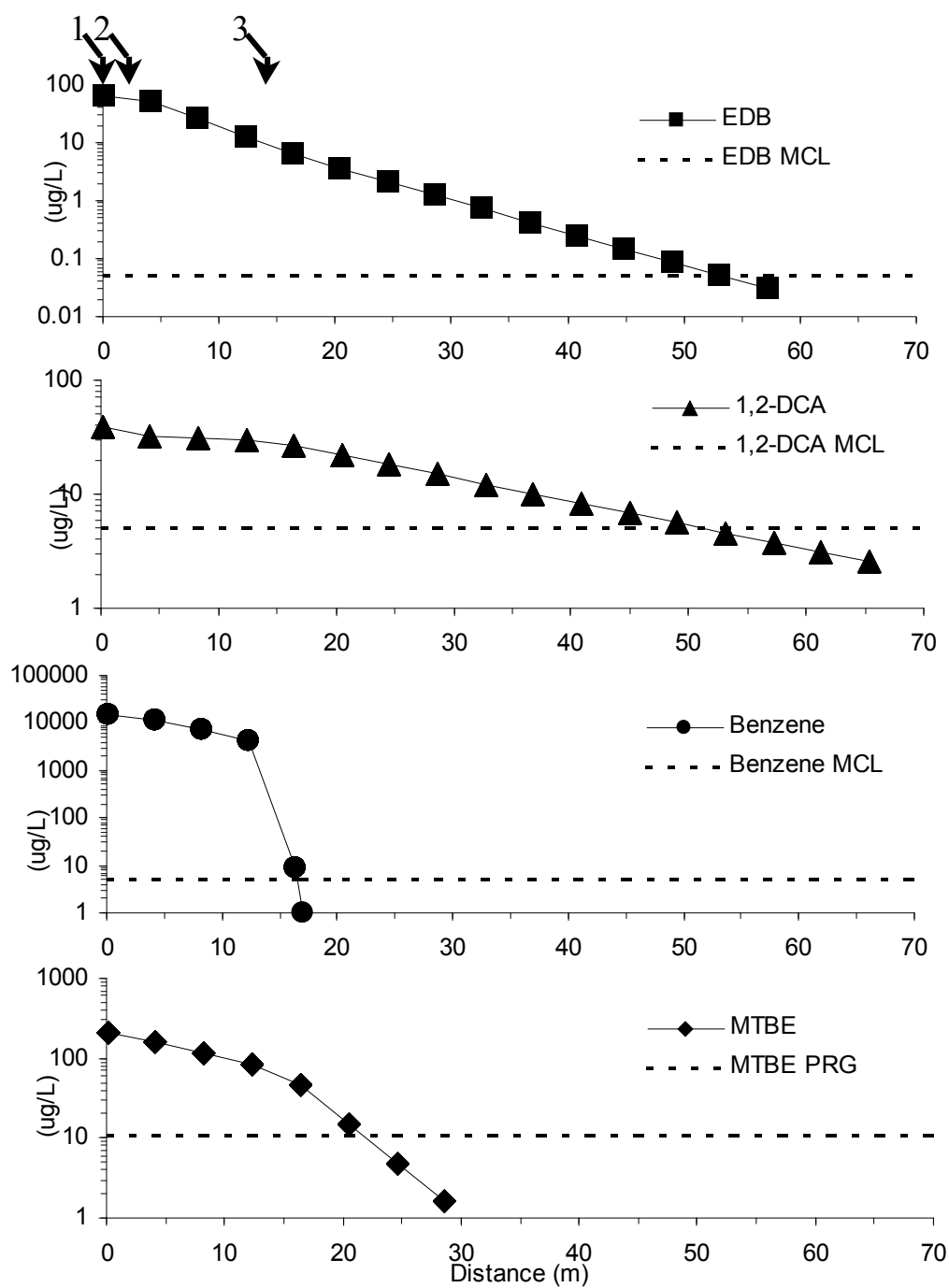


FIGURE 3.5 REMChlor simulations of natural attenuation short plume scenario, 2012. Zone 1, 2, and 3 markers are suspended above graphs at 0, 5 and 15 meters downgradient, respectively.

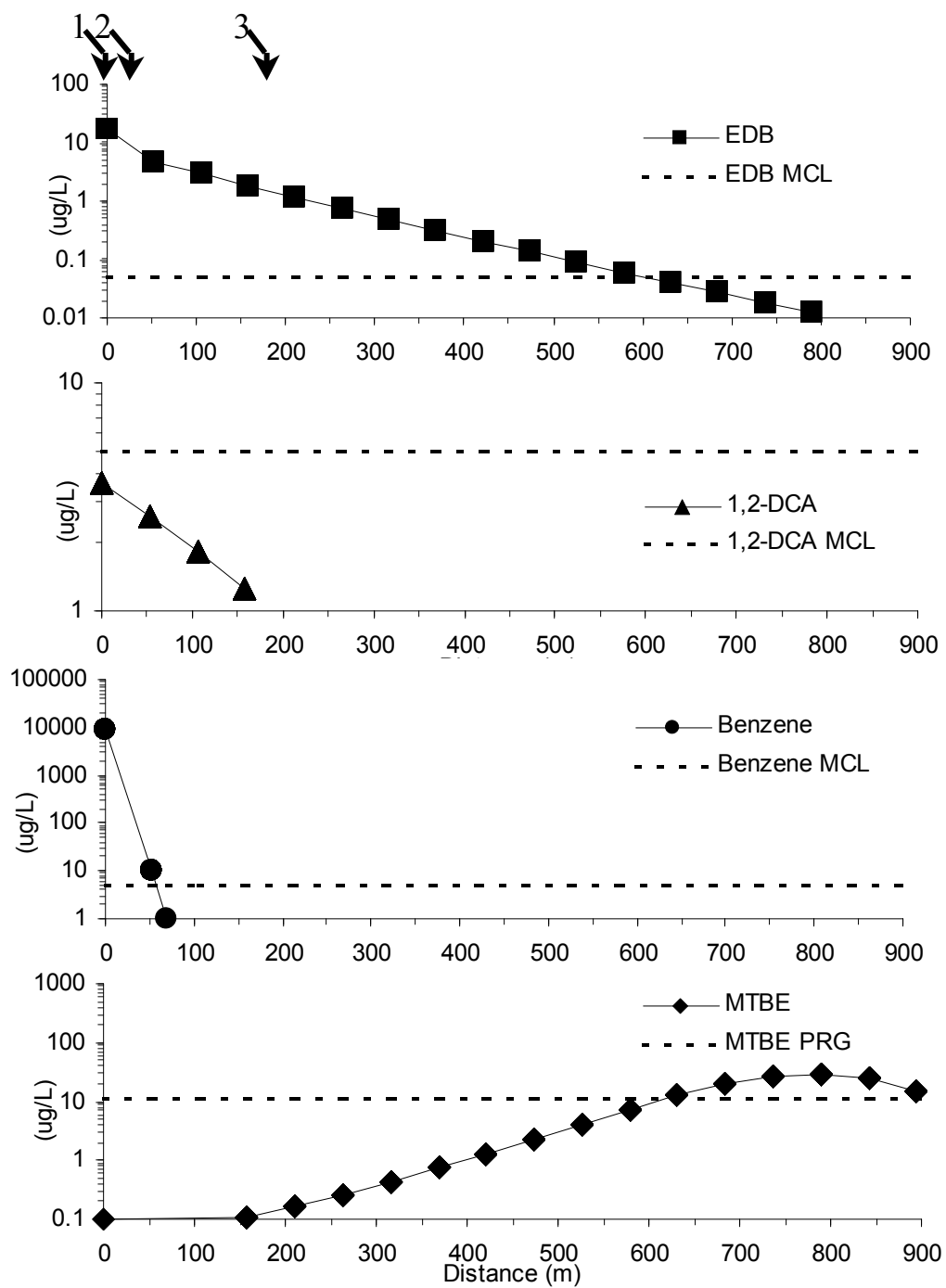


FIGURE 3.6 REMChlor simulations of natural attenuation long plume scenario, 2012. Zone 1, 2, and 3 markers are suspended above graphs at 0, 5 and 15 meters downgradient, respectively..

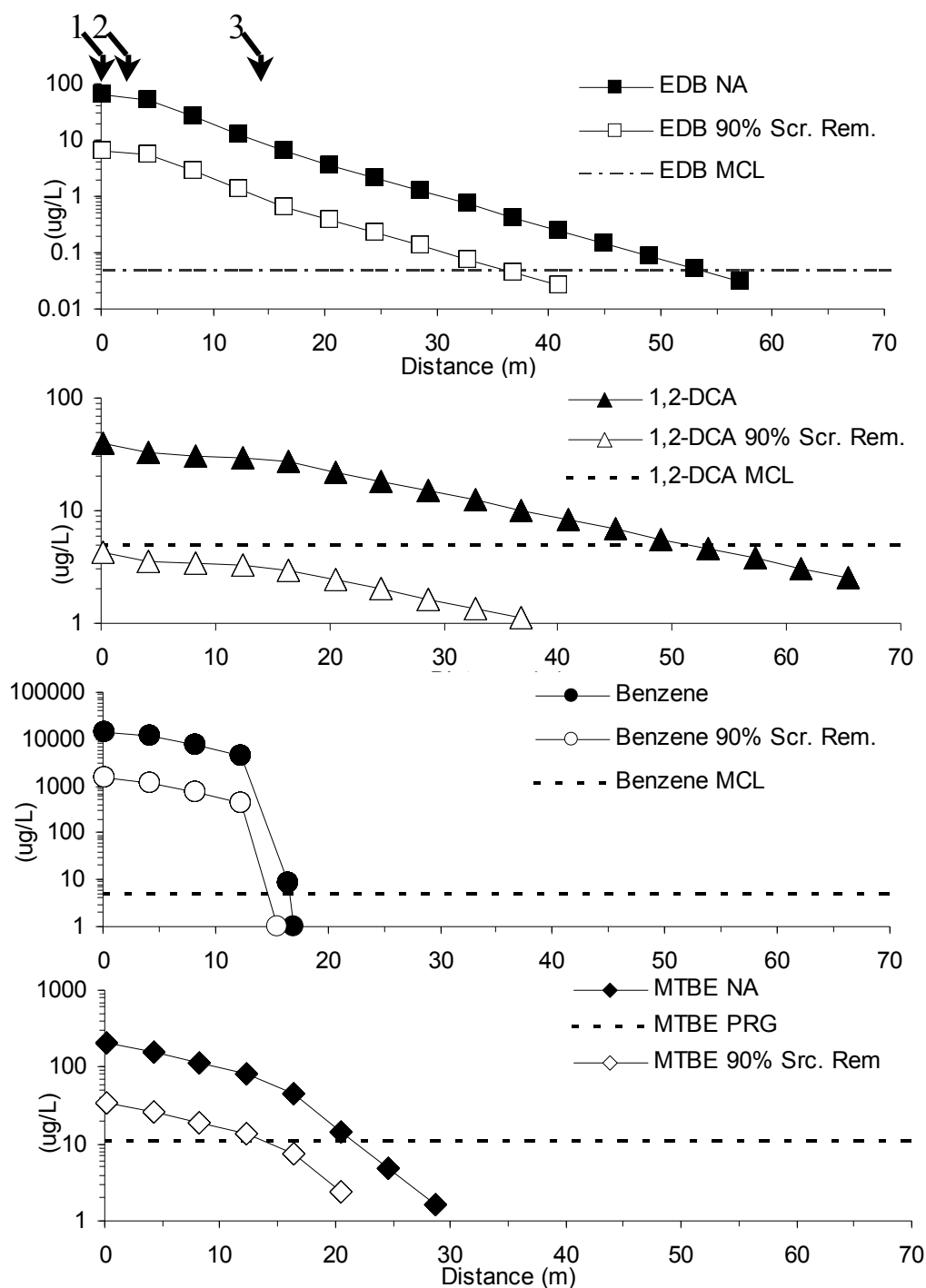


FIGURE 3.7 REMChlor simulation results of 90% source removal, short plume scenario, 2012. Zone 1, 2, and 3 markers are suspended above graphs at 0, 5 and 15 meters downgradient, respectively.

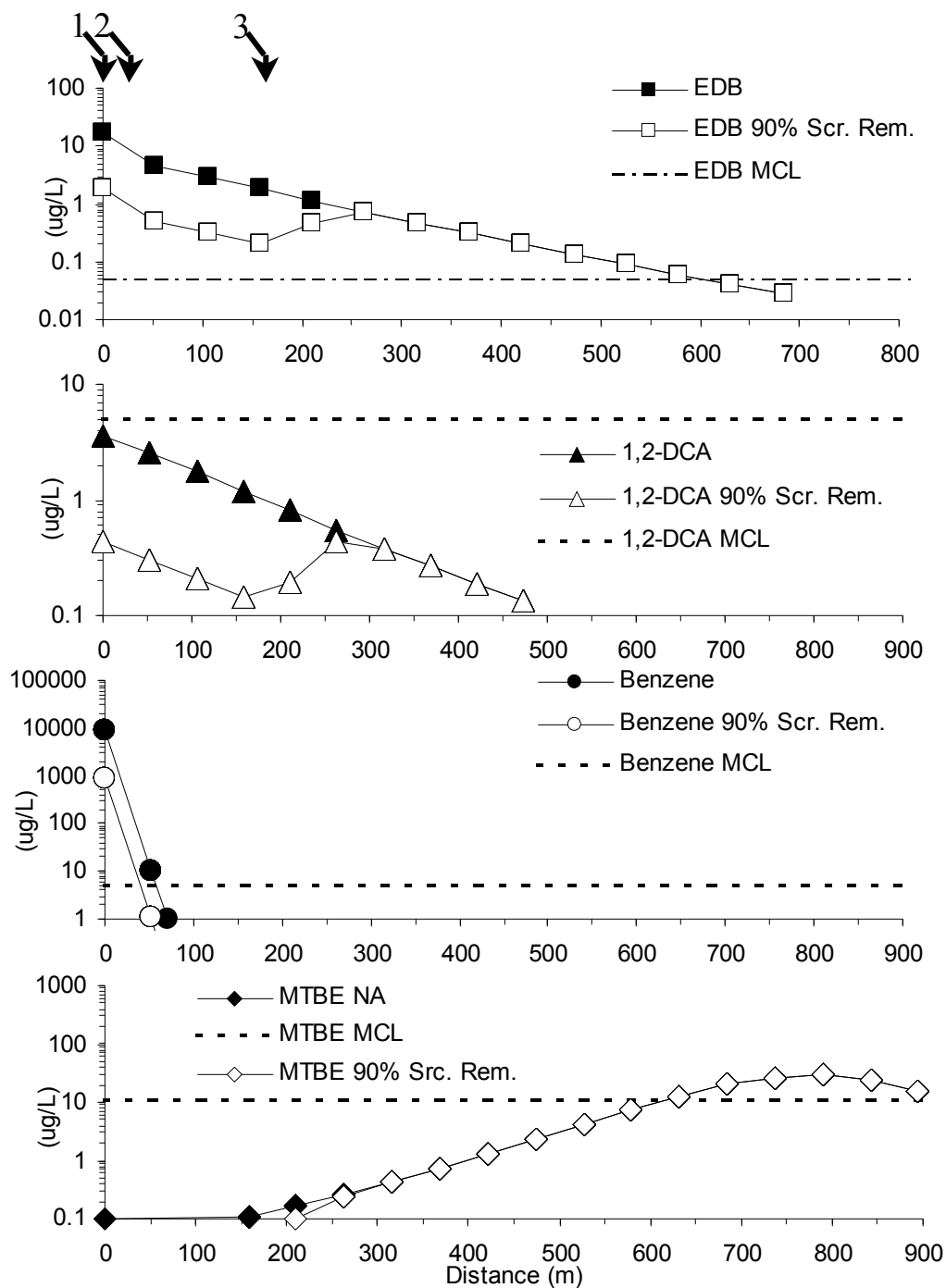


FIGURE 3.8 REMChlor simulation results of 90% source removal, long plume scenario, 2012. Zone 1, 2, and 3 markers are suspended above graphs at 0, 5 and 15 meters downgradient, respectively.

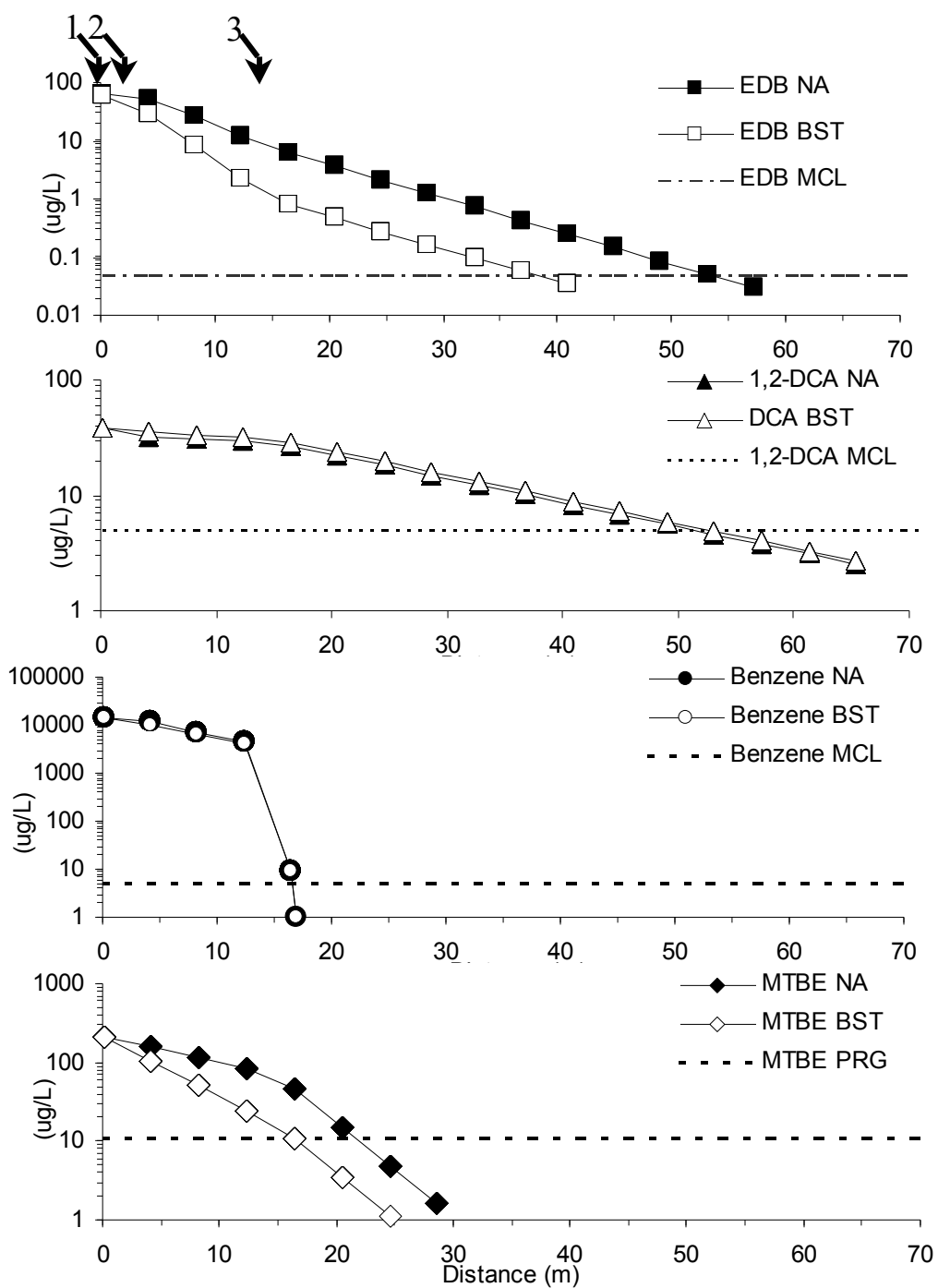


FIGURE 3.9 REMChlor simulation results of biostimulation (BST), short plume scenario, 2012. Zone 1, 2, and 3 markers are suspended above graphs at 0, 5 and 15 meters downgradient, respectively.

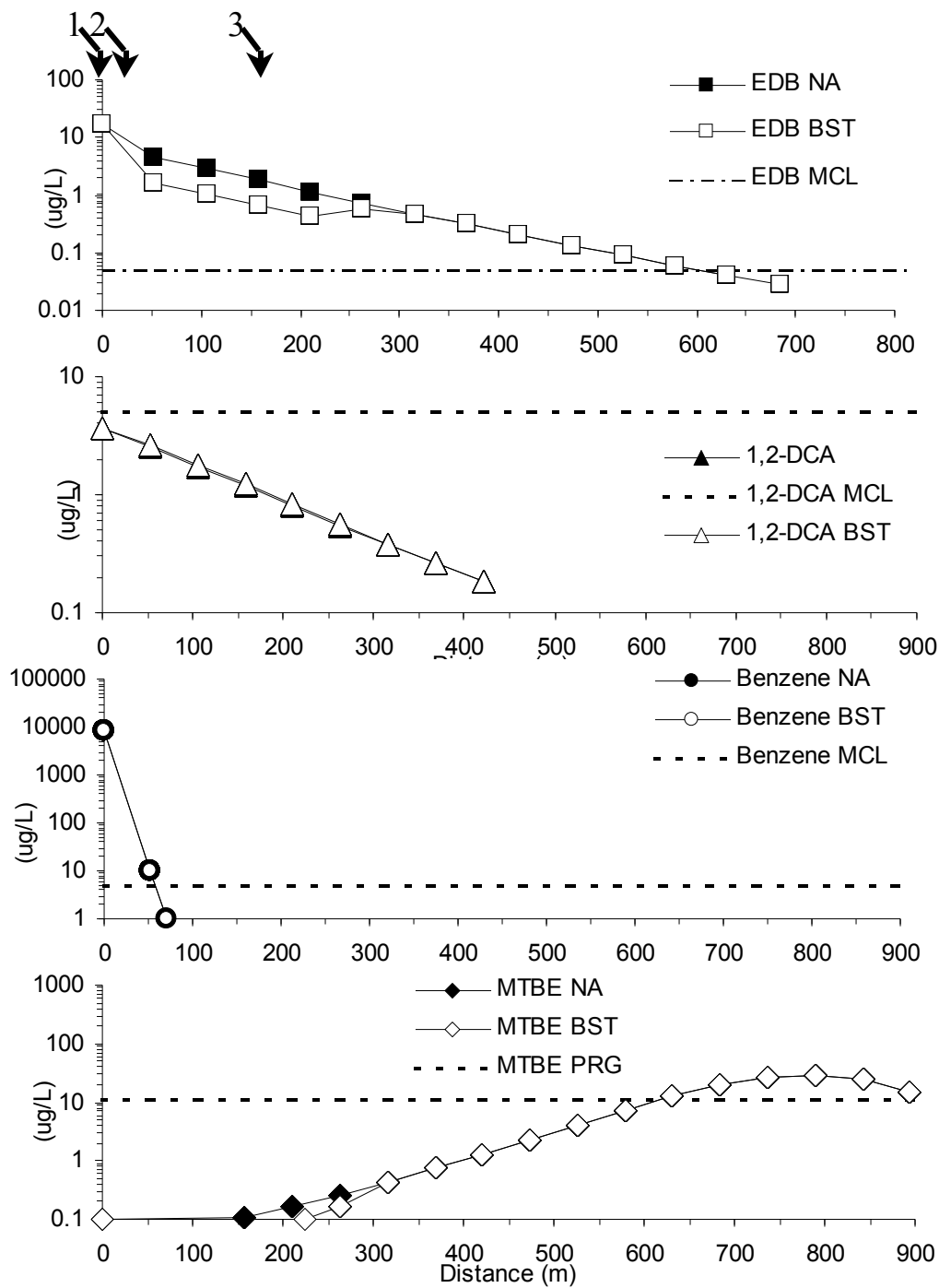


FIGURE 3.10 REMChlor simulation results of biostimulation (BST), long plume scenario, 2012. Zone 1, 2, and 3 markers are suspended above graphs at 0, 5 and 15 meters downgradient, respectively.

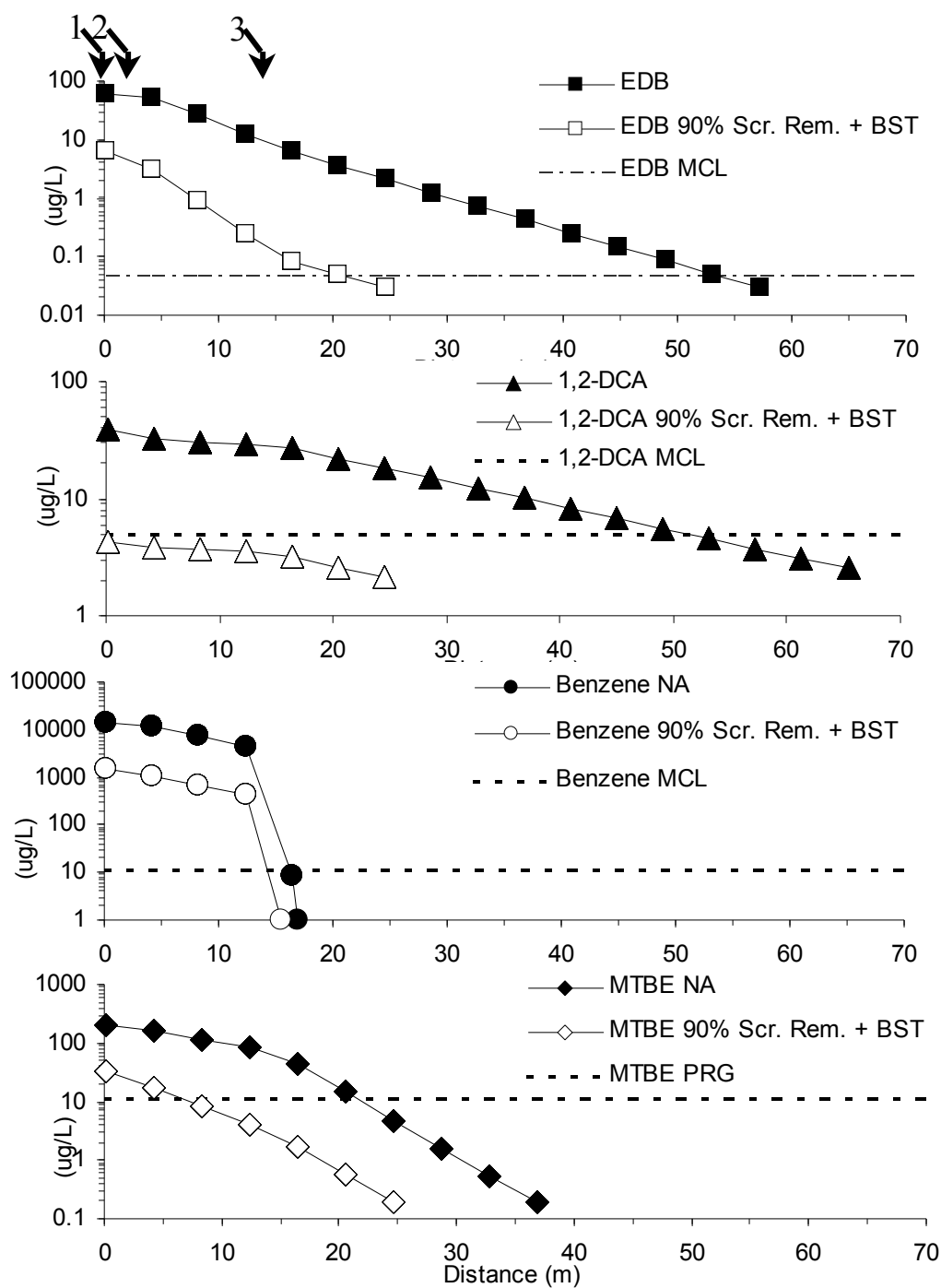


FIGURE 3.11 REMChlor simulation results of 90% source removal combined with biostimulation (BST), short plume scenario, 2012. Zone 1, 2, and 3 markers are suspended above graphs at 0, 5 and 15 meters downgradient, respectively

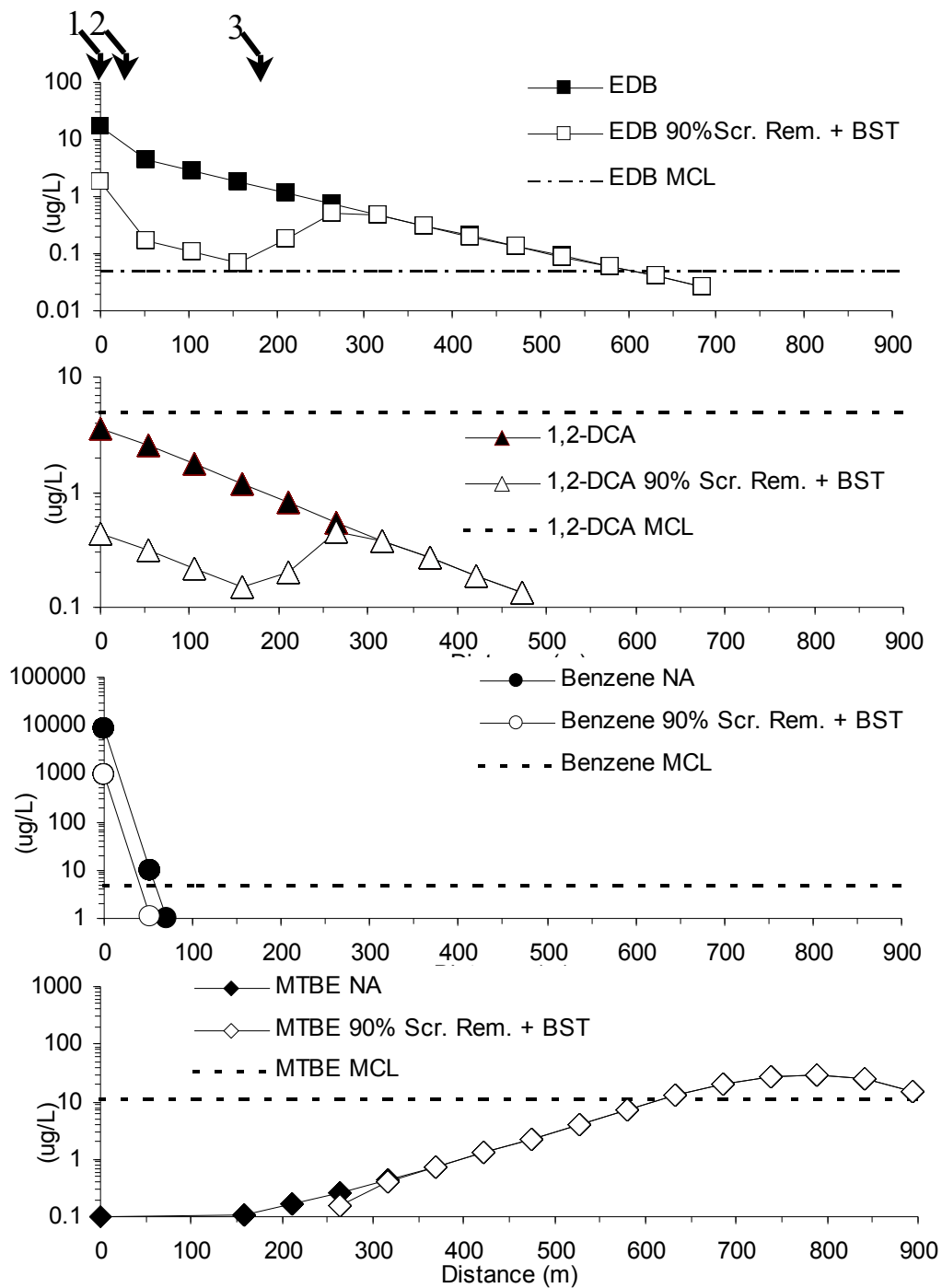


FIGURE 3.12 REMChlor simulation results of 90% source removal combined with biostimulation (BST), long plume scenario, 2012. Zone 1, 2, and 3 markers are suspended above graphs at 0, 5 and 15 meters downgradient, respectively

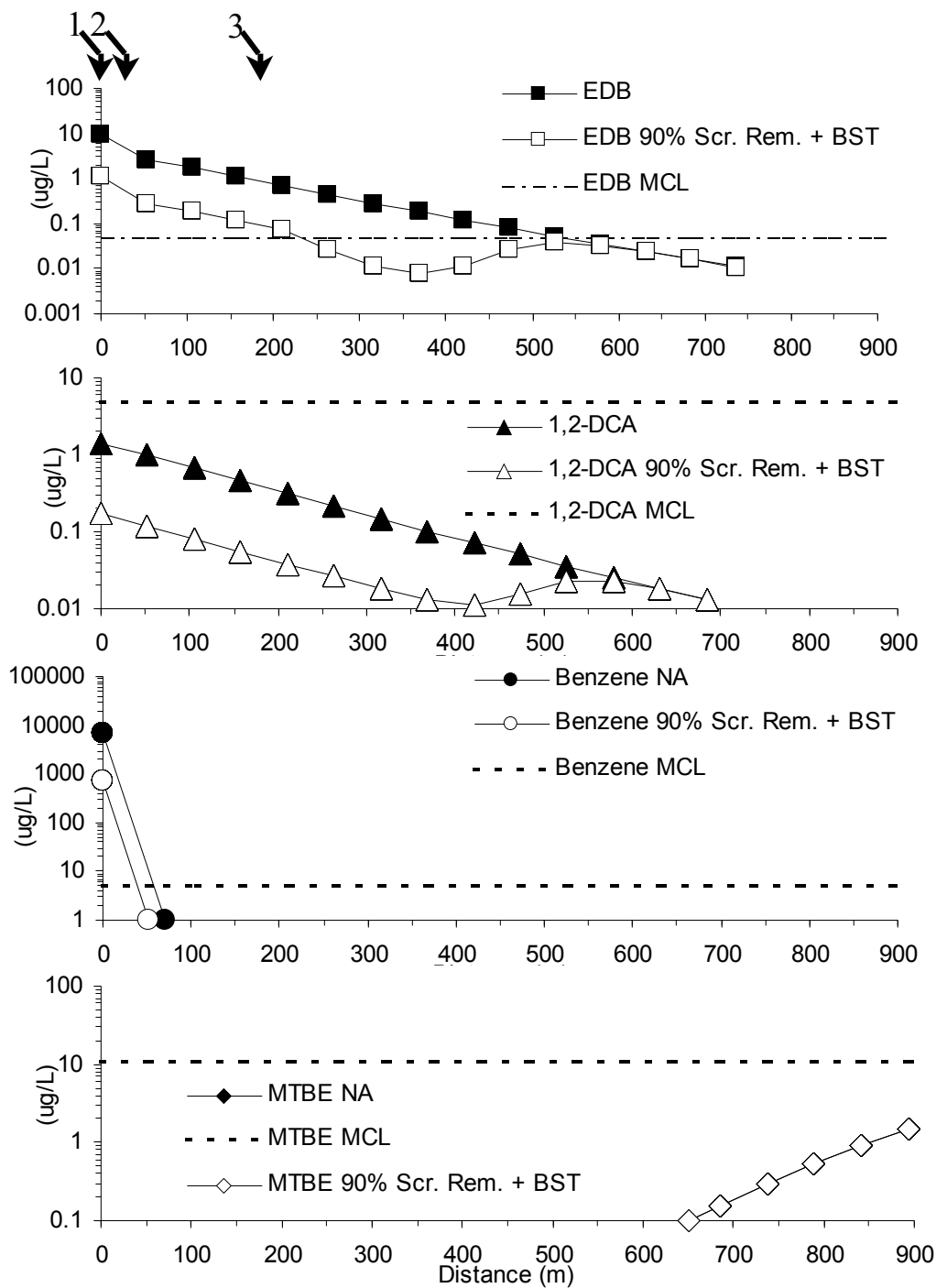


FIGURE 3.13 REMChlor simulation results of 90% source removal combined with biostimulation (BST), long plume scenario, 2017. Zone 1, 2, and 3 markers are suspended above graphs at 0, 5 and 15 meters downgradient, respectively.

CHAPTER FOUR

EVALUATION OF POTENTIAL MUTUAL INHIBITION OF EDB AND 1,2-DCA ON AN ENRICHMENT CULTURE

4.1 Introduction

Chapter 2 describes the biodegradability of EDB and apparent recalcitrance of 1,2-DCA in the presence of fuel hydrocarbons in both a laboratory and field setting. 1,2-DCA biodegradation in the presence of EDB has not been documented under any circumstances. Only one pure culture, *Dehalococcoides ethenogenes* strain 195, is known to degrade both EDB and 1,2-DCA (46). If a species of *Dehalococcoides* is responsible for the EDB degradation observed in laboratory microcosms described in Chapter 2, it may do so in preference to 1,2-DCA, given that respiration of EDB is thermodynamically more favorable than that of 1,2-DCA (Appendix A, Table A3). As a consequence, the presence of EDB may inhibit biodegradation of 1,2-DCA in groundwater, contributing to its persistence at UST sites. Conversely, it is possible that under certain circumstances 1,2-DCA inhibits EDB biodegradation, especially if the same type of enzymes are required to dehalogenate both compounds. This chapter describes experiments designed to evaluate the inhibitory interactions that may occur during biodegradation of EDB and 1,2-DCA.

Previous research on the anaerobic biodegradability of EDB and 1,2-DCA provides insight into likely biodegradation pathways. Destruction of EDB and 1,2-DCA has been achieved under a variety of low reduction-oxidation potential (redox) conditions (52, 53, 16, 29, 40, 45, 65, 66). Field evidence indirectly suggests 1,2-DCA is also

metabolized in the presence of $\text{Fe}(\text{OH})_3$ and MnO_2 (29). Gerritse et al. (29) observed consumption of 1,2-DCA in a groundwater treatment system with proportional amounts of reduced iron and Mn produced. This would tend to indirectly indicate that 1,2-DCA served as an electron donor, and was thus oxidized, so it is possible that 1,2-DCA oxidation occurs at UST sites, depending on geochemical conditions (29). Another study found mixed and pure cultures to be capable of oxidizing 1,2-DCA, with nitrate as the terminal electron acceptor (16). No information is available on whether EDB biodegradation occurs when nitrate, $\text{Fe}(\text{III})$ and $\text{Mn}(\text{IV})$ are available as terminal electron acceptors.

In low redox environments (i.e., $E_h < -100$ mV), biodegradation of EDB proceeds primarily via dihaloelimination to ethene, as is the case for 1,2-DCA (Fig. 4.1). Dehydrohalogenation to vinyl bromide and reductive dehalogenation to bromoethane are considered minor pathways, though the latter was found to be operative in laboratory microcosm experiments described in Chapter 2. In addition to chlorinated ethenes, *Dehalococcoides ethenogenes* strain 195 uses EDB and 1,2-DCA as growth-linked terminal electron acceptors, with hydrogen serving as the electron donor and acetate as the carbon source (46). The kinetics of chlorinated ethene reduction by various strains of *Dehalococcoides* is well characterized in terms of yield, maximum specific growth rate, and half saturation coefficient. In contrast, no information on the kinetics of EDB bromorespiration is available. At least one other organism, *Desulfitobacterium dichloroeliminans* strain DCA1, is known to utilize 1,2-DCA as a terminal electron acceptor. Wildeman et al. (66) demonstrated the reduction of high levels of 1,2-DCA (40

mg/L) by strain DCA1 to ethene in a matter of days (66). However, utilization of EDB by strain DCA1 has not yet been examined.

Inhibitory interactions in mixtures of contaminants have been studied by various researchers. Many possible combinations of contaminants are possible, so most researchers have focused on mixtures of two or three contaminants (35). Adamson and Parkin (1) showed that degradation of commingled 1,1,1-trichloroethane (1,1,1-TCA) and carbon tetrachloride (CT) by a mixed methanogenic culture slowed when the concentration of either compound was increased. Adding tetrachloroethene (PCE) had no effect on 1,1,1-TCA and/or CT transformation (1). Hughes and Parkin (35) found that 1,1,1-TCA was inhibited by both CT and chloroform (CF), but that CT and CF were only degraded by a mixed anaerobic culture when both were present as co-contaminants. In another study, a PCE-degrading enrichment culture was found to simultaneously degrade CT and 1,1,1-TCA with no prior exposure to these contaminants, though CT concentrations over 10 μ M were found to slow PCE degradation (2). Grostern and Edwards (31) co-innoculated microcosms with a 1,1,1-TCA-degrading anaerobic mixed culture and KB-1, which rapidly dechlorinates TCE. The presence of 1,1,1-TCA initially inhibited the *c*-DCE and VC transformation steps in the co-innoculated microcosms, but once 1,1,1-TCA was reduced to 1,1-DCA, the KB-1 culture was able to reduce both *c*-DCE and VC (31).

The above studies demonstrate the importance of inhibitory interactions in mixtures of contaminants. Given the persistence of 1,2-DCA in the field and laboratory (Chapter 2), and the number of UST sites likely impacted by EDB and 1,2-DCA,

inhibition may have particular relevance here. This chapter describes research exploring potential inhibitory interactions between EDB and 1,2-DCA. No studies have evaluated EDB and 1,2-DCA degradation as co-contaminants, or in mixture with other compounds. To evaluate potential inhibition of one or the other compound systematically, it was first necessary to identify a culture capable of growing on both compounds. *Dehalococcoides ethenogenes* strain 195 is known to degrade both EDB and 1,2-DCA (46), but the culture's ability to degrade them simultaneously was not tested. The results presented here describe inhibition tests on a mixed halorespiring culture.

4.2 Materials and Methods

4.2.1 Chemicals and Media

Chemicals used in this evaluation are described in Section 2.2.3. The medium used for the enrichment culture is described elsewhere (17) with the following modifications: the phosphate buffer was made using 52.5 g K_2HPO_4 per liter instead of 27.2 g KH_2PO_4 and 34.8 g K_2HPO_4 ; 4.7 g $\text{CaCl}_2 \cdot 2\text{H}_2\text{O}$ and 1.8 g $\text{FeCl}_2 \cdot \text{H}_2\text{O}$ were used instead of 7.0 g $\text{CaCl}_2 \cdot 6\text{H}_2\text{O}$ and 2.0 g $\text{FeCl}_2 \cdot 2\text{H}_2\text{O}$ for the salt solution; 0.2 g $\text{ZnSO}_4 \cdot 7\text{H}_2\text{O}$ was used instead of 0.1 g ZnCl_2 for the trace metal solution; the bicarbonate solution was made with 16 g NaHCO_3 per liter instead of 260 g/L; 50 mL of the bicarbonate solution was added to the medium instead of 10 mL; and instead of adding a vitamin solution, 50 mg/L of yeast extract was added (using a 5 g/L stock solution and adding 10 mL of filter sterilized stock per liter of media). These changes were made based on the availability of chemicals and the solubility of sodium bicarbonate in water.

4.2.2 SRS Chloroethene Respiring Culture

Preliminary experiments were conducted to determine if an enrichment culture that chlororespires PCE and TCE was also capable of respiring EDB and 1,2-DCA. This culture was developed with sediment and groundwater from the Twin Lakes area of the Savannah River Site (SRS) and enriched for growth on PCE and TCE (68). The culture is capable of rapidly dechlorinating all of the chlorinated ethenes to ethene, and is populated with several novel species of *Dehalococcoides*. Lactate is used as the electron donor.

To determine if the culture uses EDB and 1,2-DCA as terminal electron acceptors, two sets of triplicate serum bottles (160 mL) with Teflon-faced septa and aluminum crimp caps were inoculated with 100 mL of the SRS enrichment culture. One set was spiked with EDB, the other with 1,2-DCA. Roughly 0.3 and 0.5 μmol s EDB and 1,2-DCA respectively were added to each bottle using saturated water solutions. Given partitioning between the headspace and liquid phases, these amounts produced aqueous phase concentrations of approximately 2.5 and 5.0 μM EDB and 1,2-DCA, respectively. Sodium lactate was provided as the electron donor at 100 times the number of electron equivalents needed for complete dehalogenation. The use of both compounds proceeded after a lag, though it took much longer to adapt the culture to 1,2-DCA. Initially slow rates of use were followed by increasing and sustained utilization in both treatments. The cultures were transferred several times and continued to use the compounds upon transfer. This strongly suggests that the SRS culture contains microbes capable of dehalorespiring EDB and 1,2-DCA, currently the only mixed culture known to do so.

Subsequent experiments have confirmed an increase in the population of *Dehalococcoides* in proportion to the amount of EDB and 1,2-DCA dehalogenated (27).

To test potential inhibitory interactions between EDB and 1,2-DCA, the SRS culture was grown individually on EDB or 1,2-DCA in separate enrichments. The EDB enrichment was developed by combining aliquots (20 mL) from the EDB serum bottles discussed above with 1.44 L media (1.5 L total liquid volume). The 1,2-DCA enrichment culture was established by collecting two 100 mL aliquots and one 50 mL aliquot from the replicates of the 1,2-DCA treatment and combining with 1.25 L media (1.5 L total liquid volume). In this way, two liter-size bottles of the culture were cultivated, one on EDB and the other on 1,2-DCA. Dihaloelimination to ethene was the predominant form of conversion of both compounds (Figures 4.2 and 4.3). Whenever EDB or 1,2-DCA was consumed below detection based on GC/FID analysis, more was added. pH was monitored weekly and maintained at 7.0 with NaOH (8 M). The dose of EDB and 1,2-DCA was gradually increased (accompanied by proportionate increases in lactate additions). Over 120 days of culture development, rapid and complete metabolism of high concentrations of both compounds was achieved. The EDB enrichment achieved a maximum consumption rate of approximately 400 μmols per bottle (262 μM , or 49 mg/L) in three days. The 1,2-DCA enrichment achieved a maximum consumption rate of 370 μmols per bottle (240 μM , or 24 mg/L) in six days. To prevent an accumulation of potentially inhibitory salts (from use of NaOH to neutralize HBr and HCl), on several occasions the contents of the bottles were allowed to settle (enhanced by the presence of iron sulfides) and 0.5 L was decanted and replaced with fresh media.

The liter-sized bottles were used to test the effect of 1,2-DCA on the rate of EDB utilization by the EDB enriched culture, and to test the effect of EDB on the rate of 1,2-DCA utilization by the 1,2-DCA enriched culture. The experimental design is summarized in Tables 4.1 and 4.2. One set of experiments was conducted with the EDB enrichment culture (Table 4.1), the other with the 1,2-DCA enrichment culture (Table 4.2). The experiment that was conducted to determine the effect of 1,2-DCA on biodegradation of EDB by the EDB enrichment culture is herein referred to as the “EDB inhibition test.” The following treatments were evaluated: EDB alone; EDB + approximately an equal amount of 1,2-DCA per bottle; EDB + approximately 4 times more 1,2-DCA per bottle; and EDB + approximately 7 times more 1,2-DCA per bottle. The treatment with EDB alone was used to verify the performance of the culture in comparison to the 2 L EDB “mother bottle” (described above). Lactate was added at the beginning of the test and at each sampling event, with the total amount added in considerable excess of the amount needed for stoichiometric dehalogenation (Table 4.1). Water controls were prepared with distilled deionized water and EDB. Each treatment consisted of duplicate serum bottles. In the event of rapid biodegradation of either compound in the treatments, the initial concentration was assumed to be the same as the initial concentration in the water controls.

The experiment that was conducted to determine the effect of EDB on biodegradation of 1,2-DCA by the 1,2-DCA enrichment culture is herein referred to as the “1,2-DCA inhibition test.” The following treatments were evaluated: 1,2-DCA alone; 1,2-DCA + approximately an equal amount of EDB per bottle; 1,2-DCA +

approximately 6 times more 1,2-DCA per bottle; and EDB + approximately 11 times more 1,2-DCA per bottle. The treatment with 1,2-DCA alone was used to verify performance of the culture in comparison to the 2 L 1,2-DCA “mother bottle” (described above). In addition, a treatment was prepared with EDB alone, to test the ability of the 1,2-DCA enrichment culture to utilize EDB in the absence of 1,2-DCA and with no prior exposure to EDB. Lactate was added at the beginning of the test and at each sampling event, with the total amount added in considerable excess of the amount needed for stoichiometric dehalogenation (Table 4.2). Water controls were prepared with distilled deionized water and 1,2-DCA. Each treatment consisted of duplicate serum bottles. In the event of rapid biodegradation of either compound in the treatments, the initial concentration was assumed to be the same as the initial concentration in the water controls.

4.2.3 Analytical Methods

The same GC headspace methods described in Chapter 2 were used in this study to quantify EDB, 1,2-DCA, bromoethane, vinyl bromide, chloroethane, vinyl chloride, methane, ethane, and ethene. The sensitivity of the ECD precludes its use for EDB quantification when concentrations are over 1 mg/L (the ECD is comparatively less sensitive to 1,2-DCA). Initial headspace analysis for EDB was conducted using the same procedure as for 1,2-DCA, i.e., using a 5890 Series II Plus Hewlett-Packard GC equipped with a flame ionization detector (FID) initially. When EDB concentrations dropped below approximately 10 µg/L, it was quantified on the ECD.

4.3 Results

4.3.1 EDB Inhibition Test

Eight serum bottles inoculated with the EDB enrichment culture and amended with EDB and varying amounts of 1,2-DCA were monitored for 26 days. GC measurements were taken initially every two to three hours until concentrations of EDB declined to approximately 10 $\mu\text{g/L}$, whereupon measurements were collected every 48 hours. The frequency of initial measurements was necessary given the culture's rapid consumption of EDB at higher concentrations, even in the presence of the highest amount of 1,2-DCA added; slower consumption at low concentrations permitted longer sampling intervals later in the test. Average EDB concentrations over the first day of the test are presented by treatment in Figure 4.4a, and for the remainder of the test in Figure 4.4b. Results by bottle are presented in Appendix B.

The first treatment in the EDB inhibition test served as a control, receiving 7 μmols EDB per bottle (resulting in an aqueous phase concentration of 65 μM , or 12 mg/L), but no 1,2-DCA, and is referred to as the "EDB only treatment" (Table 4.1). EDB concentrations declined rapidly as expected, though variability among the duplicates was noted initially (Figure 4.4a). After 24 hours, the average EDB concentration in the treatment was 124 $\mu\text{g/L}$. As expected, consumption slowed at low concentrations, and 14 days elapsed before the treatment average reached EDB's MCL of 0.05 $\mu\text{g/L}$. The EDB only treatment was the first to attain the MCL, but overlap among treatment error bars suggests it was not significantly faster than other treatments. The next treatment to reach the MCL was the one with the highest amount of 1,2-DCA added (Figure 4.4b). Ethene

was the primary daughter product of EDB conversion (Figure 4.5), though less than 100% recovery was noted, likely as a consequence of error in the response factors.

To determine the effect of equimolar amounts of 1,2-DCA on EDB consumption, five μmols of 1,2-DCA per bottle were added to the second treatment (termed “EDB + Low 1,2-DCA”), producing an aqueous 1,2-DCA concentration of 52 μM , or 5.0 mg/L (Table 4.1). The presence of roughly equimolar amounts of 1,2-DCA and EDB had no significant effect on the initial rate of EDB consumption (Figure 4.4a). Final EDB concentrations were slightly above the MCL, but overlap of error bars indicate only minor statistical differences among treatments (Figure 4.4b). Over this same period, there was no significant decrease in 1,2-DCA (Figure 4.6). The EDB enrichment culture was thus able to continue its rate of EDB consumption unaffected by 1,2-DCA, even when the concentration of 1,2-DCA was orders of magnitude greater than that of EDB. 1,2-DCA showed no change in concentration for 26 days (Figure 4.6). As with the EDB only treatment, ethene was the primary daughter product of EDB conversion, though as above, recovery was less than 100% in the “EDB + Low 1,2-DCA” bottles (Figure 4.5).

The third treatment (“EDB + Mid 1,2-DCA”) received approximately five times more 1,2-DCA (26 μmols) per bottle than EDB, resulting in an initial aqueous phase concentration of 250 μM (25 mg/L). Despite this higher concentration of 1,2-DCA, EDB consumption initially increased (Figure 4.4a), though at the conclusion of the test concentrations were not significantly different than other treatments (Figure 4.4b). Ethene was the predominant biodegradation product from EDB in the “EDB + Mid 1,2-DCA”

bottles (Figure 4.5). No drop in 1,2-DCA concentrations was observed over the course of the experiment in this treatment (Figure 4.6).

Approximately ten times more 1,2-DCA was added to the final treatment (“EDB + High 1,2-DCA,”). As with the mid-DCA treatment, the high initial concentration of 1,2-DCA appeared to increase the initial rate of EDB utilization (Figure 4.4a), although at the conclusion of the test the final concentrations were similar (Figure 4.4b). Ethene was the predominant biodegradation product from EDB (Figure 4.5). 1,2-DCA exhibited no appreciable decline over 624 hours of monitoring (Figure 4.6).

EDB can also be converted by reductive dehalogenation to bromoethane or via abiotic dehydrohalogenation to vinyl bromide (Figure 4.1), but neither daughter product was detected in these experiments above their detection limits (3.2 and 1.9 $\mu\text{g/L}$ for bromoethane and vinyl bromide, respectively). These aqueous concentrations correspond to 0.002 μmol of bromoethane and 0.004 μmol of vinyl bromide per bottle. Methane was monitored during the test (Figure 4.7). Initially 1 μmol of methane per bottle was present in all treatments (Figure 4.7). Over time, levels of methane increased to approximately 14.5 μmol s in the EDB only, EDB + Low 1,2-DCA and EDB + Mid 1,2-DCA treatments, accounting for roughly 2.1% of the electron equivalents of lactate provided. Methane levels were lower in the EDB + High 1,2-DCA treatment (11.9 μmol s, or 1.7% of the electron equivalents of lactate added), but overlap among error bars indicates this difference was not significant.

4.3.1 1,2-DCA Inhibition Test

Ten serum bottles inoculated with the 1,2-DCA enrichment culture and amended with 1,2-DCA and varying amounts of EDB were monitored for 107 days. Two control treatments were established in the 1,2-DCA inhibition test, receiving approximately the same amount of 1,2-DCA or EDB (7-8 μmol), and are termed here “1,2-DCA only” and “EDB only” (Table 4.2). This equates to an initial aqueous phase concentration of 65 μM (7 mg/L) of 1,2-DCA and 80 μM of (15 mg/L) EDB. Both compounds disappeared within two days of initiation of the experiment (Figures 4.8 and 4.9). In the case of 1,2-DCA, this was expected since the culture was enriched for growth with 1,2-DCA as the terminal electron acceptor. However, the fact that EDB also was immediately consumed with no apparent lag was unexpected, since the 1,2-DCA enrichment culture had never previously been exposed to EDB. As in the case of the EDB test, approximately stoichiometric amounts of ethene were recovered in both treatments (Figure 4.10), indicating the SRS culture degrades these compounds through similar metabolic pathways, i.e., dihaloelimination.

To determine the effects of equimolar amounts of EDB on 1,2-DCA consumption by the 1,2-DCA enrichment culture, 7 μmol s 1,2-DCA (65 μM , or 7 mg/L) and 8 μmol s EDB (80 μM , 15 mg/L) were added together to the third treatment (“1,2-DCA + Low EDB”). EDB was completely consumed in two days (Figure 4.9) but 1,2-DCA was not (Figure 4.8), demonstrating a clear preference by the culture for EDB, despite its enrichment on 1,2-DCA. 1,2-DCA consumption slowed throughout the test, even after the amount of EDB remaining was well below 1 μmol per bottle. A total of 31 days was

required for complete consumption of the 1,2-DCA, in stark contrast to the 1,2-DCA only treatment, in which the compound was completely consumed to below detection after two days. This demonstrates a lasting negative impact of EDB on the culture's ability to consume 1,2-DCA, long after complete consumption of EDB. Ethene was the predominant product of EDB and 1,2-DCA conversion, though as above incomplete conversion was noted (Figure 4.10).

To test the effect of higher concentrations of EDB, 40 μmol per bottle (resulting in an initial aqueous phase concentration of 400 μM or 75 mg/L) were added to the fourth treatment, approximately five times the amount of 1,2-DCA ("1,2-DCA + Mid EDB") (Table 4.2). By day 2 of the test EDB was depleted (Figure 4.9), but only 1 μmol of 1,2-DCA was consumed (Figure 4.8). This is one-sixth the 1,2-DCA utilization rate at the same point in the treatment that received equimolar amounts of the two compounds (1,2-DCA + Low EDB treatment). Ninety-one days elapsed before 1,2-DCA decreased to below detection in this treatment.

Inhibition of 1,2-DCA was even more pronounced when EDB was added at a ratio of 11 to 1 ("1,2-DCA + High EDB"). Each bottle in the last treatment received 80 μmol of EDB (resulting in an initial aqueous phase concentration of 800 μM or 150 mg/L) (Table 4.2). Like the other treatments, the culture showed a clear preference for EDB over 1,2-DCA, though more time (8 days) was required for complete consumption of EDB to below to level of detection for the FID (Figure 4.9). At the test's conclusion (107 days), over 2 μmol 1,2-DCA remained in the bottles (Figure 4.8). Thus, higher concentrations of EDB produced proportionately greater inhibition of 1,2-DCA.

1,2-DCA can also be converted by reductive dehalogenation to chloroethane or via abiotic dehydrohalogenation to VC. Chloroethane was not detected during this test above its detection limit of $1.1 \mu\text{g/L}$, which corresponds to $0.002 \mu\text{mols}$ per bottle. Figure 4.11 shows VC concentrations over time in the treatments. A maximum of $0.05 \mu\text{mols}$ per bottle was detected on day 2 in the 1,2-DCA only treatment, and this level declined quickly. Roughly the same amount of VC accumulated in the 1,2-DCA + Low EDB treatment on days 5 and 10, respectively, which then declined over time. VC levels peaked at roughly $0.045 \mu\text{mols}$ per bottle in the 1,2-DCA + Mid EDB treatment from days 24 through 44, declining to below detection by day 91. VC exhibited an increasing trend in the 1,2-DCA + High EDB treatment, gradually increasing to $0.03 \mu\text{mols}$ per bottle by day 107.

Figure 4.12 shows methane production in the treatments over the duration of the test. All treatments contained roughly the same amount of methane at the start of the test ($4\text{-}5 \mu\text{mols/bottle}$). Over time, gradually increasing methane levels were noted in all three treatments to which both 1,2-DCA and EDB were added. A maximum of $514 \mu\text{mols}$ per bottle was observed in the treatment to which approximately equal amounts of 1,2-DCA and EDB were added. This level of methane translates into roughly 73% of the electron equivalents of lactate provided as electron donor at the start of the test. Less methane was detected in treatments to which more EDB was added. In the 1,2-DCA + Mid EDB treatment, $299 \mu\text{mols}$ had accumulated by day 91 (21% of the lactate electron equivalents added). Roughly $144 \mu\text{mols}$ (9.6% the lactate electron equivalents added) were present in the 1,2-DCA + High EDB treatment on day 107.

4.4 Discussion

Previous studies have shown the importance of inhibitory interactions between CT and PCE (2), 1,1,1-TCA, PCE and CT (1), 1,1,1-TCA, CT and CF (35), PCE and TeCA , and 1,1,1-TCA and TCE (31). The research described above demonstrates conclusively that EDB inhibits the SRS culture's ability to degrade 1,2-DCA. Though the culture rapidly consumed EDB and 1,2-DCA individually, when fed both simultaneously it degraded EDB at the expense of 1,2-DCA in all cases. When the culture was enriched on EDB, activity on 1,2-DCA was completely inhibited, even after EDB was gone. Even the highest amount of 1,2-DCA tested did not inhibited the rate of EDB degradation, down to part-per-trillion levels. Any prior exposure to EDB precluded the culture's ability to consume 1,2-DCA. Remarkably, when the culture was enriched on 1,2-DCA and subsequently exposed to both EDB and 1,2-DCA, EDB was consumed first. EDB clearly inhibited 1,2-DCA biodegradation, and the degree of 1,2-DCA inhibition was roughly proportional to the initial concentration of EDB.

Few studies have evaluated potential inhibitory interactions between brominated and chlorinated compounds, and none have focused on EDB and 1,2-DCA specifically. Gu et al. (32) found that vinyl bromide and VC were mutually inhibitory in a mixed *cis*-1,2-DCE dechlorinating enrichment culture, though VC was slightly more so than vinyl bromide (32). This may be due to the slight thermodynamic advantage of hydrogenolysis of vinyl chloride relative to that of vinyl bromide (Table A.3). Bedard and Van Dort (4) found that brominated biphenyls were superior dehalogenation substrates to chlorinated biphenyls (4). One brominated compound known to inhibit dechlorination is 2-

bromoethanesulfonate (BES) (43), though the mechanism by which it does so is unclear. Chiu and Lee (13) found that 2-bromoethanesulfonate (BES) did not inhibit the activity of a TCE-dechlorinating culture but did change the mechanism by which the culture degraded TCE. In microcosms containing the culture, but not BES, TCE was dechlorinated to ethane via *cis*-DCE, VC and ethene. However, when BES was added, TCE was degraded to ethene (not ethane) via a mixture of *cis*- and 1,1-DCE (roughly at a 3:1 ratio) and VC, leading the authors to speculate that its presence altered bacterial community structure.

None of the above studies evaluated inhibition over ranges of different concentrations. The experiments conducted here showed that the consumption of 1,2-DCA by the 1,2-DCA enrichment culture slowed significantly in the 1,2-DCA + Low EDB treatment, was slower in the 1,2-DCA + Mid EDB treatment, and was slowest in 1,2-DCA + High EDB, which received the most EDB. The presence of EDB significantly impeded the ability of the enrichment culture to degrade 1,2-DCA at low levels, and the rate in the 1,2-DCA + Low EDB treatment, which exhibited the most extensive 1,2-DCA degradation, showed extended tailing at low levels.

Inhibition of 1,2-DCA by EDB may contribute to its observed persistence in laboratory and field studies. EDB and 1,2-DCA were co-released at UST sites as components of leaded gasoline. This release scenario provides no expectation of prior exposure to 1,2-DCA, which might predispose indigenous communities of microorganisms to consume 1,2-DCA preferentially. Within this context, these

experiments raise the possibility that EDB precludes the ability of microorganisms at these sites to biodegrade 1,2-DCA anaerobically.

Where the SRS culture was enriched for 1,2-DCA consumption, it was able to biodegrade 1,2-DCA to a limited degree while consuming EDB. When equivalent amounts of the compounds were provided, concurrent consumption was greatest; 8 μ mol EDB and 3 μ mol 1,2-DCA were degraded in two days. Less 1,2-DCA was degraded if EDB concentrations were higher. Both compounds were degraded without appreciable lagtime to ethene via dehaloelimination. This would tend to indicate the same organisms and/or enzymes are involved. The culture's preference for EDB may relate to the thermodynamic advantage of its respiration over 1,2-DCA (Appendix A). If different enzymes and/or microbes are required for reduction of EDB and 1,2-DCA, there would be no expectation for competitive inhibition. Further investigation into the culture's preference for EDB would permit a better understanding of the persistence of 1,2-DCA at UST sites. Cultivating the SRS culture's ability to degrade both compounds simultaneously might permit bioaugmentation of commingled EDB and 1,2-DCA in potential field application. These experiments were conducted at aqueous concentrations that are higher than those likely to be encountered at UST sites, and further research is needed to evaluate potential inhibition among EDB and 1,2-DCA at concentrations more relevant to those likely to be encountered at UST sites. Given the clear-cut results presented here, research into inhibitory interactions among commingled compounds of all classes may have important applicability to the science and application of in situ bioremediation.

Table 4.1 Treatments Used to Test the Effect of 1,2-DCA on EDB

	EDB			1,2-DCA			Lactate Provided ^a			Lactate Required ^b
	<u>μmol/</u> <u>bot.</u>	<u>μM</u>	<u>mg/L</u>	<u>μmol/</u> <u>bot.</u>	<u>μM</u>	<u>mg/L</u>	<u>μmol/</u> <u>bot.</u>	<u>meq/</u> <u>bot.</u>	<u>mM</u>	<u>meq/bot.</u>
EDB Only	7	65	12	-	-	-	0.07	0.8	0.7	0.014
EDB + Low 1,2-DCA	7	65	12	5	52	5	0.07	0.8	0.7	0.024
EDB + Mid 1,2-DCA	7	65	12	26	250	25	0.07	0.8	0.7	0.066
EDB + High 1,2-DCA	7	65	12	53	520	52	0.07	0.8	0.7	0.120
Water Controls	7	65	12	50	480	48	-	-	-	-

Table 4.2 Treatments Used to Test the Effect of EDB on 1,2-DCA

	1,2-DCA			EDB			Lactate Provided ^a			Lactate Required ^b
	<u>μmol/</u> <u>bot.</u>	<u>μM</u>	<u>mg/L</u>	<u>μmol/</u> <u>bot.</u>	<u>μM</u>	<u>mg/L</u>	<u>μmol/</u> <u>bot.</u>	<u>meq/</u> <u>bot.</u>	<u>mM</u>	<u>meq/bot</u>
1,2-DCA Only	7	65	7	-	-	-	0.07	0.8	0.7	0.014
EDB Only	-	-	-	8	80	15	0.07	0.8	0.7	0.016
1,2-DCA + Low EDB	7	65	7	8	80	15	0.07	0.8	0.7	0.024
1,2-DCA + Mid EDB	7	65	7	40	400	75	0.07	0.8	0.7	0.066
1,2-DCA + High EDB	7	65	7	80	800	150	0.07	0.8	0.7	0.120
Water Controls	7	65	7	8	80	15	-	-	-	-

^aLactate was added whenever EDB/1,2-DCA was added

^bLactate required calculated as meq EDB/1,2-DCA present in each bottle the start of an experiment

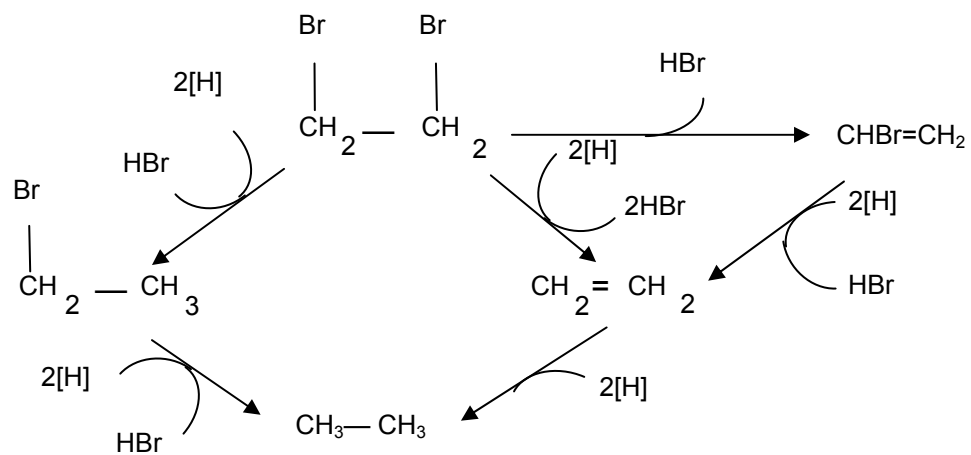


Figure 4.1 Pathways for anaerobic reduction of EDB; $[H] = H^+ + e^-$. The pathways for anaerobic transformation of 1,2-DCA are identical.

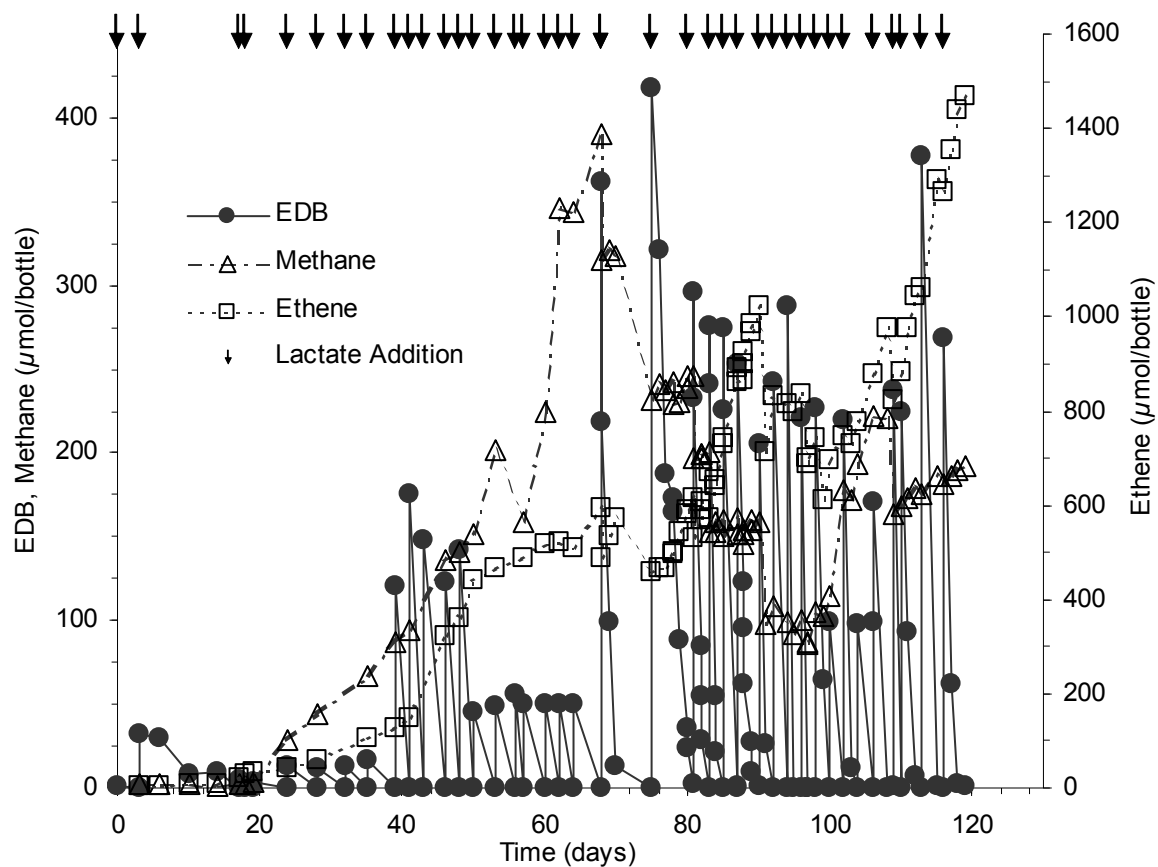


FIGURE 4.2 EDB mother bottle. Arrows (\downarrow) indicate when lactate was added to the bottle. New lactate additions were made with each addition of EDB.

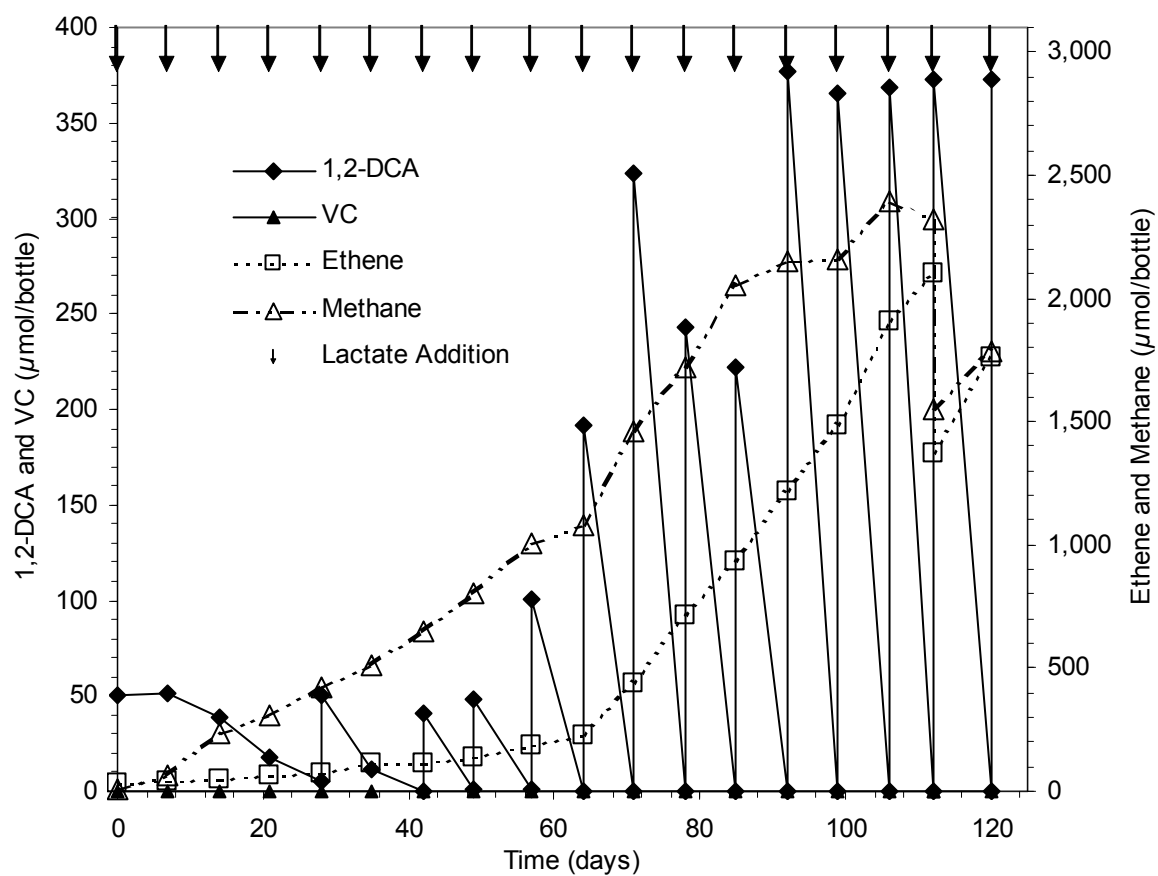


FIGURE 4.3 1,2-DCA mother bottle. Arrows (\downarrow) indicate when lactate was added to the bottle. New lactate additions with each addition of 1,2-DCA.

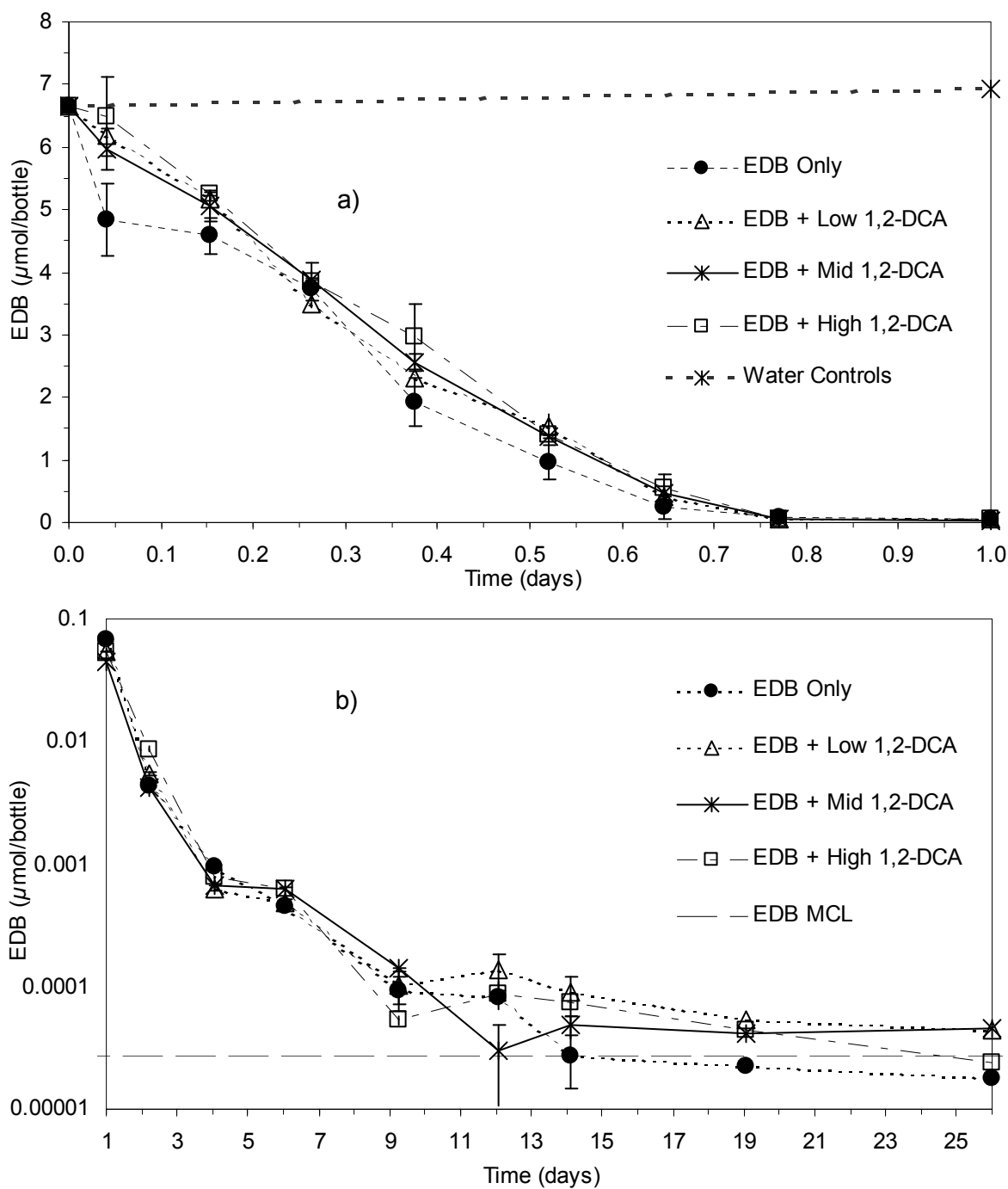


FIGURE 4.4 EDB inhibition test, comparison of average EDB amount per bottle by treatment from 0 to 1 days (a), and 1 to 26 days (b). Error bars represent one standard deviation on treatment mean.

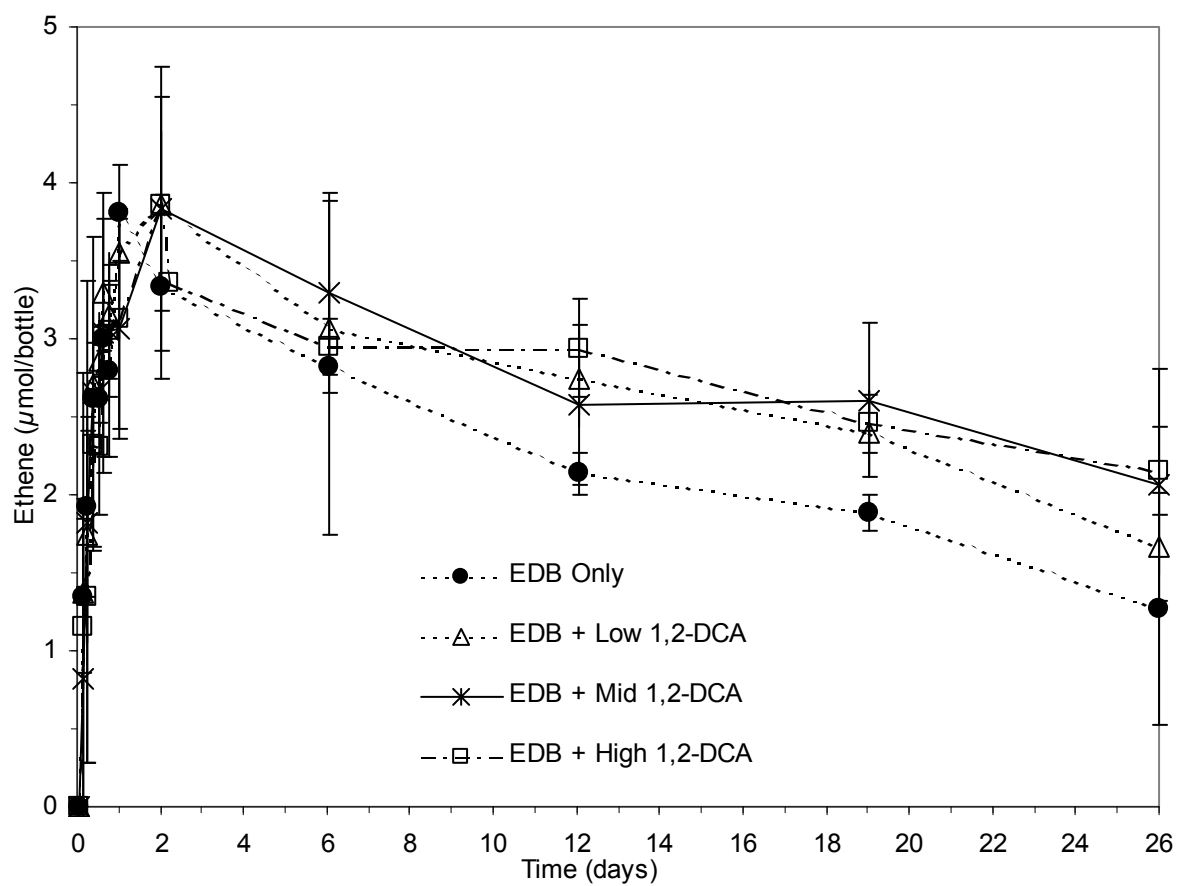


FIGURE 4.5 EDB inhibition test, comparison of average ethene amount per bottle by treatment. Error bars represent one standard deviation on treatment mean.

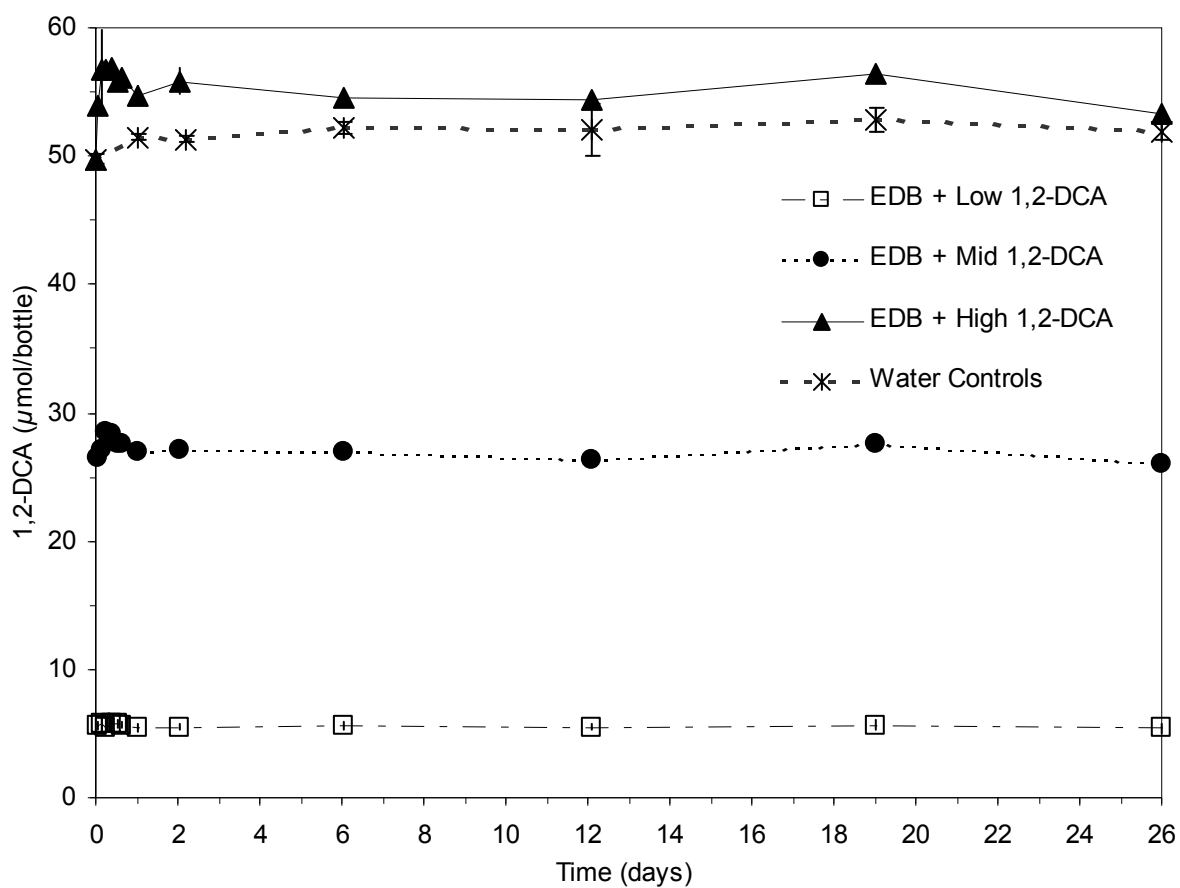


FIGURE 4.6 EDB inhibition test, comparison of average 1,2-DCA amount per bottle by treatment. Error bars represent one standard deviation on treatment mean.

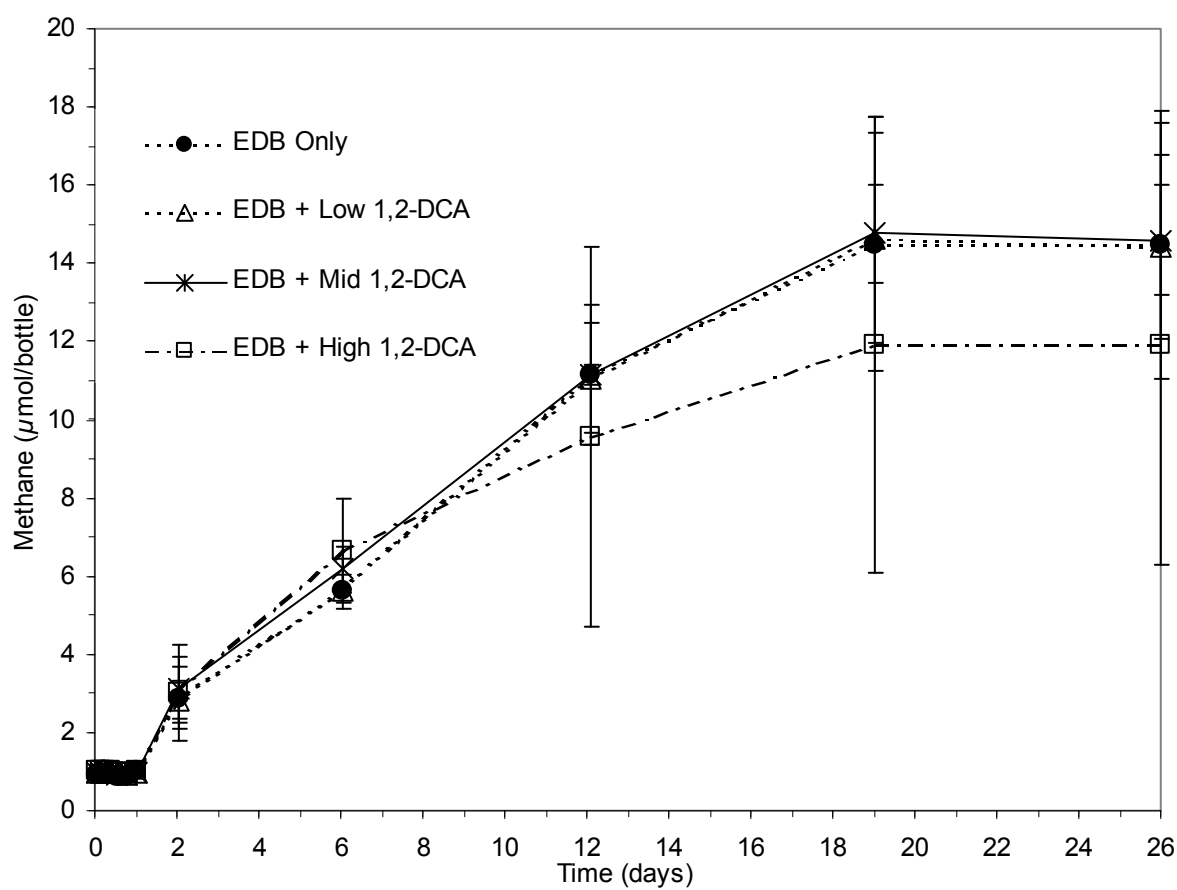


FIGURE 4.7 EDB inhibition test, comparison of average methane amount per bottle by treatment. Error bars represent one standard deviation on treatment mean.

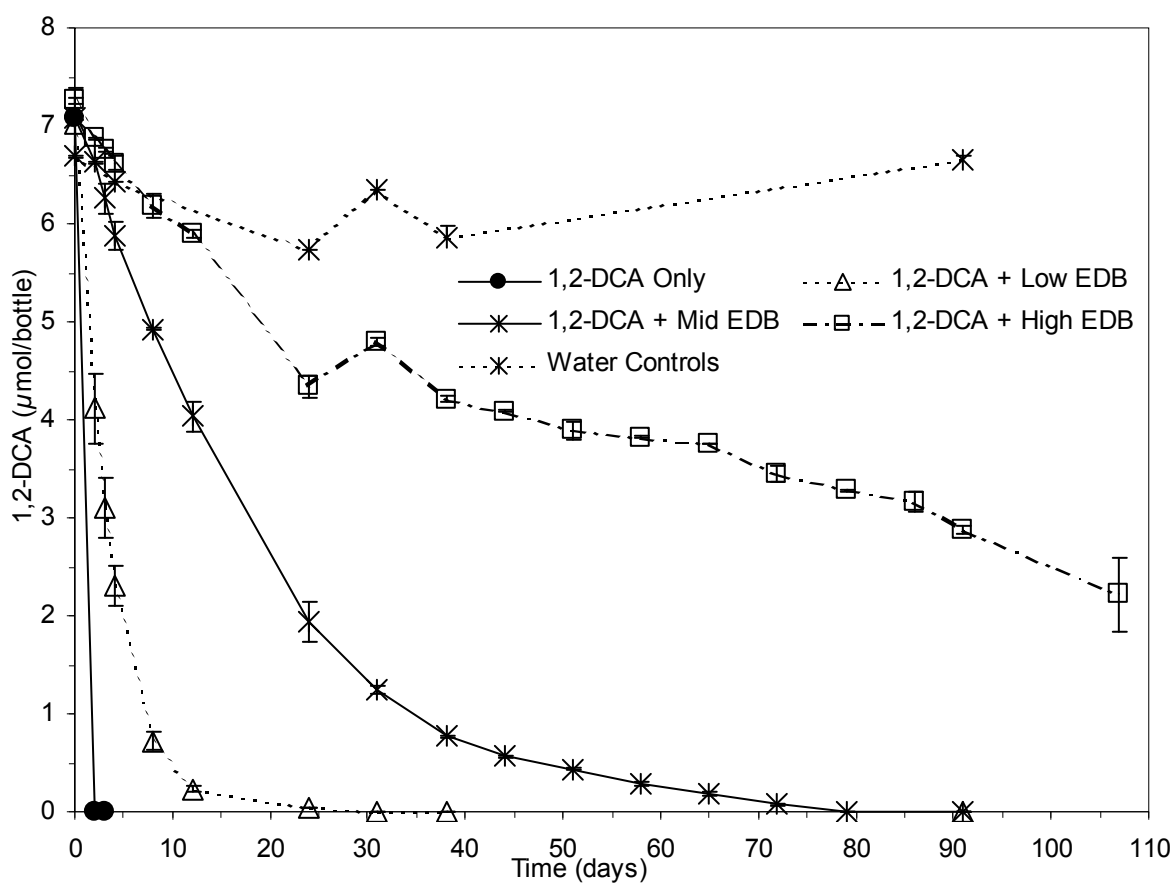


FIGURE 4.8 1,2-DCA inhibition test, comparison of average 1,2-DCA amount per bottle by treatment. Error bars represent one standard deviation on treatment mean.

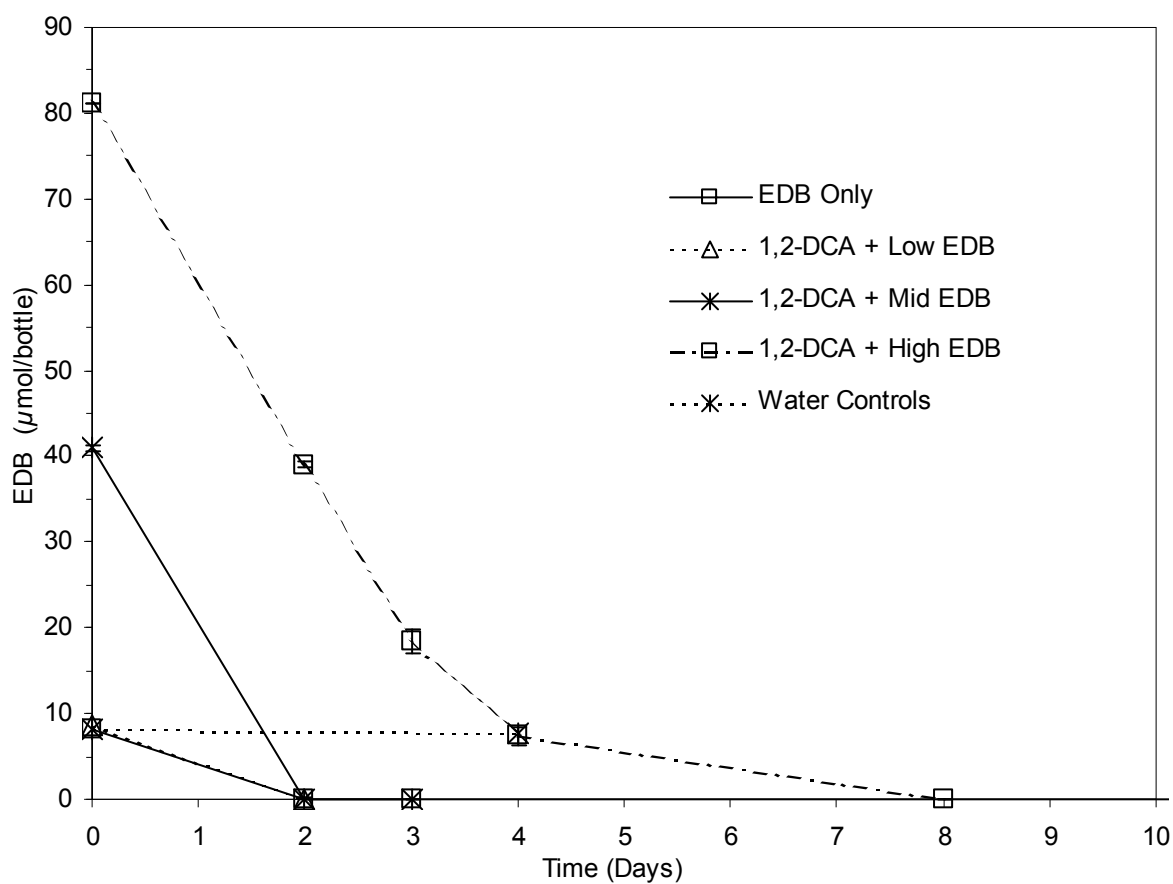


Figure 4.9 1,2-DCA inhibition test, comparison of average EDB amount per bottle by treatment. Error bars represent one standard deviation on treatment mean.

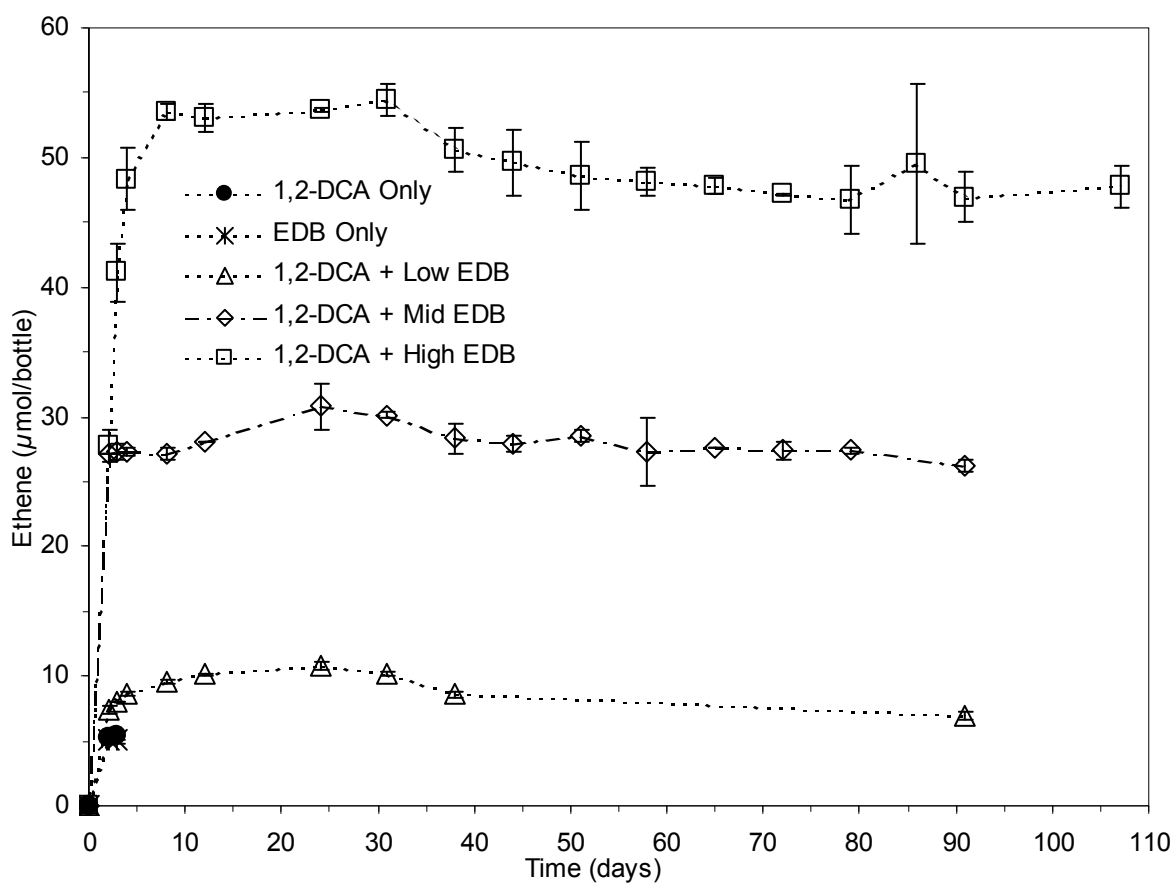


FIGURE 4.10 1,2-DCA inhibition test, comparison of average ethene amount per bottle by treatment. Error bars represent one standard deviation on treatment mean.

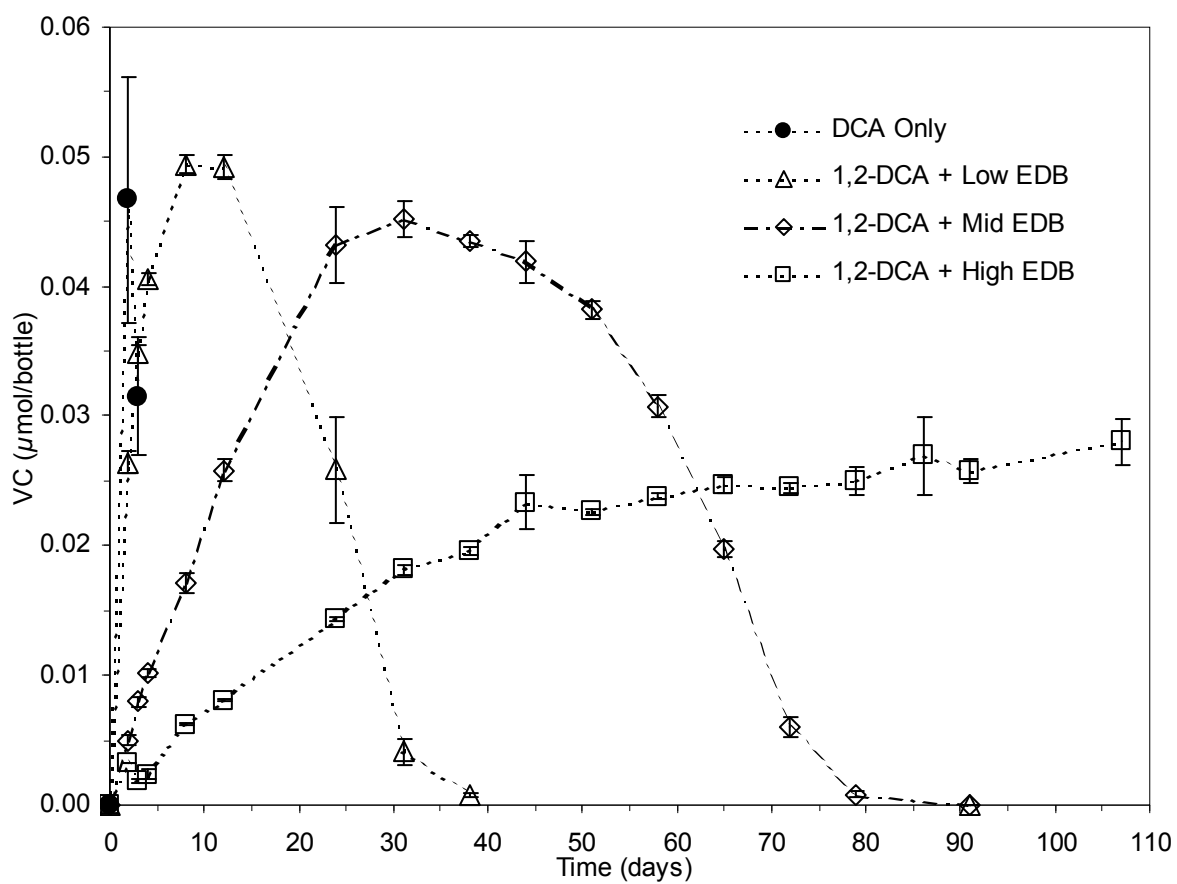


FIGURE 4.11 1,2-DCA inhibition test, comparison of average VC amount per bottle by treatment. Error bars represent one standard deviation on treatment mean.

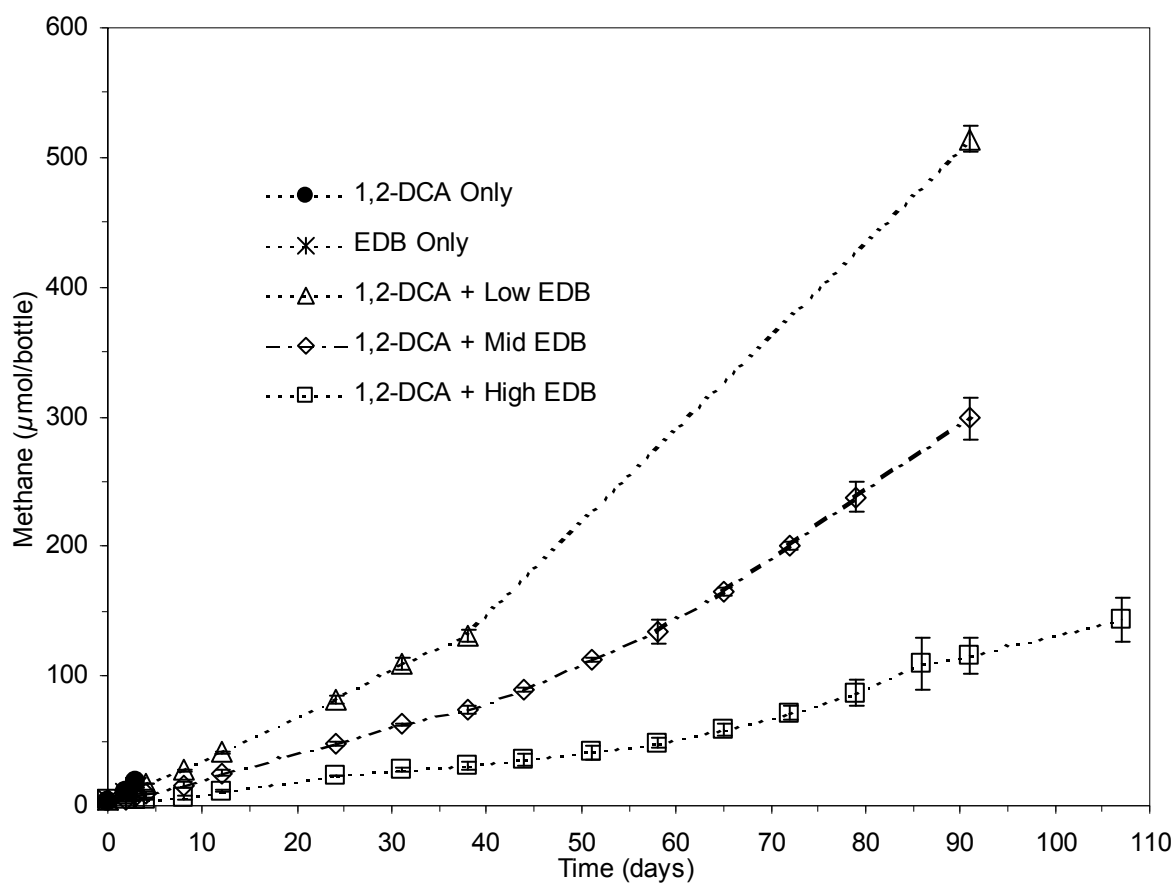


FIGURE 4.12 1,2-DCA inhibition test, comparison of average methane amount per bottle by treatment. Error bars represent one standard deviation on treatment mean.

CHAPTER FIVE

SUMMARY AND IMPLICATIONS

This research demonstrates that EDB is anaerobically biodegradable to below its MCL in the presence of 1,2-DCA and fuel hydrocarbons. Biodegradation of EDB in microcosms was confirmed by carbon specific isotope analysis at the University of Oklahoma. More consistent EDB removal was achieved when lactate was added to laboratory microcosms. Anaerobic biodegradation of EDB is commonly thought to occur via dihaloelimination to ethene, but hydrogenolysis to bromoethane was prominent in the microcosm portion of this study, particularly in the less contaminated microcosms. Several toxicological effects are associated with bromoethane, including neurotoxicity, hematological and hepatic toxicity, so the possibility that bromoethane is present in groundwater at UST sites is a concern. Unlike EDB, 1,2-DCA was recalcitrant in a majority of the experiments performed, and did not respond to lactate addition. This observation is in keeping with field data indicating 1,2-DCA may be the more persistent of the lead additives. Varying rates of decay were observed for the BTEX components of gasoline, and notably, anaerobic degradation of benzene was observed and corroborated by carbon specific isotope analysis. The effect of lactate addition on BTEX biodegradation was beneficial in the case of benzene, negligible in the case of toluene, and inhibitory for ethylbenzene and *o*-xylene when the concentrations of these compounds were high.

Experiments conducted with an enrichment culture originally developed with chlorinated ethenes as terminal electron acceptors showed conclusively that EDB

inhibited biodegradation of 1,2-DCA. Thermodynamic calculations indicate reduction of EDB and its daughter products is more favorable than that of its 1,2-DCA analogs. The degree of 1,2-DCA inhibition was roughly proportional to the initial concentration of EDB. Higher EDB concentrations produced more extensive and with longer lasting inhibition of 1,2-DCA. When enriched on 1,2-DCA, the culture was able to effect limited concurrent degradation of both compounds. In these cases, EDB degradation was much faster and more extensive, and less concurrent degradation of 1,2-DCA was observed at higher EDB concentrations. This clear pattern of inhibition of 1,2-DCA by EDB suggests that inhibition may be a contributing factor to the persistence of 1,2-DCA at UST sites. EDB and 1,2-DCA were co-released at UST sites, so there would be little expectation of prior exposure of indigenous microorganisms to 1,2-DCA; concurrent degradation was only possible if the culture was enriched on 1,2-DCA before it was exposed to EDB, so complete inhibition of 1,2-DCA at UST sites might be expected. Bioaugmentation with microorganisms that have been enriched simultaneously for EDB and 1,2-DCA consumption may be necessary to achieve concurrent bioremediation of these compounds.

Little is known about EDB and 1,2-DCA degradation in aerobic zones at UST sites. Further work is needed to determine the factors controlling their persistence in oxygenic environments. It is anticipated that this knowledge would assist remedial decision makers at sites where long aerobic EDB and 1,2-DCA plumes exist. A relevant consideration is how aerobes respond to the very low concentrations likely to be

encountered in aerobic zones and whether they are below S_{min} , the minimum substrate level capable of supporting growth.

Modeling was conducted with an analytical model (REMChlor) to determine the effects of source and plume remediation on plume extent at UST sites. REMChlor uses mass balance approaches to track changes in source mass and plume concentration, and unlike commonly used screening models such as BIOCHLOR, is able to simulate plume response to variable source depletion and plume remediation. Plume degradation rates were derived from laboratory studies described above, the first to evaluate EDB and 1,2-DCA biodegradation in the presence of fuel hydrocarbons. Simulation results indicate that the relative risk posed by each compound varies greatly over time and space, especially when multiple releases of leaded and unleaded gasoline have occurred. Compounds likely to exceed regulatory standards based on dissolution characteristics in near-source plume zones (i.e., benzene) may not exceed these standards downgradient, due to differences in biodegradation rates. Conversely, EDB and 1,2-DCA, which are likely to be less biodegradable than nonhalogenated fuel hydrocarbons in the aerobic environment, pose far greater relative risk downgradient of the source. If later releases of unleaded fuel occur, MTBE may represent the greatest risk near the source, though its rapid dissolution pattern makes the risk short-lived. EDB will partition out of the NAPL phase much more slowly, so it will likely sustain dissolved plumes for longer timeframes. Extensive plume lengths of EDB and 1,2-DCA result when aerobic biodegradation rates are low, so longer remedial timeframes are necessary prior to seeing beneficial effects of remediation downgradient. Given its rapid dissolution profile, detached plumes of MTBE

are possible. Source removal produces an immediate drop in source discharge concentrations, but given that in the best case a 90% removal efficiency can be expected, the applicability of this technique as a stand alone remedial method is limited to compounds like 1,2-DCA that are likely to be encountered near their risk-based screening value. Source removal is less effective for EDB, which dissolves from gasoline at concentrations that are orders of magnitude above its MCL ($0.05 \mu\text{g/L}$). If remediation is undertaken decades after the release, natural dissolution and attenuation processes may be sufficiently advanced to limit the gains achievable from expensive source removal. Of the four compounds evaluated here, remedial challenges are likely to be highest for EDB, given its very low MCL, extensive downgradient plumes, and relative recalcitrance in the aerobic zone. Even where the best possible combination of source removal and plume bioremediation are combined, significant remedial timeframes will likely be required for this compound where long plumes exist.

The environmental community has grappled with a legacy of UST contamination for over 20 years. An assessment of the risk to human health and the environment posed by BTEX and MTBE was possible only after understanding their behavior in the subsurface. This research advances our understanding of the behavior of EDB and 1,2-DCA at UST sites, but further work is needed. A better understanding of the factors controlling the persistence of EDB and 1,2-DCA will permit a more informed response to this problem on the part of practitioners, researchers, and regulators. Should the occurrence of lead scavengers be as widespread as preliminary evidence would indicate,

having this knowledge in hand before deleterious impacts to human health and the environment occur can only prove beneficial.

APPENDICES

Appendix A

6.1 Microcosm Sampling and Analytical Methods

6.1.1 Microcosm Sampling

Volatile compounds in the microcosms were quantified using a headspace method. This required taking samples of the headspace by puncturing the septum with a syringe. Because of excessive diffusive losses of some of the volatile compounds (in particular, BTEX) during storage with punctured septa, a different procedure was used for sampling that allowed for storage of the microcosms with unpunctured septa. The next section of Appendix A provides a comparison of diffusive losses during the two methods of microcosm storage (i.e., with punctured versus unpunctured septa). This section describes how the headspace sampling was accomplished, followed by descriptions of the GC methods, CSIA, and methods for anions, iron and organic acids.

Headspace sampling began by shaking the microcosms to homogenize the sediment and groundwater and placing the microcosms in the anaerobic chamber in an upright position the night before samples were to be taken. At least one hour before sampling, the unpunctured septa that were on the bottles were quickly removed and replaced with septa that were designated for puncturing (i.e., they may have already been punctured several times). It took less than five seconds to exchange the septa. Duplicate headspace samples (0.5 mL) were then taken in separate syringes (1.0 mL series A-2 with a side-port needle, Precision Scientific) inside the chamber; the syringes were immediately removed and walked over to the GC. One sample was injected to the ECD, the other to the FID (see below). After confirming that the samples had been run

successfully on the GC, the punctured septa on the microcosms were exchanged for unpunctured ones, the microcosms were removed from the chamber, shaken to homogenize the sediment and groundwater, and then stored in the inverted position until the next sampling event. As needed, liquid samples were removed at the same time as headspace samples. Supernatant was removed using a 2 mL glass syringe.

6.1.2 GC Methods

As mentioned above, the two headspace samples were injected onto the GC, one immediately after the other. A single temperature program (40°C for 5 min, ramped at 10°C/min to 200°C, hold for 12 min) resolved all of the contaminants of interest. To quantify EDB, 1,2-DCA, bromoethane, and vinyl bromide, one of the headspace samples was injected onto an RTX 624 column (60-m, 0.53 mm inner diameter, 3.0 μ m film thickness) connected to the ECD, with injector and detector temperatures set at 200°C and 260°C, respectively. Helium (3 mL/min) and nitrogen (33 mL/min) served as the carrier and make-up gases, respectively. A split flow rate of 220 mL/min (73.1:1 split ratio) was used for EDB concentrations greater than approximately 1.0 μ g/L and a splitless mode was used thereafter (0.75 min splitless injections). To quantify hydrocarbons, the second headspace sample was injected onto an RTX-5 column (30-m, 0.53 mm inner diameter, 0.25 μ m film thickness) connected to the FID was used, with injector and detector temperatures set at 250°C and 310°C, respectively. Helium (5.88 mL/min) and nitrogen (33.0 mL/min) served as the carrier and makeup gases, respectively. A split flow rate of 26.0 mL per minute was used, and injections were made in splitless mode (0.75 min).

6.1.3 Carbon Specific Isotope Analysis

Samples for CSIA were prepared by diluting 2 mL of groundwater from a microcosm tenfold in 25 mL vials with Teflon-backed septa to prevent volatilization losses. EDB and 1,2-DCA samples were preserved with HCl (3 drops). The analytes were extracted by a purge and trap (P&T model OI 4660) interfaced to a GC-IRMS instrument (Finnigan MAT 252 IRMS). Due to chromatographic complexity of the samples, satisfactory resolution of EDB and 1,2-DCA required a 2-dimensional chromatographic approach (separation on polar GC phase followed by separation on non-polar GC phase). The P&T-GCIRMS interface described previously (41) was programmed for collecting 2 min heart-cuts of the sample eluting from the polar pre-column. The heart-cuts were directed onto a non-polar phase GC column for final separation followed by on-line combustion and analysis of isotope composition.

6.1.4 Anions, Iron, and Organic Acids

Liquid samples were filtered (0.45 μ m PVDF, Pall Life Sciences) and analyzed for bromide, chloride, nitrate and sulfate on a Dionex DX-100 Ion Chromatograph using a AS5A-5 μ (4 x 150 mm) column and 0.01 N H₂SO₄ as eluant (0.6 mL/min). Lactate, acetate and propionate were quantified by high performance liquid chromatography using an anion exchange column (Aminex HPX-87H, BioRad) (18). Iron (II) was analyzed using the ferrozine method (15).

6.2 The Effect of Incubation Method on Losses of Volatile Compounds During Storage of the Microcosms

Prior microcosm experiments (39) suggested that loss of BTEX compounds may be significant when the microcosms are incubated with septa that have been repeatedly punctured. An alternative approach is to incubate the test bottles with unpunctured septa, as described above. The hypothesis was that the losses that occur during the brief time when swapping the unpunctured and punctured septa are smaller in comparison to not changing the septa and incubating the bottles for extended periods (i.e., months) with septa that have been punctured. To test this hypothesis, two sets of triplicate water controls were prepared using the same type of bottles as the microcosms, with 1.7 L of distilled deionized water present. Both sets were spiked with the same amounts of EDB, 1,2-DCA and BTEX. One set (“punctured septa”) was sampled and incubated without changing the septa. For the other set (“unpunctured septa”), the septa were exchanged prior to and after sampling, as described above.

Data were collected for 120 days. Results are shown in Figure S.1. The data were fit to a first order model. For the unpunctured treatment, none of the trend lines were statistically significant ($\alpha=0.05$), so no trend line is shown. This confirmed the lack of diffusive losses with this method of microcosm operation. A summary of the pseudo first order rates of loss for the punctured treatment is given in Table A.1. It is evident that diffusive losses were significantly greater for EDB, benzene, toluene, ethylbenzene and *o*-xylene in the bottles that were incubated with punctured septa. There was virtually no difference for 1,2-DCA. These results confirm the importance of incubating the

microcosms with unpunctured septa rather than punctured ones, and that the process of exchanging septa just before and after sampling resulted in minimal (if any) losses of the volatile compounds.

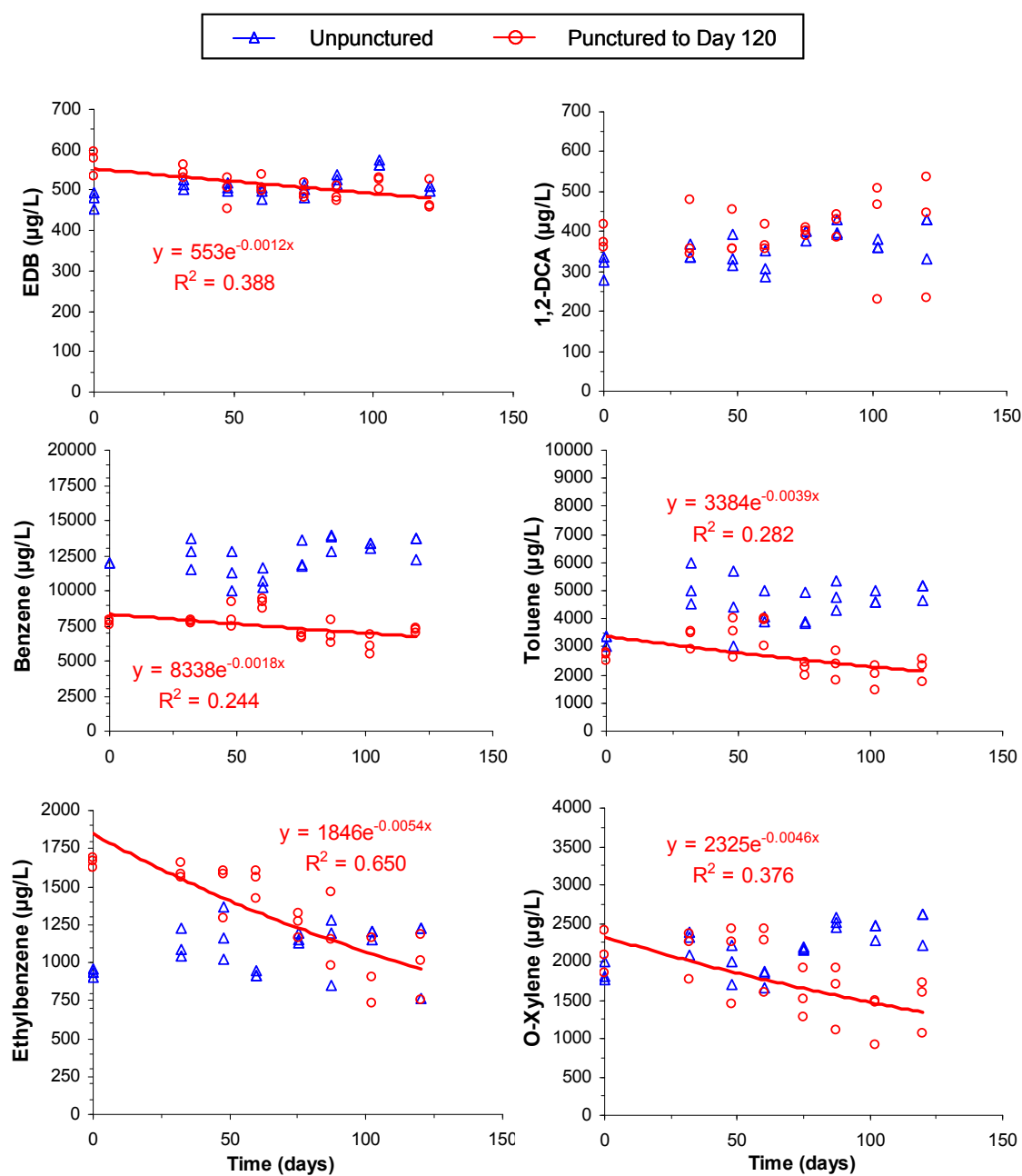


Figure A-1. Behavior of EDB, 1,2-DCA and BTEX in triplicate water control microcosms that were incubated with unpunctured septa (blue symbols) and punctured ones (red symbols). Trend lines are shown only when the first order regression line was statistically significant; for the compounds that had a slope that was not different from zero, no trend line is shown.

Table A-1. Summary of First Order Loss Rates from Water Controls with Punctured and Unpunctured Septa.

	Unpunctured		Punctured		
Compound	Rate (yr⁻¹)^a	R²	Rate (yr⁻¹)	R²	Comparison^b
EDB	0 ^c	-	0.428 ± 0.115	0.388	Significant
1,2-DCA	0	-	0	-	Insignificant
Benzene	0	-	0.650 ± 0.244	0.244	Significant
Toluene	0	-	1.42 ± 0.483	0.282	Significant
Ethylbenzene	0	-	1.99 ± 0.311	0.650	Significant
<i>o</i> -Xylene	0	-	1.67 ± 0.458	0.376	Significant

^a Rates were determined based on regression of pooled data from triplicate bottles.

^b Student's *t*-tests ($\alpha = 0.05$) were performed to compare the rates for the unpunctured and punctured bottles. Where statistical differences were observed, "significant" was entered. If no statistical difference was observed, "insignificant" was entered.

^c The slope was not statistically different from zero or was positive.

6.3 Comparison of EDB Quantification by EPA Method 8011 and Headspace Analysis

Care was taken prior to beginning the experiments to develop an analytical method capable of attaining EDB's very low MCL of $0.05 \mu\text{g/L}$. USEPA's method 8011 was compared to quantification by headspace analysis, on the basis of the amount of EDB delivered in a sample to the GC when $0.05 \mu\text{g/L}$ is present in the aqueous phase of the microcosms. Method 8011 analyzes for EDB and 1,2-dibromo-3-chloropropane by extracting an aqueous sample into hexane (58). The headspace method is based on 0.5 mL samples from the gas phase of the microcosms.

With USEPA Method 8011, a 35 mL aqueous sample is extracted into 2.0 mL hexane, concentrating the sample by a factor of 17.5 (58). The extraction procedure was modified for the purposes of this study in order to conserve aqueous volume, by reducing the aqueous and solvent volumes seven fold; i.e., 5.0 mL of microcosm water was extracted into 0.3 mL pentane. (Pentane was used rather than hexane, since pentane elutes faster than hexane and the hexane peak overlapped with 1,2-DCA, which elutes faster than EDB). Assuming 100% extraction efficiency (i.e., all mass in the aqueous phase is extracted by the solvent) and $0.05 \mu\text{g/L}$ EDB in the water, the mass injected onto the GC in a $1 \mu\text{L}$ sample is $8.33\text{E-}4 \text{ ng}$.

With the headspace method, the amount injected is based on the concentration in the gas phase that is in equilibrium with $0.05 \mu\text{g/L}$ EDB in the aqueous phase. This concentration is obtained based on a mass balance for the microcosm:

$$M_T = C_l V_l + C_g V_g \quad (\text{A1})$$

where M_T is the total amount of EDB ($\mu\text{g}/\text{bottle}$); C_l is the concentration of EDB in the aqueous phase ($\mu\text{g}/\text{L}$), V_l is the aqueous volume (L), C_g is the gas phase concentration ($\mu\text{g}/\text{L}$), and V_g is the gas volume (L). Using Henry's law constant ($H_c = C_g/C_l$) and substituting C_l for C_g yields:

$$M_T = C_l V_l + H_c C_l V_g \quad (\text{A2})$$

When $V_l = 1.5 \text{ L}$, $V_g = 0.3 \text{ L}$, $C_l = 0.05 \mu\text{g}/\text{L}$, and $H_c = 0.0251$, then $M_T = 7.54\text{E-}2 \mu\text{g}$.

Equation A1 may also be solved in terms of C_g by substituting for C_l :

$$C_g = \frac{M_T}{\frac{V_l}{H_c} + V_g} \quad (\text{A3})$$

Using the value calculated for M_T from equation S-2 and the values above for V_l , V_g , and H_c , equation A3 yields a value of $1.26\text{E-}3 \mu\text{g}/\text{L}$ for C_g . The amount of EDB injected onto the GC in a 0.5 mL headspace sample is $6.28\text{E-}4 \text{ ng}$. This amount is approximately 75% of the amount injected based on the modified version of Method 8011. Since the assumption regarding complete extraction efficiency for Method 8011 is unrealistic and the headspace method delivers an amount to the GC sufficient to allow detection to below the MCL for EDB, the headspace method was selected for quantification. This approach avoids the need to perform extractions and does not disturb the amount of liquid in the microcosms.

6.4 EDB and 1,2-DCA Results for Individual Microcosms.

Figure 1 in the manuscript shows average results for EDB and 1,2-DCA in triplicate microcosms. Data for each bottle are presented in Figure A.2 for the source zone and Figure A.3 for the midgradient zone, in order to reveal the extent of variability among the replicates. Especially noteworthy is the rapid biodegradation of EDB and 1,2-DCA in NA source zone replicate #3 (also described in the manuscript). EDB was added a second time to this microcosm to confirm its biodegradation activity. NA source zone replicate #4 also needed to be respiked with EDB, although it did not consume the second addition of EDB as rapidly as replicate #3. The BST and AC replicates in the source zone behaved more similarly. All of the midgradient replicates behaved similarly, both with respect to EDB and 1,2-DCA (Figure A.3) and BTEX (data not shown).

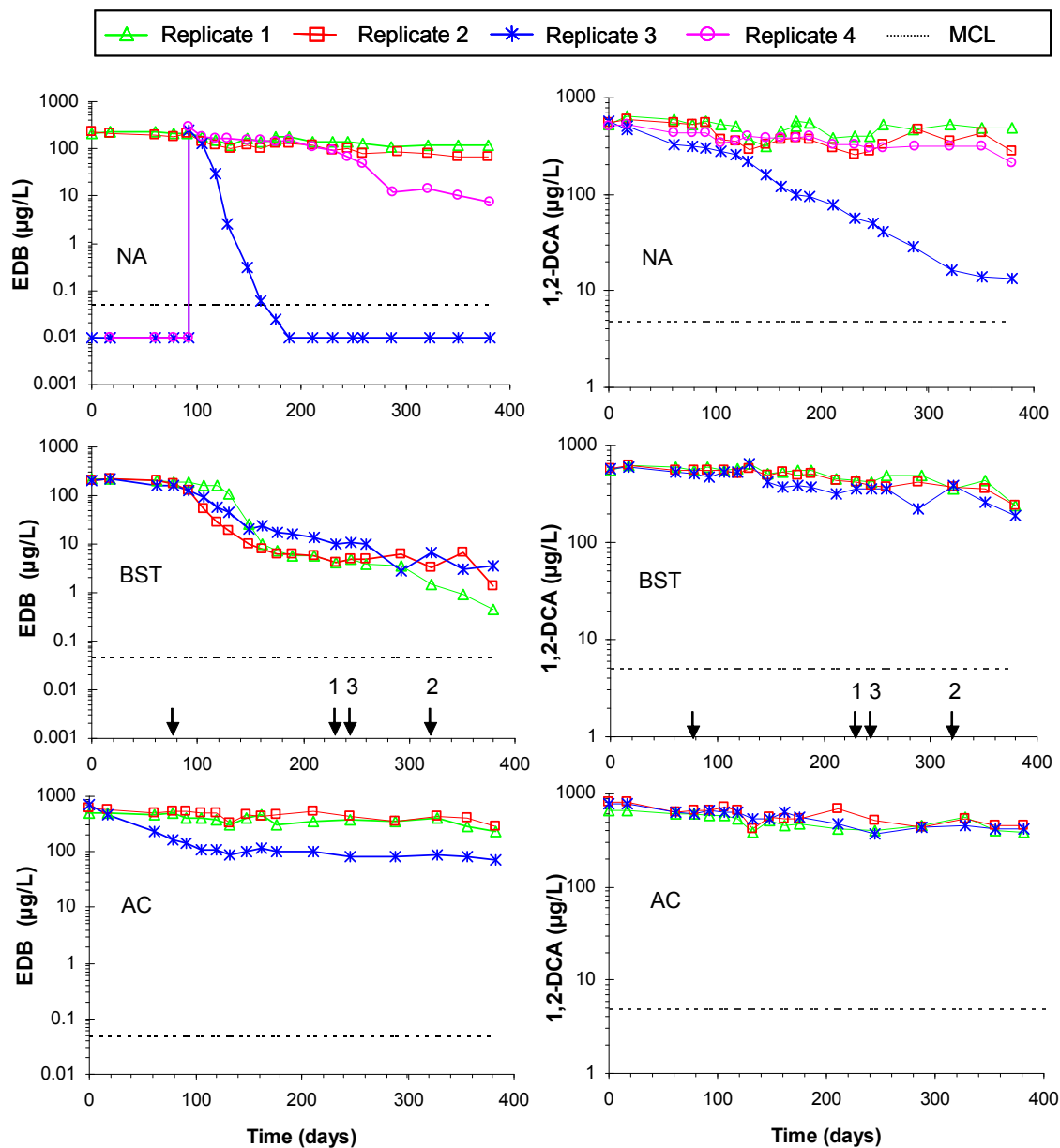


Figure A-2. Source zone EDB and 1,2-DCA microcosm replicates; dashed horizontal lines indicate the MCL for EDB and 1,2-DCA.

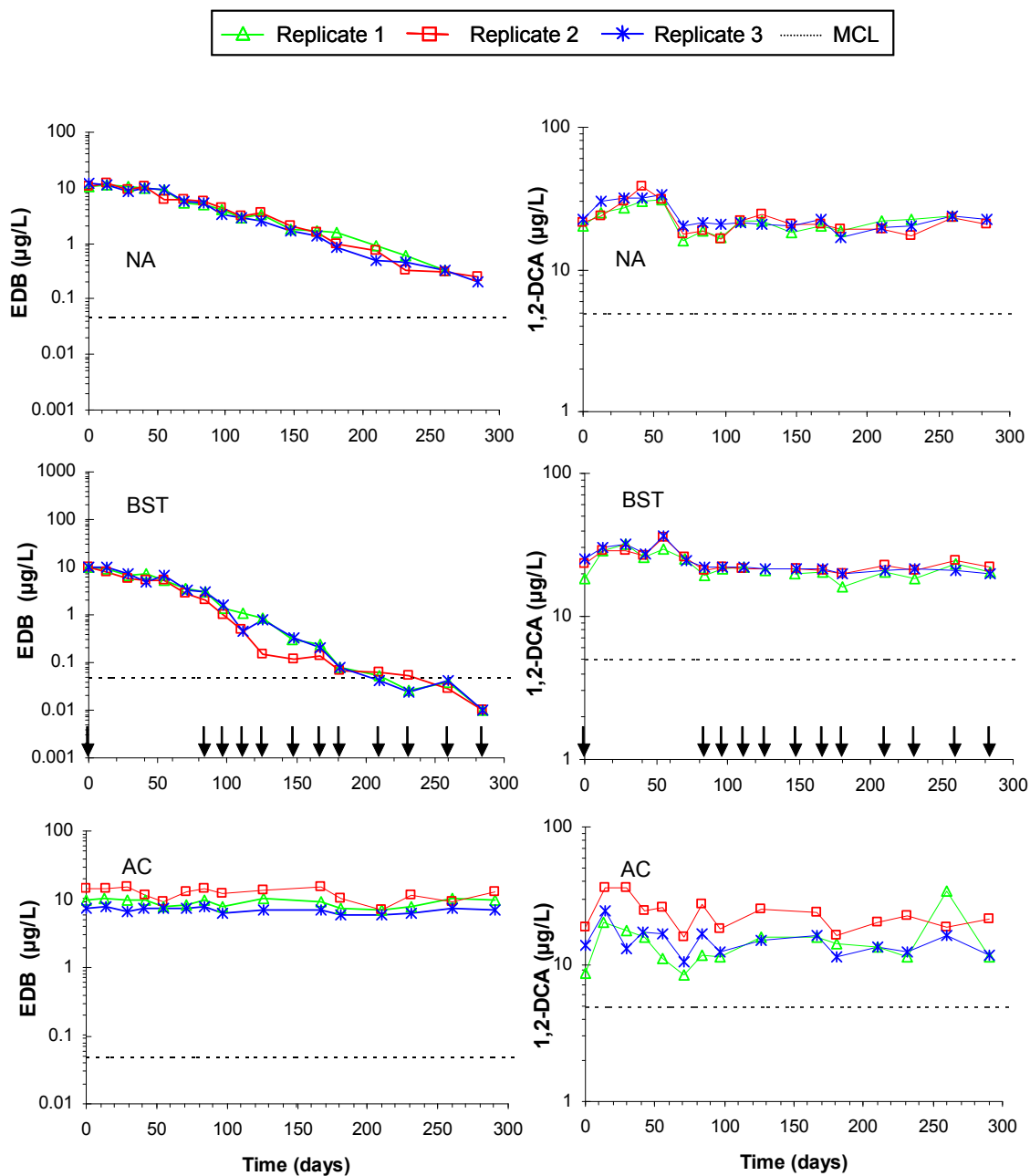


Figure A-3. Midgradient zone EDB and 1,2-DCA microcosm replicates; dashed horizontal lines indicate the MCL for EDB and 1,2-DCA.

6.5 Characteristics of Soil from the Source and Midgradient Zones.

Table A.2 shows various properties of the soil taken from the source and midgradient zones at the Clemson, South Carolina UST site sampled for this study. The soils contain a lower level of total iron than would be expected for clays that are native to the area. However, the soil at the site consists of clays along with poorly-sorted fill material consisting of a mixture of sand, silt and clay.

Table A.2 Soil Characteristics^a

Compound	Source Zone	Midgradient Zone
Phosphorus (mg/kg)	2.5	1.0
Potassium (mg/kg)	20	20
Calcium (mg/kg)	350	41
Magnesium (mg/kg)	23	14
Zinc (mg/kg)	5.2	2.3
Manganese (mg/kg)	27	22
Copper (mg/kg)	0.30	0.35
Boron (mg/kg)	0.1	0.05
Sodium (mg/kg)	9.0	9.0
Nitrate Nitrogen (mg/kg)	2.0	1.0
pH	5.1	4.8
Iron (mg/kg)	35	16
Carbon (%)	0.30	0.01

^a Analyses performed by the Agricultural Services Laboratory at Clemson University.

6.6 Comparison of Gibbs Free Energies for Dehalogenation of EDB, 1,2-DCA, and Associated Daughter Products

Table A.3 compares Gibbs free energy values for hydrogenolysis, dihaloelimination, and dehydrohalogenation of EDB, 1,2-DCA and their associated daughter products under standard and actual conditions for the source and midgradient microcosms. Table A.4 lists Gibbs free energy of formation values, Henry's law constants, and aqueous concentrations that were used in calculations for Table A.3. Transformations of EDB and its potential brominated daughter products are more thermodynamically favorable than for 1,2-DCA and its chlorinated daughter products in all reactions, with one exception: hydrogenolysis of vinyl chloride is slightly more favorable than vinyl bromide. It should be noted, however, that vinyl chloride and vinyl bromide did not accumulate in any of the microcosms in this study.

Table A.3 Comparison of Gibbs Free Energies for Transformation of EDB, 1,2-DCA and Associated Daughter Products

Transformation Process	Reaction	$\Delta G^{o' a}$	ΔG , Source Zone ^b	ΔG , Midgradient Zone ^b
Dihaloelimination	EDB + H ₂ → ethene + 2Br ⁻ + 2H ⁺	-195.0	-244.9	-259.8
	1,2-DCA + H ₂ → ethene + 2Cl ⁻ + 2H ⁺	-188.3	-225.5	-247.9
Hydrogenolysis	EDB + H ₂ → bromoethane + Br ⁻ + H ⁺	-153.5	-169.9	-177.4
	1,2-DCA + H ₂ → chloroethane + Cl ⁻ + H ⁺	-152.3	-162.4	-154.9
	bromoethane + H ₂ → ethane + Br ⁻ + H ⁺	-140.4	-156.8	-164.3
	chloroethane + H ₂ → ethane + Cl ⁻ + H ⁺	-134.9	-145.0	-137.5
	vinyl bromide + H ₂ → ethene + Br ⁻ + H ⁺	-148.4	-151.3	-158.7
	vinyl chloride + H ₂ → ethene + Cl ⁻ + H ⁺	-149.8	-159.8	-152.4
	ethene + H ₂ → ethane	-99.0	-99.4	-100.0
Dehydrohalogenation	EDB → vinyl bromide + Br ⁻ + H ⁺	-46.6	-63.0	-70.4
	1,2-DCA → vinyl chloride + Cl ⁻ + H ⁺	-38.5	-48.5	-41.1

^aCalculated using the aqueous Gibbs free energies of formation in Table A-4. Temperature = 25°C; all reactants and products at 1 M or 1 atm except H⁺, pH = 7.0.

^b ΔG calculated from $\Delta G^{o'}$ using the Nernst equation and the field conditions specified in Table A-4.

Table A.4 Data Used for Gibbs Free Energy Calculations Presented in Table A.3

Compound	$\Delta G^{\circ}_{f(g)}$		Henry's law constant ^a		$\Delta G^{\circ}_{f(aq)}$		Field Concentrations	
	kJ/mol	Source	atm·m ³ /mol	Source	kJ/mol	Source	Source Zone	Midgradient Zone
EDB	-10.60	(53)	0.0006664	(42)	-11.82 ^b	-	1.33E-06 M	6.67E-08 M
1,2-DCA	-73.90	(53)	0.0014400	(42)	-73.22 ^b	-	1.00E-05 M	4.00E-07 M
Bromoethane	-26.33	(53)	0.0075006	(36)	-21.34 ^b	-	1.00E-06 M	1.00E-06 M
Chloroethane	-60.00	(53)	0.0104458	(60)	-54.20 ^b	-	1.00E-06 M	1.00E-06 M
Vinyl bromide	81.06	(30)	0.0062300	(59)	23.83 ^b	-	1.00E-06 M	1.00E-06 M
Vinyl chloride	51.54	(53)	0.0263497	(42)	59.46 ^b	-	1.00E-06 M	1.00E-06 M
Ethene	68.16	(53)	0.1771136	(26)	80.97 ^b	-	2.75E-02 M	6.67E-03 M
Ethane	-32.95	(53)	0.4232135	(26)	-18.04 ^b	-	2.41E-02 M	5.00E-03 M
Bromide	-	-	-	-	-103.97	(6)	1.33E-06 M	6.67E-08 M
Chloride	-	-	-	-	-131.30	(6)	1.73E-05 M	3.47E-04 M
H ⁺ (pH = 7)	-	-	-	-	-39.83	(44)	6.40E-07 M	6.40E-07 M
H ₂	-	-	-	-	0.00	(44)	1.00E-03 atm	1.00E-03 atm

^a T = 25°C^b $\Delta G^{\circ}_{f(aq)} = \Delta G^{\circ}_{f(g)} + RT(\ln H)$

6.6 Comparison of EDB, 1,2-DCA and BTEX First Order Biodegradation Rates.

First order biodegradation rates observed in the microcosms (Figure 2.2) were compared to in situ rates of decay at the Clemson, South Carolina UST site sampled for this study. Rates for the UST site were estimated with the following first order decay model, assuming steady state conditions :

$$C(x) = C_o e^{\frac{-x}{v} \lambda_p} \quad (\text{A4})$$

where $C(x)$ is the contaminant concentration ($\mu\text{g/L}$) as a function of distance downgradient of the source, C_o is the source zone monitoring well concentration ($\mu\text{g/L}$), x is distance (m) between the source and midgradient monitoring wells, v is seepage velocity (m/yr), and λ_p is the pseudo-first order rate of decay (yr^{-1}). The resulting in situ decay rates are quite similar to the source zone microcosm decay rates (Table A.5). In the case of EDB, the two rates are nearly identical; the 1,2-DCA microcosm rate is 30% higher than the field rate. It should be noted that this comparison is based upon concentrations trends between the source and midgradient monitoring wells (MW-1 and MW-3, respectively) from which soil and groundwater samples were taken to prepare the microcosms. Since only two wells were utilized for this comparison, calculated field decay rates may not be strictly representative of actual in situ decay rates. The BTEX microcosm rates are 1.5 to 2.6 times higher than the rates estimated from the Clemson UST field data.

Table A.5 Comparison of First Order Biodegradation Rates (yr⁻¹)

Compound	This Study ^a				Clemson UST Site ^b	Other Field Studies ^c
	Source Zone		Midgradient Zone			
	NA	BST	NA	BST		
EDB	1.5 ± 1.0	5.5 ± 1.2	5.4 ± 0.3	9.4 ± 0.2	1.3	1.2 - 137
1,2-DCA	1.3 ± 0.3	0.8 ± 0.1	0.3 ± 0.1	0.7 ± 0.2	0.9	0.73
Benzene	1.5 ± 0.2	2.3 ± 0.2	3.5 ± 0.8	3.1 ± 0.4	1.0	4.4
Toluene	2.7 ± 0.3	2.3 ± 0.3	15 ± 3.3	12 ± 1.0	1.1	83
Ethylbenzen e	2.6 ± 0.3	1.7 ± 0.2	9.3 ± 1.2	11 ± 1.0	0.9	30
<i>o</i> -Xylene	2.3 ± 0.3	1.3 ± 0.1	9.5 ± 1.7	11 ± 1.2	0.6	4.4

^aFrom figure 2.2 in Chapter 2.

^bCalculated using equation S4, based on concentration data in Table S-6, $x = 5.97$ m, and $v = 3.79$ m/yr.

^cFrom reference (57).

Table A.6 Field Concentration Data Used to Calculate First Order Biodegradation Rates for the Clemson UST Site

Compound	Source Zone Concentration (μg/L)	Midgradient Zone Concentration (μg/L)
EDB	320	13
1,2-DCA	860	96
Benzene	35,578	2,669
Toluene	17,068	1,063
Ethylbenzene	2,581	243
<i>o</i> -Xylene	3,286	623

APPENDIX B

7.1 Inhibition Test Results by Bottle

Results of inhibition tests described in Chapter 4 are presented for each treatment. Replicates 1 and 2 are presented as a) and b) panels, respectively. The EDB inhibition test is presented in figures B-1 through B-4. The 1,2-DCA inhibition test results are presented in figures B-5 through B-9.

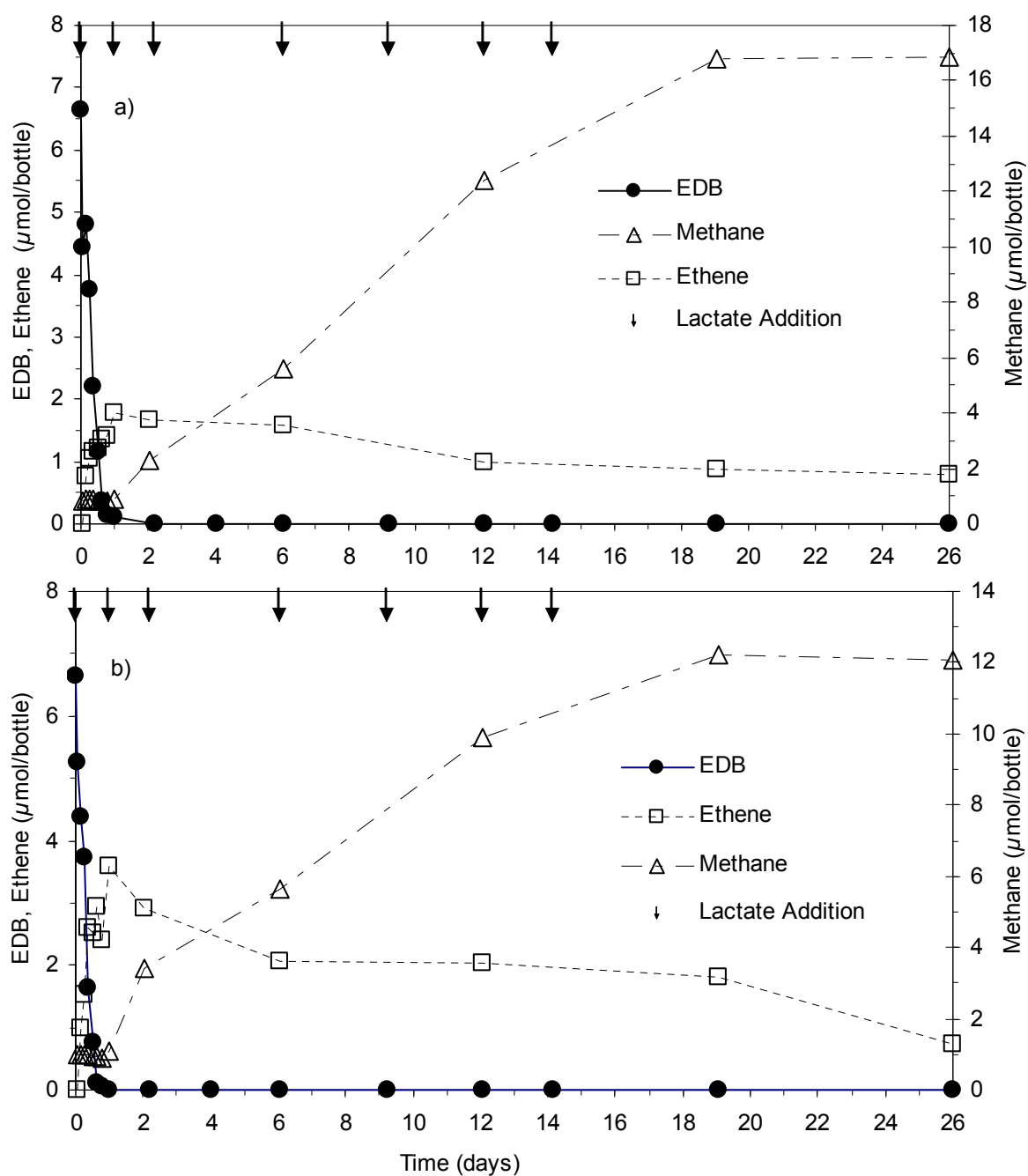


FIGURE B-1 EDB inhibition test, EDB only, replicates 1 (a) and 2 (b). Arrows (\downarrow) indicate when lactate was added.

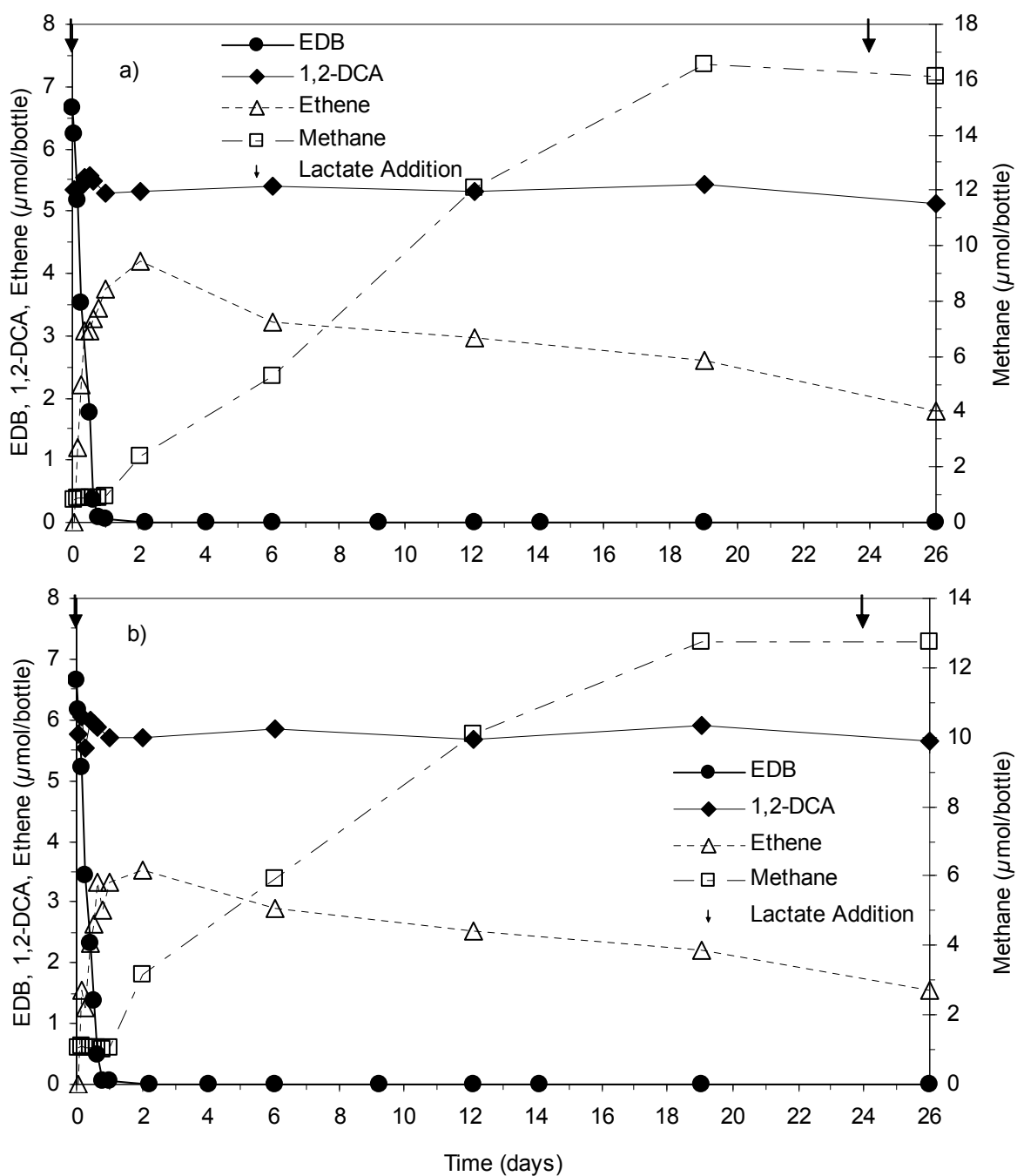


FIGURE B-2 EDB inhibition test, EDB + Low 1,2-DCA, replicates 1 (a) and 2 (b). Arrows (\downarrow) indicate when lactate was added.

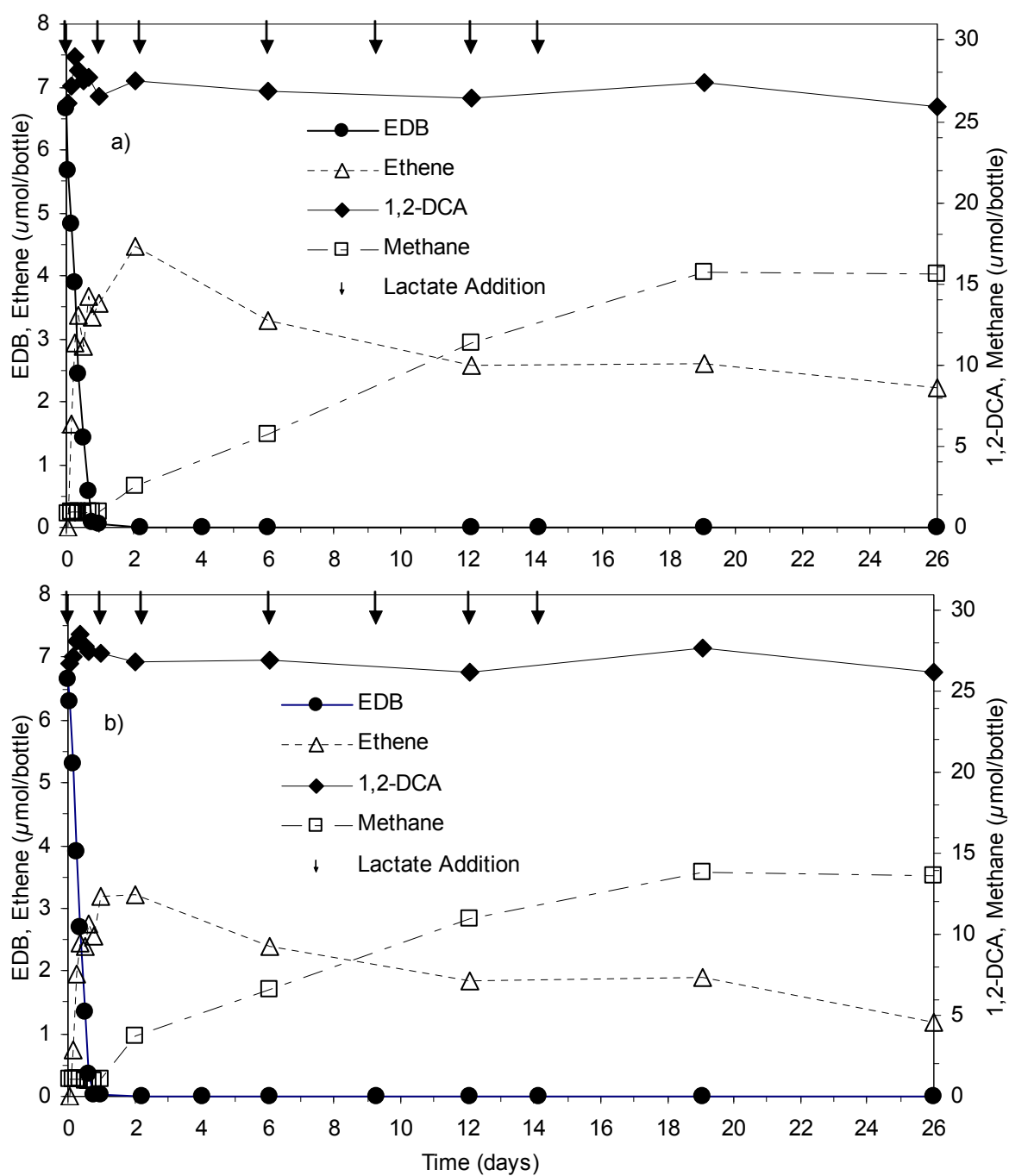


FIGURE B-3 EDB inhibition test, EDB + Mid 1,2-DCA, replicates 1 (a) and 2 (b). Arrows (\downarrow) indicate when lactate was added.

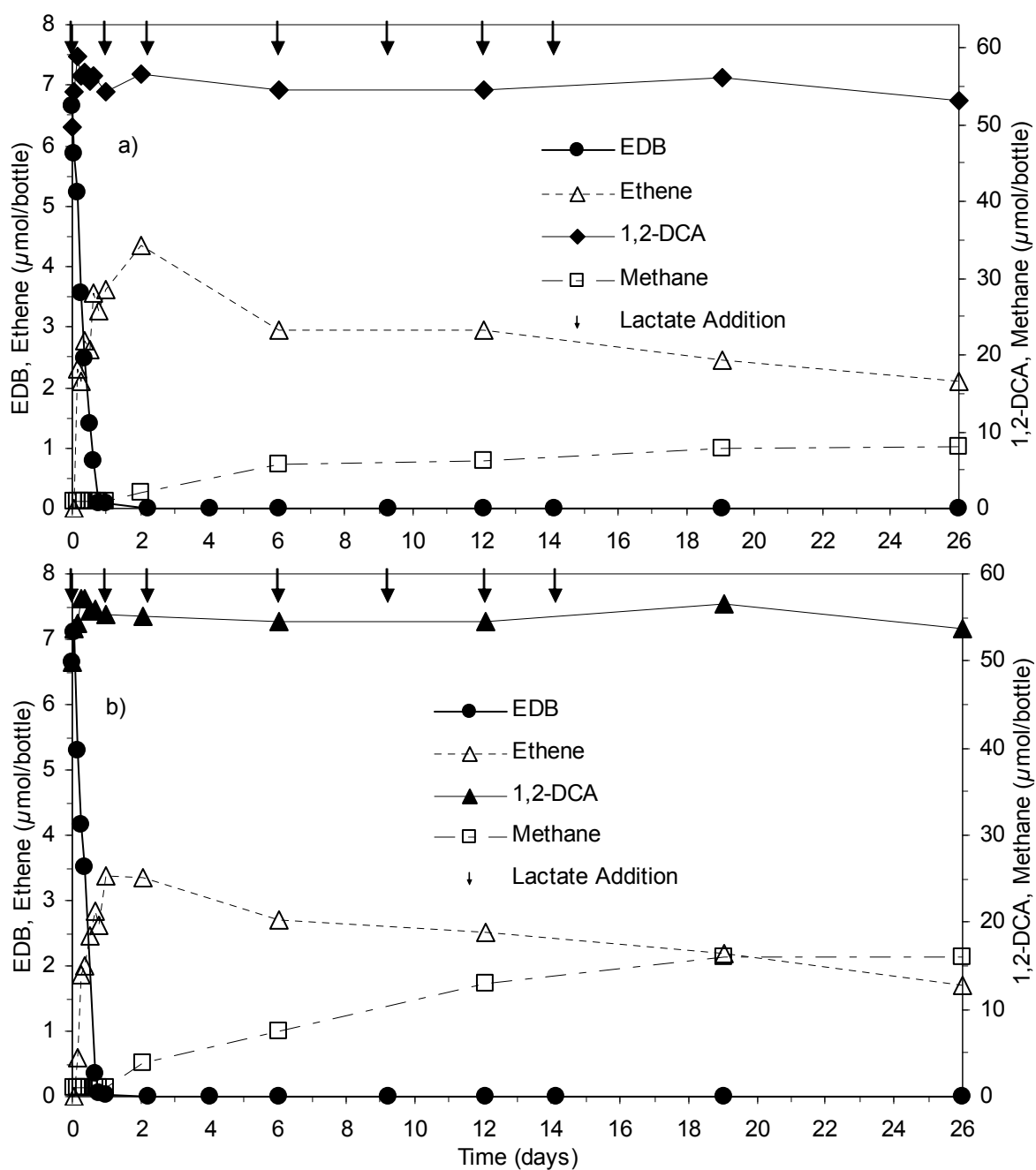


FIGURE B-4 EDB inhibition test, EDB + High 1,2-DCA, replicates 1 (a) and 2 (b). Arrows (\downarrow) indicate when lactate was added.

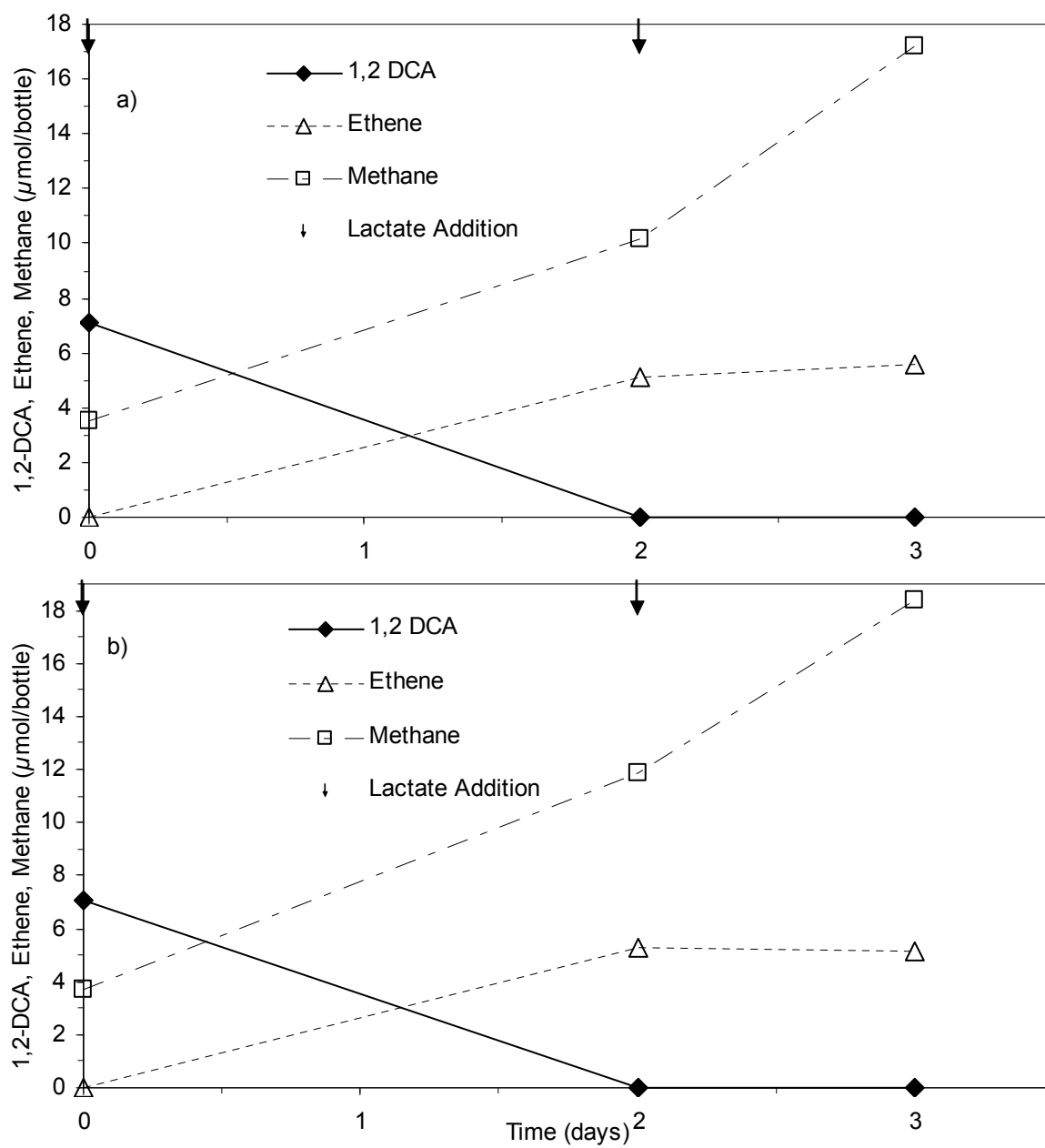


FIGURE B-5 1,2-DCA inhibition test, 1,2-DCA only, replicates 1 (a) and 2 (b). Arrows (\downarrow) indicate when lactate was added.

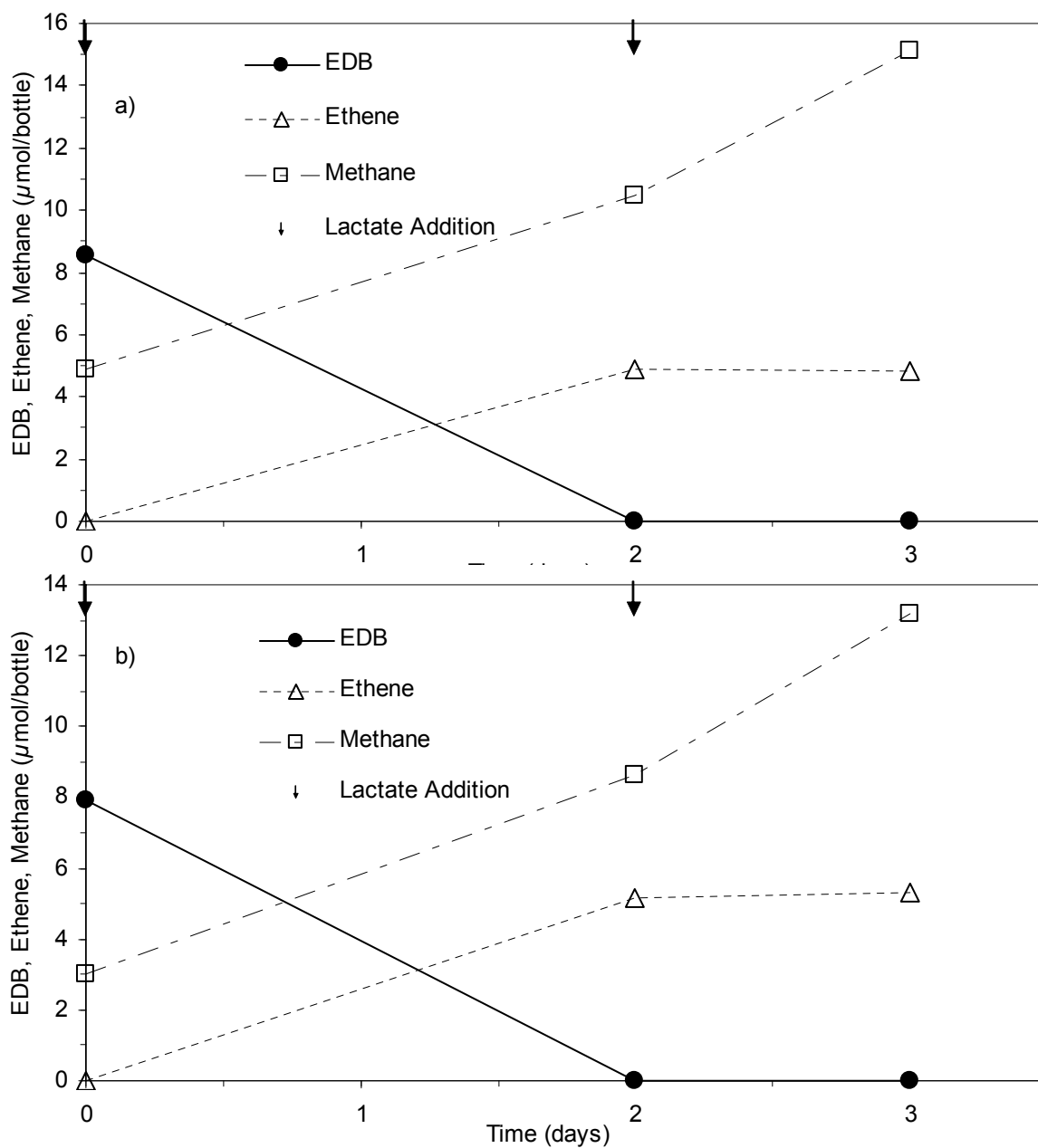


FIGURE B-6 1,2-DCA inhibition test, EDB only, replicates 1 (a) and 2 (b). Arrows (\downarrow) indicate when lactate was added.

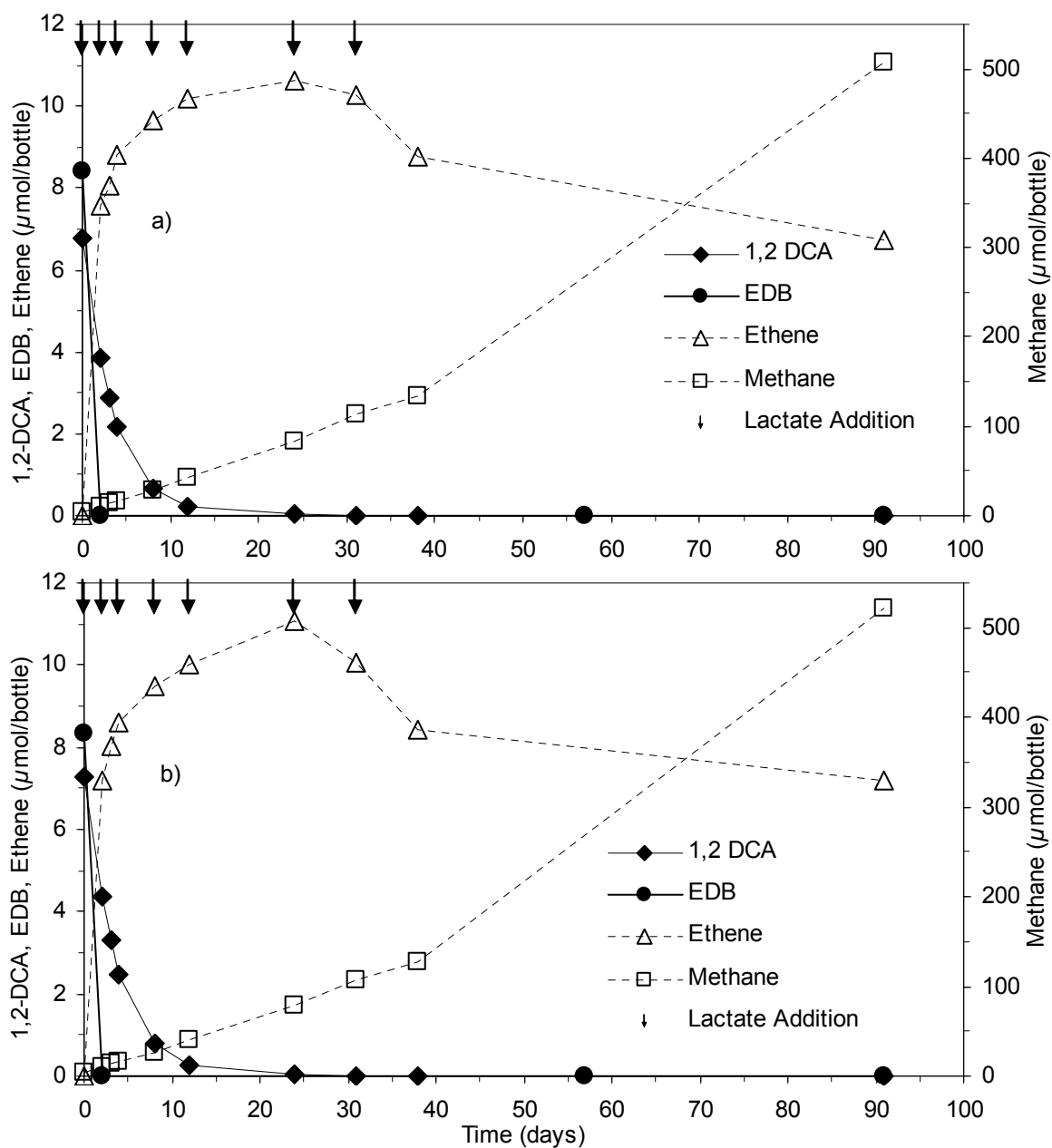


FIGURE B-7 1,2-DCA inhibition test, 1,2-DCA + Low EDB, replicates 1 (a) and 2 (b). Arrows (\downarrow) indicate when lactate was added.

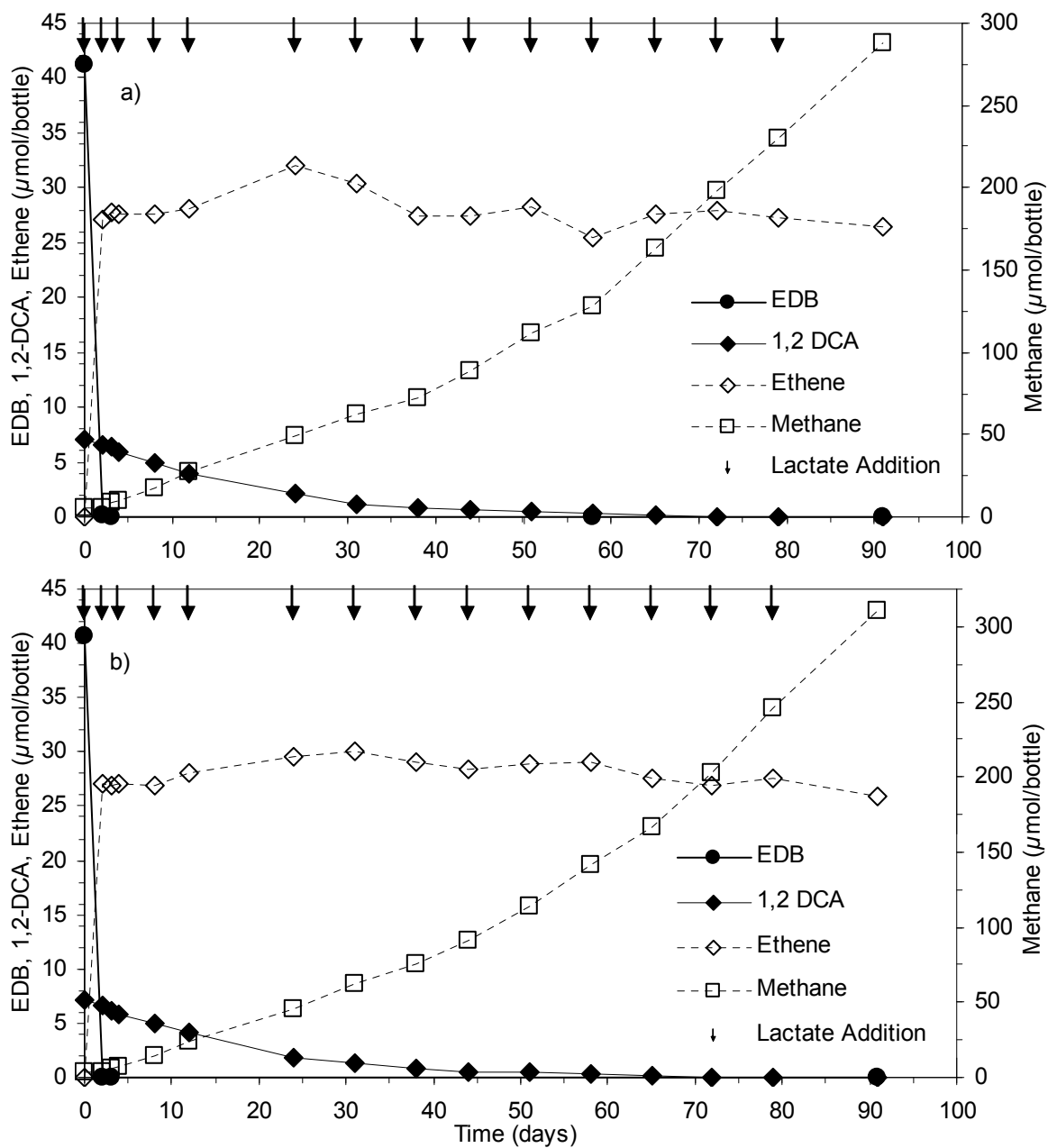


FIGURE B-8 1,2-DCA inhibition test, 1,2-DCA + Mid EDB, replicates 1 (a) and 2 (b). Arrows (\downarrow) indicate when lactate was added.

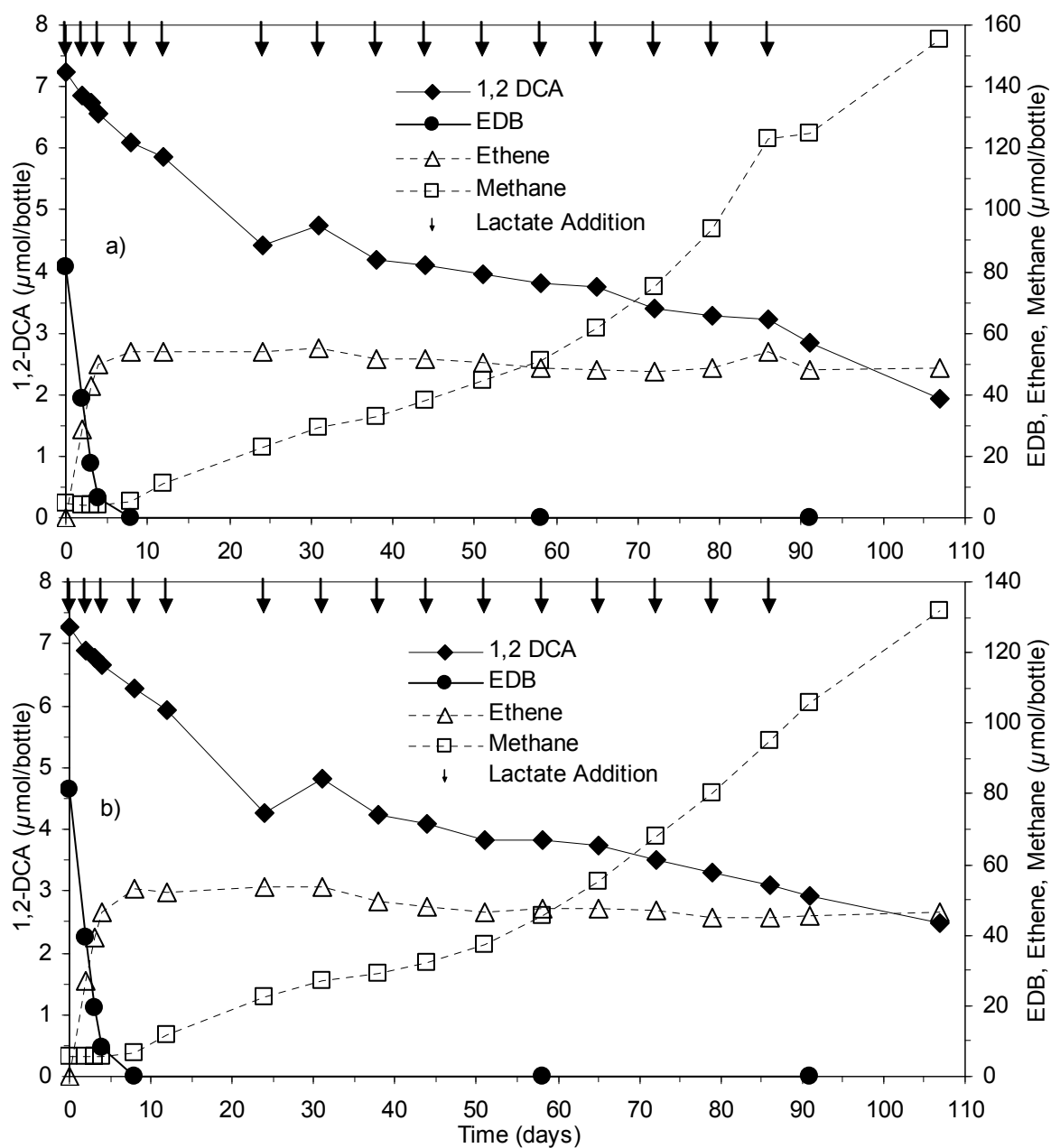


FIGURE B-9 1,2-DCA inhibition test, 1,2-DCA + High EDB, replicates 1 (a) and 2 (b). Arrows (\downarrow) indicate when lactate was added.

REFERENCES

1. **Adamson, D. T., and G. F. Parkin.** 1999. Biotransformation of mixtures of chlorinated aliphatic hydrocarbons by an acetate-grown methanogenic enrichment culture. *Wat. Res.* **33**:1482-1494.
2. **Adamson, D. T., and G. F. Parkin.** 2000. Impact of mixtures of chlorinated aliphatic hydrocarbons on a high-rate, tetrachloroethene-dechlorinating enrichment culture. *Environ. Sci. Technol.* **34**:1959-1965.
3. **Aziz, C. E., C. J. Newell, J. R. Gonzales, P. Hass, T. P. Clement, and Y. Sun.** 2000. BIOCHLOR Natural Attenuation Decision Support System User's Manual Version 1.0. U.S. Environmental Protection Agency, EPA/600/R-00/008.
4. **Bedard, D. L., and H. M. V. Dort.** 1998. Complete reductive dehalogenation of brominated biphenyls by anaerobic microorganisms in sediment *Appl. Environ. Microbiol.* **64**:940-947.
5. **Bedient, P. B., H. S. Rifai, and C. J. Newell.** 1999. *Ground Water Contamination Transport and Remediation*, 2nd Edition ed. Prentice Hall, Upper Saddle River, New Jersey.
6. **Benjamin, M. M.** 2002. *Water Chemistry*. McGraw Hill, New York.
7. **BLE.** 2005. Report of Tier II Assessment Former Tiger Mart. Bunnell-Lammons Engineering, Greenville, SC.
8. **Boyd, T. A.** 1950. Pathfinding in fuels and engines. *SAE Quarterly Transactions* **4**:182-195.
9. **Bradley, P. M., and F. H. Chapelle.** 2002. Microbial mineralization of ethene under sulfate-reducing conditions. *Bioremediation Journal* **6**:1-8.
10. **Bradley, P. M., and F. H. Chapelle.** 1996. Anaerobic mineralization of vinyl chloride in Fe(III)-reducing, aquifer sediments. *Environ. Sci. Technol.* **30**:2084-2086.
11. **Bradley, P. M., and F. H. Chapelle.** 1998. Microbial mineralization of VC and DCE under different electron accepting conditions. *Anaerobe* **4**:81-87.
12. **CH2MHILL.** 2004. Final Fuel Spill-F1 2003 Annual System Performance and Ecological Impact Monitoring Report. CH2MHILL, Otis Air National Guard Base, MA, Massachusetts Military Reservation.

13. **Chiu, P. C., and M. Lee.** 2001. 2-Bromoethanesulfonate affects bacteria in a trichloroethene-dechlorinating culture. *Appl. Environ. Microbiol.* **67**:2371-2374.
14. **Cline, P. V., J. J. Deletion, and P. S. Rao.** 1991. Partitioning of aromatic constituents into water from gasoline and other complex solvent mixtures. *Environ. Sci. Technol* **25**:914-920.
15. **Cwiertny, D. M., and A. L. Roberts.** 2005. On the nonlinear relationship between k_{obs} and reductant mass loading in iron batch systems. *Environ. Sci. Technol.* **39**:8948-8957.
16. **Dinglasan-Panlilio, M. J., S. Dworatzek, S. Mabury, and E. A. Edwards.** 2006. Microbial oxidation of 1,2-dichloroethane under anoxic conditions with nitrate as electron acceptor in mixed and pure cultures. *FEMS Microbiol. Ecol.* **56**:355–364.
17. **Edwards, E. A., and D. Grbic-Galic.** 1994. Anaerobic degradation of toluene and o-xylene by a methanogenic consortium. *Appl. Environ. Microbiol.* **60**:313-322.
18. **Ehrlich, G. G., D. F. Goerlitz, J. H. Bourell, G. V. Eisen, and E. M. Godsy.** 1981. Liquid chromatographic procedure for fermentation product analysis in the identification of anaerobic bacteria. *Appl. Environ. Microbiol.* **42**:878-885.
19. **Elsner, M., L. Zwank, D. Hunkeler, and R. P. Schwarzenbach.** 2005. A new concept linking observable stable isotope fractionation to transformation pathways of organic pollutants. *Environ. Sci. Technol.* **39**:6896-6916.
20. **Falta, R. W.** 2008. Methodology for comparing source and plume remediation alternatives. *Ground Water* **46**:272-285.
21. **Falta, R. W.** 2004. The potential for ground water contamination by the gasoline lead scavengers ethylene dibromide and 1,2-dichloroethane. *Ground Water Monit. Remediat.* **24**:76-87.
22. **Falta, R. W.** 2006. REMChlor Remediation Evaluation Model for Chlorinated Solvents. User's Manual Beta Version 1.0.
23. **Falta, R. W., N. Basu, and P. S. Rao.** 2005. Assessing the impacts of partial mass depletion in DNAPL source zones: I. Analytical modeling of source strength functions and plume response. *J. Contam. Hydrol.* **78**:259-280.
24. **Falta, R. W., and N. Bulsara.** 2004. Lead scavengers: A leaded gasoline legacy? *L.U.S.T.Line* **47**:6-10.

25. **Falta, R. W., N. Bulsara, J. K. Henderson, and R. A. Mayer.** 2005. Leaded-gasoline additives still contaminate groundwater. *Environ. Sci. Technol.* **39**:378A-384A.
26. **Freedman, D. F., and S. D. Herz.** 1996. Use of ethylene and ethane as primary substrates for aerobic cometabolism of vinyl chloride. *Water Environ. Res.* **68**:320-328.
27. **Freedman, D. L.** 2008. Personal Communication.
28. **Freedman, D. L., and J. M. Gossett.** 1989. Biological reductive dechlorination of tetrachloroethylene and trichloroethylene to ethylene under methanogenic conditions. *Appl. Environ. Microbiol.* **55**:2144-2151.
29. **Gerritse, J., A. Borger, E. Van Heiningen, H. H. M. Rijnaarts, N. P. Bosma, J. Taat, B. Van Winden, J. Dijk, and J. A. M. De Bont.** 1999. Assessment and monitoring of 1,2-dichloroethane dechlorination, In: *Engineered Approaches for In Situ Bioremediation of Chlorinated Solvent Contamination*, A. Leeson and B. C. Allemean (eds.), 73-79.
30. **Gokel, G. W.** 2004. *Dean's Handbook of Organic Chemistry*, 2nd ed. McGraw-Hill, New York.
31. **Groster, A., and E. Edwards.** 2006. A 1,1,1-trichloroethane-degrading anaerobic mixed microbial culture enhances biotransformation of mixtures of chlorinated ethenes and ethanes. *Appl. Environ. Microbiol.* **72**:7849-7856.
32. **Gu, A. Z., H. D. Stensel, J. M. H. Pietari, and S. E. Strand.** 2003. Vinyl bromide as a surrogate for determining vinyl chloride reductive dechlorination potential. *Environ. Sci. Technol.* **37**:4410-4416.
33. **He, J., K. M. Ritalahti, K.-L. Yang, S. S. Koeningsberg, and F. E. Löffler.** 2003. Detoxification of vinyl chloride to ethene coupled to growth of an anaerobic bacterium. *Nature* **424**:62-65.
34. **Henderson, J. K., D. L. Freedman, R. W. Falta, T. Kuder, and J. T. Wilson.** 2008. Anaerobic biodegradation of ethylene dibromide and 1,2-dichloroethane in the presence of fuel hydrocarbons. *Environ. Sci. Technol.* **42**:864-870.
35. **Hughes, J. B., and G. F. Parkin.** 1992. The effect of mixtures of xenobiotics and primary electron donor on the anaerobic biotransformation of high concentrations of chlorinated aliphatics. *Wat. Sci. Tech.* **26**:117-126.

36. **IPCS.** 2006. International Programme on Chemical Safety Home Page. www.inchem.org/documents/cicads/cicads/cicad42.htm, (accessed February 16, 2006).
37. **Jacobs, E. S., Ed.** 1980. Use and air quality impact of ethylene dichloride and ethylene dibromide scavengers in leaded gasoline. In Banbury Report 5: Ethylene Dichloride: A Potential Health Risk? Ed. B. N. Ames, P. Infante, and R Reitz, 239-255. Cold Spring Harbor Laboratory, New York.
38. **Johnson, R., J. Pankow, D. Bender, C. Price, and J. Zogorski.** 2000. MTBE: To what extent will past releases contaminate community water supply wells? *Environ. Sci. Technol.* **34**:210a-217a.
39. **Kelly, W. R., M. P. Saliga, M. L. Machesky, and D. L. Freedman.** 1996. Biodegradation of BTEX under iron-reducing conditions in batch microcosms. Presented at the Proceeding of the Water Environment Federation 69th Annual Conference.
40. **Klecka, G. M., C. L. Carpenter, and S. J. Gonsior.** 1999. Biological transformation of 1,2-dichloroethane in subsurface soils and groundwater. *J. Contam. Hydrol.* **34**:139-154.
41. **Kuder, T., J. T. Wilson, P. Kaiser, R. Kolhatkar, P. Philp, and J. Allen.** 2005. Enrichment of stable carbon and hydrogen isotopes during anaerobic biodegradation of MTBE: microcosm and field evidence. *Environ. Sci. Technol.* **39**.
42. **LaGrega, M. D., P. L. Buckingham, and J. C. Evans.** 1994. Hazardous Waste Management. McGraw-Hill, Inc., New York.
43. **Loffler, F. E., K. M. Ritalahti, and J. M. Tiedje.** 1997. Dechlorination of chloroethenes is inhibited by 2-bromoethanesulfonate in the absence of methanogens. *Appl. Environ. Microbiol.* **63**:4982-4985.
44. **Madigan, M. T., J. M. Martinko, and J. Parker.** 2000. Brock Biology of Microorganisms, 9th ed. Prentice Hall, Upper Saddle River, New Jersey.
45. **Maes, A. V., H.; Smith, K.; Ossieur, W.; Lebbe, L.; Verstraete, W.** 2006. Transport and activity of *Desulfitobacterium dichloroeliminans* strain DCA1 during bioaugmentation of 1,2-DCA-contaminated groundwater. *Environ. Sci. Technol.* **40**.
46. **Maymó-Gatell, X., Y.-t. Chien, J. M. Gossett, and S. H. Zinder.** 1997. Isolation of a bacterium that reductively dechlorinates tetrachloroethene to ethene. *Science* **276**:1568-1571.

47. **Meckenstock, R. U., B. Morasch, C. Griebler, and H. H. Richnow.** 2004. Stable isotope fractionation analysis as a tool to monitor biodegradation in contaminated aquifers. *J. Contam. Hydrol.* **75**:215-255.
48. **Montgomery, J. H.** 1997. *Agrochemicals Desk Reference*, 2nd edition, 2nd ed. CRC Lewis Publishers, Boca Raton, Florida.
49. **Newell, C. J., R.K. McLeod, and J.R. Gonzales.** 1996. BIOSCREEN Natural Attenuation Decision Support System User's Manual Version 1.3. U.S. EPA National Risk Management Research Laboratory, EPA/600/R-96/087.
50. **NRC.** 2000. *Natural Attenuation for Groundwater Remediation*. National Research Council, National Academy Press, Washington, DC.
51. **Parker, J. C., and E. Park.** 2004. Modeling field scale dense nonaqueous phase liquid dissolution in heterogeneous aquifers. *Water Resour. Res.* **40**:W051091.
52. **Pignatello, J. J., and C. Z. Cohen.** 1990. Environmental chemistry of ethylene dibromide in soil and ground water. *Review of Environmental Contaminant Toxicology* **112**:1-47.
53. **Reid, R. C., J. M. Prausnitz, and B. E. Poling.** 1987. *The Properties of Gases & Liquids*, Fourth Edition ed. McGraw-Hill Book Company, New York.
54. **Rittmann, B. E., and P. L. McCarty.** 2001. *Environmental Biotechnology: Principles and Applications*. McGraw-Hill, New York.
55. **Rothermich, M. M., L. A. Hayes, and D. R. Lovley.** 2002. Anaerobic, sulfate-dependent degradation of polycyclic aromatic hydrocarbons in petroleum-contaminated harbor sediment. *Environ. Sci. Technol.* **36**:4811-4817.
56. **Schmidt, T. C., M. Schirmer, H. Weib, and S. B. Haderlein.** 2003. Microbial degradation of methyl *tert*-butyl ether and *tert*-butyl alcohol in the subsurface. *J. Contam. Hydrol.* **70**:173-203.
57. **Suarez, M. P., and H. S. Rifai.** 1999. Biodegradation rates for fuel hydrocarbons and chlorinated solvents in groundwater. *Bioremediation Journal* **3**:337-362.
58. **USEPA.** 2000. United States Environmental Protection Agency Test Methods Home Page. http://www.epa.gov/epaoswer/hazwaste/test/8_series.htm 1,2-Dibromoethane and 1,2-dibromo-3-chloropropane by microextraction and gas chromatography (accessed May 2007).

59. **USEPA.** 2007. US EPA Region 9 Superfund Preliminary Remediation Goals Home Page. Region 9 Preliminary Remediation Goals 2004 Table (<http://www.epa.gov/region09/waste/sfund/prg/index.html>) (accessed August 22, 2007).
60. **USEPA.** 2006. USEPA Athens Lab Home Page. <http://www.epa.gov/ATHENS/learn2model/part-two/onsite/esthenry.htm>, (accessed February 16, 2006).
61. **Wackett, L. P., M. S. P. Logan, F. A. Blocki, and C. Bao-li.** 1992. A mechanistic perspective on bacterial metabolism of chlorinated methanes. *Biodegradation* **3**:19-36.
62. **Watt, R. J.** 1998. Hazardous Wastes: Sources, Pathways, Receptors. Wiley Publishers, New York.
63. **Weaver, J.** 2007. Unpublished data.
64. **Wiedemeier, T. D., H.S. Rifai, C.J. Newell, and J.T. Wilson.** 1999. Natural Attenuation of Fuels and Chlorinated Solvents in the Subsurface.
65. **Wijngaard van den, A. J., K. W. H. J. Van der Kamp, F. Van der Ploeg, B. Pries, B. Kazemier, and D. B. Janssen.** 1992. Degradation of 1,2-dichloroethane by *Ancyclobacter aquaticus* and other facultative methylotrophs. *Appl. Environ. Microbiol.* **58**:976-983.
66. **Wildeman, S. D., G. Linthout, H. V. Langenhove, and W. Verstraete.** 2004. Complete lab-scale detoxification of groundwater containing 1,2-dichloroethane. *Appl. Microbiol. Biotechnol.* **63**:609-612.
67. **Wilson, J. T.** 2007. Personal communication.
68. **Wood, E. A.** 2007. Development and Evaluation of an Enrichment Culture for Bioaugmentation of the P-Area Chlorinated Ethene Plume at the Savannah River Site. MS Thesis, Clemson University. Clemson University, Clemson.
69. **Zhu, J., and J. F. Sykes.** 2004. Simple screening models of NAPL dissolution in the subsurface. *J. Contam. Hydrol.* **72**:245-258.